Aus der Neurologischen Universitätsklinik Tübingen

Abteilung Neurologie mit Schwerpunkt Neurodegenerative Erkrankungen

# Electrophysiological activity of basal ganglia under deep brain stimulation in the rat model

**Inaugural-Dissertation**
**zur Erlangung des Doktorgrades**
**der Medizin**

**der Medizinischen Fakultät**
**der Eberhard Karls Universität**
**zu Tübingen**

**vorgelegt von**

**Slewa, Barbara Lidia**

**2020**

Dekan: Professor Dr. B. Pichler

1. Berichterstatter: Privatdozent Dr. S. Breit
2. Berichterstatter: Professor Dr. C. Schwarz

Tag der Disputation: 19.10.2020

## Contents

## List of figures

## List of tables

## List of abbreviations

| | |
|---|---|
| **CM** | centromedian nucleus |
| **COMT** | catechol-*O*-methyltransferase |
| **COX1** | cytochrome c oxidase subunit I |
| **CV-ISI** | coefficient of variation of the interspike intervals |
| **DBS** | deep brain stimulation |
| **DDH** | discharge density histogram |
| **dopamine** | 3,4-dihydroxyphenethylamin |
| **EP** | entopeduncular nucleus |
| **GABA** | gamma-aminobutyric acid |
| **Glu** | glutamate |
| **GP** | lateral globus pallidus (equivalent to GPe in primates) |
| **GPe** | external globus pallidus |
| **GPi** | internal globus pallidus |
| **HFS** | high-frequency stimulation |
| **ISI** | inter-spike interval |
| **LDTg** | laterodorsal tegmental nucleus |
| **levodopa** | L-3,4-dihydroxyphenylalanine |
| **MAO-B** | monoamine oxidase B |
| **mRNA** | messenger RNA |
| **MSNs** | medium-sized spiny neurons |
| **n.s.** | not significant |
| **NMDA** | *N*-methyl-D-aspartate |
| **p** | probability value |
| **PBS** | phosphate-buffered saline |
| **PD** | Parkinson's disease |
| **PFA** | paraformaldehyde |
| **PPN** | pedunculopontine nucleus |
| **rsfMRI** | resting-state functional magnetic resonance imaging |
| **SD** | standard deviation |
| **SEM** | standard error of the mean |
| **SNc** | substantia nigra pars compacta |

| | |
|---|---|
| **SNr** | substantia nigra pars reticulata |
| **STN** | subthalamic nucleus |
| **STN-DBS** | Tiefe Hirnstimulation des Nucleus subthalamicus;<br>*engl.* deep brain stimulation of the subthalamic nucleus |
| **STN-HFS** | Hochfrequenzstimulation des Nucleus subthalamicus;<br>*engl.* high-frequency stimulation of the subthalamic nucleus |

# 1 Introduction

In the past three decades, deep brain stimulation (DBS) has become the neurosurgical procedure of choice for patients in an advanced stadium of Parkinson's disease. Pharmacotherapeutic limitations led to the development of surgical strategies and over the years, DBS emerged as an effective and less invasive surgical option compared to ablative procedures. It has replaced ablative surgeries and contributed to reducing the number of patients struggling with motor fluctuations and dyskinesias associated with the high doses of levodopa therapy in the later stages of Parkinson's disease (Thanvi BR & Lo TCN, 2004). DBS has shown an advantage in numerous other neurological disorders and is currently a subject of various medical trials.

It is well known that high-frequency stimulation (HFS) of the subthalamic nucleus (STN), alleviates the cardinal symptoms of Parkinson's disease. However, the underlying physiological mechanisms are not entirely understood. The data obtained in this field from experimental models based on anatomical, neurochemical and electrophysiological *in vitro* and *in vivo* research is often contradictory.

Our *in vivo* study in anesthetized rats explores the effects HFS of the STN has on the electrophysiological activity of the three basal ganglia involved in the motor circuit- that is, the external globus pallidus (GPe), the substantia nigra pars reticulata (SNr) and the pedunculopontine nucleus (PPN).

## 1.1 Etiology, pathophysiology and pathogenesis of Parkinson's disease

Parkinson's disease (PD) is a neurodegenerative movement disorder with a high prevalence (1600 per 100´000 individuals among 70 - 79-year-olds in Europe, Australia, and North America) which increases with demographic aging

(Pringsheim T, et al., 2014) and is expected to have a–significant worldwide economic impact in the near future (Dorsey ER, et al., 2007).

Its diverse range of symptoms include rigidity, tremor, bradykinesia and postural instability, as well as a variety of other motor, autonomic, neuropsychiatric, gastrointestinal, and neuro-ophthalmologic manifestations (Greenland JC & Barker RA, 2018).

The hallmark of Parkinson's disease is the loss of dopaminergic neurons in the substantia nigra pars compacta (SNc) resulting in a balance disruption in the basal ganglia network. Another prominent feature of Parkinson's disease is the presence of eosinophilic inclusion bodies primarily composed of misfolded α-synuclein and other ubiquitinated proteins called Lewy bodies (Engelender S, 2008). The precise role of Lewy bodies in the pathogenesis of Parkinson's disease remains unknown. Interestingly, Lewy body pathology affects not only the dopaminergic areas of the brain but is also found in peripheral tissues. The occurrence of Lewy bodies in the sympathetic autonomic denervation of the heart or the myenteric plexus is associated with several non-motor symptoms such as orthostatic hypotension and alterations in gastrointestinal motility (Orimo S, et al., 2005; Fujishiro H, et al., 2008). Lewy bodies are also found in the olfactory bulb and brain centers such as the amygdala, and perirhinal nucleus, resulting in hyposmia (Witt, et al., 2009).

Most patients are diagnosed with the idiopathic form of Parkinson's disease, around 10 % have a positive family history. The discovery of gene mutations responsible for the hereditary Parkinson's disease brought some light into the mechanisms underlying its pathogenesis. Among them are mutations that cause altered proteolysis which in turn are responsible for the aggregation of α-synuclein, others are responsible for mitochondrial dysfunctions leading to increased oxidative stress. These genes encode the proteins involved in the molecular pathways that overlap with the pathologies seen in the idiopathic form (Dexter DT & Jenner P, 2013). Neuroinflammation, a broken blood-brain barrier, and excitotoxicity, resulting from the increased activity of the glutamatergic STN

input the SNc, also seem to play a role in neuronal cell death (Hirsch EC, et al., 2003; Steigerwald F, et al., 2008).

Several environmental factors, such as rural living, farming, pesticide use, or a history of head injury, have been linked to an increased risk of Parkinson's disease (Noyce AJ, et al., 2012). There is also some data supporting an inverse association of smoking and coffee consumption with Parkinson's disease (Hancock DB, et al., 2007).

The pathophysiology of the basal ganglia in Parkinson's disease is further discussed below in section 1.3.8.

## 1.2 Pharmacological treatment of Parkinson's disease

Dopaminergic depletion disrupts the finely tuned basal ganglia network. L-3,4-dihydroxyphenylalanine (levodopa), a precursor of 3,4-Dihydroxyphenethylamin (dopamine), is so far the most effective pharmacotherapy alleviating the motor symptoms of Parkinson's disease. It is administered in combination with a peripheral aromatic L-amino acid decarboxylase inhibitor (carbidopa or benserazide), which inhibits the conversion of levodopa to dopamine before crossing the blood-brain barrier and reduces the side effects of dopamine while improving its availability in the brain. The response to the levodopa treatment fluctuates. Moreover, within 5 – 10 years of treatment, levodopa leads to motor complications including involuntary movements and dyskinesias such as athetosis or dystonia in most patients (> 90 %). Patients experience "wearing-off" phenomena leading to "on" and "off" states, in which symptoms return or worsen before the next dose of levodopa is administered. Dopamine precursors, as well as other pharmacological strategies including monoamine oxidase B (MAO-B) inhibitors, catechol-*O*-methyltransferase (COMT) inhibitors, dopamine receptor agonists, anticholinergics or *N*-methyl-D-aspartate (NMDA) receptor antagonists, only offer symptomatic treatment (Connolly BS & Lang AE, 2014).

## 1.3 Basal ganglia

### 1.3.1 Neuroanatomical and physiological organization

The basal ganglia are a group of interconnected nuclei located at the base of the forebrain. A variety of anatomical, molecular and imaging techniques was required to shed some light on their complex organization and function. They include four structures: the striatum, the globus pallidus, the STN, and the substantia nigra. Together these nuclei create a highly organized network involved in movement control, associative learning, memory, and emotion (Obeso JA, et al., 2008). The basal ganglia receive projections from the cerebral cortex and send their output to the brain stem and, via the thalamus, back to the prefrontal, premotor and motor cortices (Graybiel AM, et al., 2003). A simplified diagram displaying the architecture of basal ganglia connections within the motor circuit is shown in Figure 1.

### 1.3.2 Striatum

The striatum is a functionally and anatomically highly heterogeneous structure. The internal capsule divides the striatum into the caudate nucleus and putamen. It receives excitatory, glutamatergic projections from the cerebral cortex, thalamus, and amygdala, as well as dopaminergic projections from the SNc within the nigrostriatal connection (Gerfen CR, et al., 1990). The existence of pendunculostriatal projections has been confirmed in primates and rats (Lavoie B & Parent A, 1994b; Nakano K, et al., 1990).

The majority of striatal neurons are GABAergic medium-sized spiny neurons (MSNs), which send their tonically inhibiting projections to the globus pallidus and substantia nigra. About half of these neurons express dopamine D1 receptors and inhibit the internal globus pallidus (GPi) and the SNr. Dopamine has an excitatory effect on the neurons with D1 receptors. The MSNs that project to the GPe express dopamine D2 receptors and decrease their inhibitory action in the

presence of dopamine (Gerfen CR, et al., 1990). The striatum also contains several different types of interneurons, which modulate the activity of projection neurons (Kawaguchi Y, et al., 1995).

### 1.3.3 Globus pallidus

The globus pallidus in primates consists of two parts: the external globus pallidus (GPe) and the internal globus pallidus (GPi), which are separated by a layer of myelinated fibers called the medial medullary lamina. In rodent terminology, we often find the entopeduncular nucleus (EP) or the medial globus pallidus in reference to the GPi, and GP or the lateral globus pallidus in reference to the GPe. Both nuclei consist of GABAergic neurons and their dendrites form disc-like structures situated perpendicularly to the striatal projections (Percheron G, et al., 1984). The GPe receives GABAergic projections from the striatal MSNs expressing dopamine D2 receptors, while the striatopallidal projections expressing D1 receptors reach to the GPi.

The GPe is in reciprocal connection with the STN which innervates it via excitatory glutamatergic projections (Shink E, et al., 1996). The centromedian nucleus (CM or Cm-Pf) of the thalamus also sends its glutamatergic projections to the GPe (Sadikot AF & Rymar VV, 2009). The inhibitory GABAergic neurons of the GPe project to the striatum, the STN, the GPi, and the SNr (Mallet N, et al., 2012; Jessell TM, et al., 1978).

Together, the GPi and the SNr play the role of output nuclei in the basal ganglia system and consist of inhibitory GABAergic neurons that fire tonically to inhibit their targets. The GPi receives inputs from the striatum, GPe, and STN. Its outputs reach the GPe, thalamus and the mesencephalon (DeLong MR, et al., 1985). The GPi is also reciprocally connected with the PPN (Martinez-Gonzalez C, et al., 2011).

### 1.3.4 Substantia nigra

The substantia nigra is located in the midbrain, dorsally to the cerebral peduncles. It consists of the pars reticulata and the pars compacta.

Dopaminergic cells of the pars compacta contain neuromelanin, a dark pigment derived from oxidized and polymerized dopamine, which accumulates in lysosomal granules of the cell bodies (Rabey JM & Hefti F, 1990). The majority of afferents to pars compacta are GABAergic neurons arising from the striatum, the GPe and GPi, as well as from the pars reticulata. The medial prefrontal cortex, STN and the PPN deliver an excitatory glutamatergic input to the SNc. The dopaminergic neurons of the pars compacta send their projections to the SNr, GPe, GPi, STN and striatum via the nigrostriatal pathway. (Tepper JM & Lee CR, 2007; Guatteo E, et al., 2009).

The neurons of the SNr are mainly GABAergic. Together with the GPi, the SNr acts as the output of the basal ganglia, from where the information travels to the thalamus. The SNr also sends its inhibitory projections to the dopaminergic cells of the SNc, the PPN, and the superior colliculus (Parent A & Hazrati LN, 1995a). The activity of the SNr is influenced by the inhibitory afferents from the striatum (Parent A & Hazrati LN, 1995b), the GPe (Smith Y & Bolam JP, 1989), and the nucleus accumbens (Deniau JM, et al., 1994), in addition to the excitatory glutamatergic projections from the STN (Kita H & Kitai ST, 1987).

### 1.3.5 Subthalamic nucleus

The STN plays a critical role in movement control and its lesion or pharmacological inhibition induce hemiballism (Crossman AR, 1987). It is currently the most common target of DBS in Parkinson's disease to reduce tremor and bradykinesia (Limousin P, et al., 1998).

The STN receives inhibitory GABAergic projections from the GPe (Parent A & Hazrati LN, 1995b), glutamatergic excitatory input from the motor cortex, primary

somatosensory cortex (Canteras NS, et al., 1988), and the thalamus (Canteras NS, et al., 1990), as well as cholinergic input from the PPN (Lavoie B & Parent A, 1994b). The SNc modulates the activity of the STN neurons via dopaminergic inputs (Hassani OK, et al., 1997; Cragg SJ, et al., 2004). The loss of dopaminergic neurons of the SNc appears to be responsible for the abnormal activity of STN neurons in Parkinson's disease (Bernheimer H, et al., 1973).

The excitatory glutamatergic projections of the STN reach to the GPi and GPe (Nambu A, et al., 2000) as well as to the SNc regulating dopamine release (Hammond C, et al., 1983; Smith Y & Parent A, 1988). Inhibitory STN projections influence the basal ganglia output nuclei, GPi and the SNr, in the indirect pathway (Perkins MN & Stone TW, 1980; Mintz I, et al., 1986).

### 1.3.6 Pedunculopontine nucleus

The PPN is a small, morphologically and neurochemically heterogeneous nucleus, located in the upper brainstem and involved in movement initiation, movement execution, sleep, and arousal (Aravamuthan BR, et al., 2008; Tsang EW, et al., 2010). Compared to other basal ganglia, the electrophysiology of the PPN, its function in the basal ganglia system, and its role in the pathophysiology of Parkinson's disease are less understood. The PPN has only recently become the subject of interest as a possible target for DBS.

Because of its irregular shape and the lack of a clear anatomical landmark, the precise boundaries of the PPN are difficult to determine. In rats, the PPN extends rostrally to the SNr, borders the laterodorsal tegmental nucleus (LDTg) caudally and the brachium conjunctivum dorsally (Garcia-Rill E, 1991).

Based on the density of cholinergic neurons, the PPN was originally divided into the pars dissipata (rostral) and pars compacta (caudal) (Olszewski J & Baxter D, 1982). The pars disspata consists mostly of GABAergic neurons and interconnects with the basal ganglia, whereas the pars compacta consists dominantly of cholinergic and glutamatergic neurons (Rye DB, et al., 1987;

Mesulam MM, et al., 1989; Lavoie B & Parent A, 1994a; Wang HL & Morales M, 2009).

The PPN receives a diverse modulation from functionally heterogeneous areas of the brain, including afferents from the cortex, thalamus, hypothalamus, pons, cerebellum, medulla, basal ganglia, as well as the sensory inputs from the spinal cord (Saper CB & Loewy AD, 1982; Semba K & Fibiger HC, 1992; Hazrati LN & Parent A, 1992). A direct excitatory input to the PPN from the STN via glutamatergic projections has been established in rats (Kita H & Kitai ST, 1987; Granata AR & Kitai ST, 1989), cats, and primates (Nauta HJ & Cole M, 1978). The afferents from the GPi and the SNr are GABAergic (Granata AR & Kitai ST, 1991; Moriizumi T & Hattori T, 1992; Shink E, et al., 1997).

The PPN itself has rich efferents projecting to the basal ganglia, thalamus, and cortex (Muthusamy KA, et al., 2007). It reaches the STN via its cholinergic, GABAergic, and glutamatergic projections (Bevan MD & Bolam JP, 1995). The projections to the GPe and GPi are also cholinergic and richer in the GPi (Charara A & Parent A, 1994). The SNc dopaminergic neurons receive direct glutamatergic and cholinergic input from the PPN (Futami T, et al., 1995; Takakusaki K, et al., 1996). Cholinergic afferents from the PPN were also found in the SNr (Woolf NJ & Butcher LL, 1986; Scarnati E, et al., 1987). The input from the PPN to the thalamus is both cholinergic and non-cholinergic (Steriade M, et al., 1988). PPN projections to the striatum have been identified in rodents (Saper CB & Loewy AD, 1982). Other ascending targets of the PPN include the lower brainstem, pons, medulla, and spinal cord (Rye DB, et al., 1988).

### 1.3.7 The role of basal ganglia in motor control

The basal ganglia participate in five functional circuits: the motor circuit, the oculomotor circuit involved in eye movement control (Hikosaka O, et al., 2000), the dorsolateral prefrontal circuit responsible for cognitive tasks, the lateral orbitofrontal circuit, which plays a major role in mediating empathetic and socially

appropriate responses, and the limbic circuit, which is focused on motivated behavior (Graybiel AM, et al., 2003).

The motor circuit is understood the best and underlies the pathophysiology of movement disorders. Movement is initiated in the cortex, and the information is then passed to the basal ganglia, which return the processed information back to the cortex. Precise movement facilitation or inhibition requires adequate neuronal excitability within each nucleus and their undisturbed functioning as a network (Obeso JA, et al., 2008). A simplified diagram of the motor circuit involving the direct and indirect pathway is shown in Figure 1.

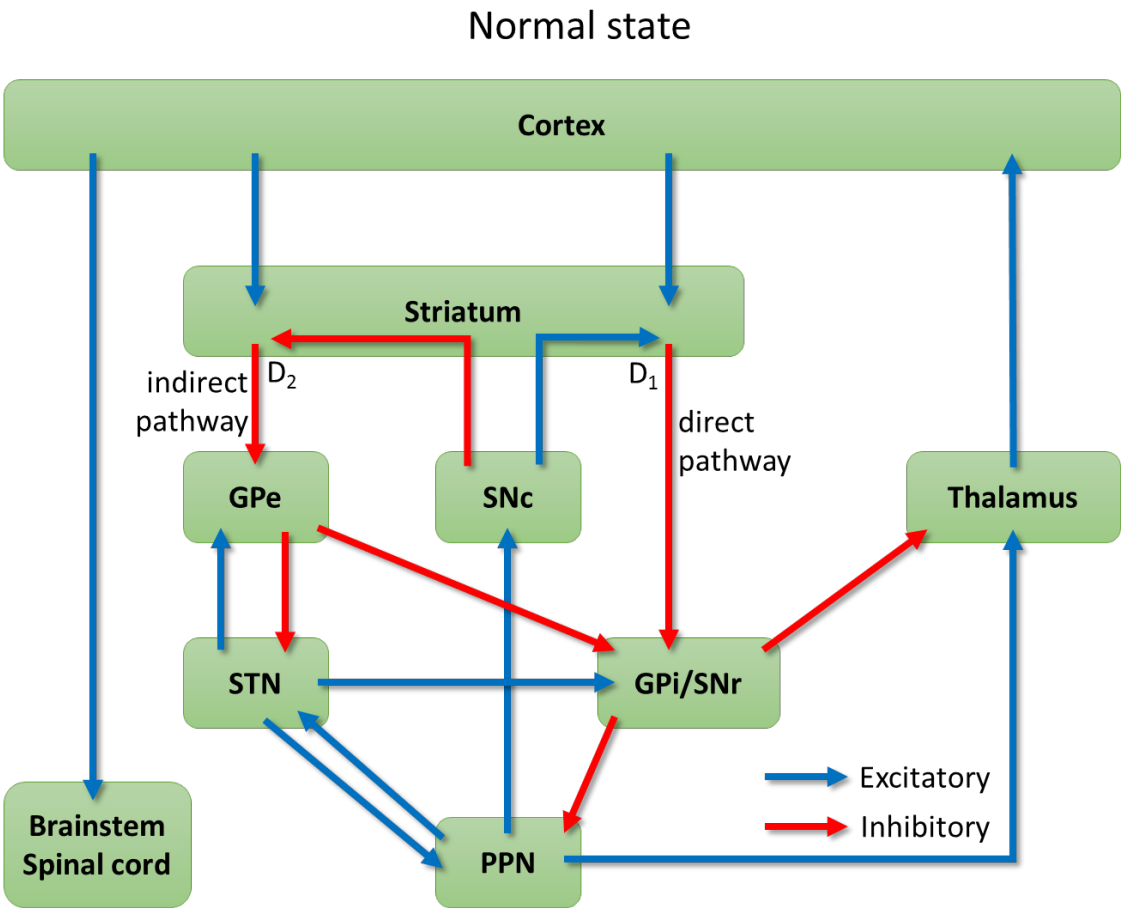


**Figure 1: Simplified diagram of the motor circuit, modified from "Functional architecture of basal ganglia circuits: neural substrates of parallel processing" by Alexander GE and Crutcher MD, Trends Neurosci. 1990, Fig. 2.**

**Inhibitory projections are shown as red arrows, excitatory projections as blue arrows. Abbreviations: D1, dopamine receptor D1; D2, dopamine receptor D2; GPe, external globus pallidus; GPi, internal globus pallidus; PPN, pedunculopontine nucleus; SNc, substantia nigra pars compacta; SNr, substantia nigra pars reticulata; STN, subthalamic nucleus.**

The input from outside the basal ganglia enters the striatum and the STN, the output nuclei are the SNr and the GPi. The striatum acts as an entry point to the basal ganglia in both the direct and indirect pathways. It receives excitatory glutamatergic input from the primary motor cortex and sends projections to the output nuclei. The GPi and the SNr tonically inhibit their target nuclei in the thalamus. Their inhibitory GABAergic output is modulated by the striatal projections via the direct and indirect pathways. In the direct pathway the striatum projects to the SNr and GPi, which in turn send inhibitory projections straight to the thalamus. The indirect pathway passes from the striatum to the GPe. The GPe sends its inhibitory GABAergic projections to the STN, from where the pathway passes to the SNr and GPi via excitatory glutamatergic projections. The output nuclei project, as in the direct pathway, to the thalamus. The thalamus excites the upper motor neurons, which facilitates the movement. Both pathways are affected by dopaminergic projections from the SNc to the striatum. In the presence of dopamine, the striatal projections in the direct pathway carrying D1 dopamine receptors increase their inhibitory influence on the SNr and GPi, whereas the striatal projections expressing D2 receptors decrease their GABAergic inhibition onto the GPe in the indirect pathway. In this way, the dopamine release results in a reduction of the inhibitory GPe influence onto the STN in the indirect pathway with a consequent increase in glutamatergic excitatory STN influence onto the output basal ganglia, which intensify their inhibition of the thalamus. The cortex stimulation via the thalamus is decreased resulting in movement inhibition. In the direct pathway, on the contrary, dopamine release increases the striatal inhibitory activity onto the SNr and GPi, which leads to a decrease in their tonic inhibition of the thalamus. The activation of the indirect pathway promotes movement inhibition. The indirect pathway is dominant in the normal state. When the movement initiation takes place, dopamine release into the striatum shifts the balance towards the direct circuit and facilitates the movement (Alexander GM & Crutcher MD, 1990).

The hyperdirect pathway has been proposed as a critical mechanism in suppressing erroneous movement (Bosch C, et al., 2012). The hyperdirect pathway bypasses the striatum, as the input from the motor cortex is transmitted

directly to the STN via fast myelinated axons. The STN sends excitatory projections to the GPi, which inhibits the thalamus. The inhibition of the thalamus in the hyperdirect pathway exceeds the inhibition resulting from the tonic discharge of the GPi, contributing to a stronger depression of the somatomotor activity. The hyperdirect pathway is faster than both the direct and indirect pathways, in which the output from the motor cortex reaches the striatum via unmyelinated axons (Mason P, 2017; Nambu A, et al., 2002).

### 1.3.8 Basal ganglia pathophysiology in Parkinson's disease

Degeneration of dopaminergic cells in the SNc causes a reduction of dopamine concentration at a striatal level resulting in the disorganization of basal ganglia activity (Bernheimer H, et al., 1973). The generally accepted firing rate model of the functional organization of basal ganglia is shown in Figure 2 below. This model predicts that dopamine depletion leads to the loss of GABAergic striatal input and increased STN excitatory input resulting in enhanced tonic inhibitory influence of the basal ganglia output nuclei, SNr and GPi, on the motor thalamic nuclei. The inhibition of the thalamus leads to the deactivation of motor cortical areas. Simultaneously, there is an excessive inhibition of the GPe in the indirect pathway (Alexander GM & Crutcher MD, 1990; Elder CM & Vitek JL, 2001).

In Parkinson's disease, alterations to the STN, GPi, and GPe activity are mainly concordant with the predictions of the firing rate model (Miller WC & DeLong MR, 1987; Pan HS & Walters JR, 1988; Filion M & Tremblay L, 1991; Hassani OK, et al., 1996; Vila M, et al., 1997; 2000; Elder CM & Vitek JL, 2001; Soares J, et al., 2004), whereas the changes in SNr activity are generally inconsistent (Sanderson P, et al., 1986; Murer MG, et al., 1997; Rohlfs A, et al., 1997).

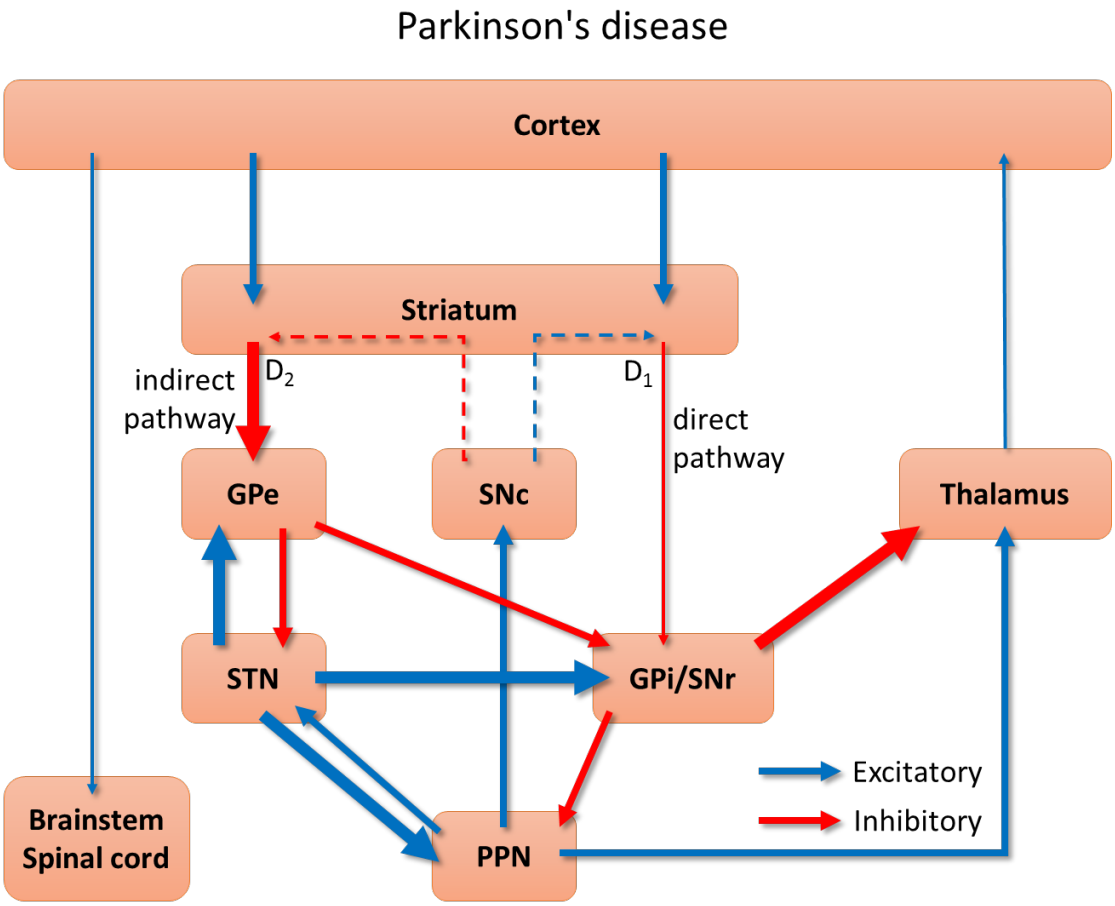


**Figure 2: Simplified diagram of basal ganglia dysfunction in Parkinson's disease, modified from "The functional anatomy of basal ganglia disorders" by Albin et al., Trends Neurosci. 1989, Fig.2 D.**

**Inhibitory projections are shown as red arrows, excitatory projections as blue arrows. Thicker arrows represent a functional increase, while thinner arrows represent a functional decrease in activity. Degeneration of the SNc dopaminergic cells resulting in dopamine depletion and ensuing changes in the activity of striatal projection neurons is shown as interrupted arrows. The parkinsonism-related changes for anatomical connections that are not a part of the standard rate model (e.g., corticostriatal and PPN projections) are not shown. Abbreviations: D1, dopamine receptor D1; D2, dopamine receptor D2; GPe, external globus pallidus; GPi, internal globus pallidus; PPN, pedunculopontine nucleus; SNc, substantia nigra pars compacta; SNr, substantia nigra pars reticulata; STN, subthalamic nucleus.**

Data regarding the activity of PPN in the parkinsonian state is limited. Studies in the 6-OHDA rat model reported overactivity of PPN with an increase of bursting firing (Breit S, et al., 2001; Jeon MF, et al., 2003).

## 1.4 Deep brain stimulation

### 1.4.1 DBS in Parkinson's disease

The origins of the brain stimulation reach back to 1878 when Dr. Robert Bartholow performed and documented the first electrical stimulation of an exposed cortex on a patient admitted to the Samaritan Hospital in Cincinnati (Morgan JP, 1982). In the 1950s, ablative surgeries such as pallidotomy and thalamotomy were developed empirically to treat Parkinson's disease and tremor (Hassler R, et al., 1960). With the progress of stereotactic surgery, the intraoperative brain stimulation was used in exploring a brain target before lesioning in the treatment of psychiatric diseases (Gildenberg PL, 2005; Hariz MI, et al., 2010). In the 1960s, Carl Wilhelm Sem-Jacobsen, a Norwegian psychiatrist and neurophysiologist, used externalized depth electrodes implanted over several months for intermittent stimulation and evaluation prior to ablation (Sem-Jacobsen CW, 1966). The first application of "therapeutic" deep brain electrostimulation, however, must be accredited to Natalia Petrovna Bechtereva, a neurophysiologist and neuroscientist at the Institute of Experimental Medicine and the Academy of Medical Sciences of the USSR in Leningrad, who also around this time treated approximately 120 patients with Parkinson's disease with external DBS of the ventrolateral thalamus and the centrum medianum in intermittent courses of stimulation for up to 1.5 years. Eventually, microlesions were performed via electrodes providing the best responses to stimulation (Blomstedt P & Hariz MI, 2010).

With the introduction of levodopa in the mid-1960s, the popularity of ablative surgeries decreased. However, the significant side effects of dopaminergic drugs and the limitations of chronic levodopa therapy observed in the following years led to a renaissance of surgical approaches in the early 1990s (DeLong M & Wichmann T, 2012). A crucial role in the shaping of modern DBS was played by a team of neurosurgeons and neurologists from Grenoble University - Benabid, Pollak and their colleagues. The Grenoble group was the first to provide a detailed study on thalamic high-frequency brain stimulation in the treatment of

Parkinson's disease (Benabid AL, et al., 1987; Benabid AL, et al., 1991), and in 1993 a bilateral subthalamic stimulation was performed proving its efficacy and safety (Pollak P, et al., 1993).

Subsequently, high-frequency DBS replaced the pallidotomy and the thalamotomy and is nowadays probably the most rapidly expanding field in neurosurgery. It can safely be performed bilaterally and does not exclude patients from benefiting from other surgical therapies in the future. Not only is the postoperative recovery time shorter and the numbers of complications lower, but it is also a reversible and dynamic treatment because the stimulation parameters can be changed at any time to minimize side effects and improve efficacy (Breit S, et al., 2004).

HFS of the STN, which is the most common target of DBS in Parkinson's disease, alleviates tremor within seconds (Blahak C, et al., 2009), rigidity and bradykinesia within minutes to hours (Temperli P, et al., 2003), whereas the relief of axial symptoms occurs after hours to days (Fasano A, et al., 2015). After termination of STN stimulation, symptoms return in the same time order (Temperli P, et al., 2003).

### 1.4.2 DBS in other neurological and psychiatric disorders

DBS has proven its efficacy in the treatment of Parkinson's disease, can be applied as an experimental treatment in severe Tourette syndrome (Viswanathan A, et al., 2012), and is also considered to be a valid option for intractable epilepsy (Baldermann JC, et al., 2016) or essential tremor (Zhang K, et al., 2010). The use of DBS is being explored for several neuropsychiatric disorders including obsessive-compulsive disorder, eating disorders, treatment-resistant depression (DeLong M & Wichmann T, 2012; Wang D, et al., 2018) and addiction (Pelloux Y & Baunez C, 2013; Bari A, et al., 2018).

### 1.4.3 The current state of knowledge of STN stimulation

High-frequency STN stimulation leads to motor improvement in patients (Benazzouz A, et al., 1993; Limousin P, et al., 1995; Limousin P, et al., 1998) and animal models of Parkinson's disease (Benazzouz A, et al., 1996) inducing a normalization of both reaction and movement times as well as activity of agonist/antagonist muscles (Benazzouz A, et al., 1993). Similar beneficial motor effects have been achieved by a lesion (Bergman H, et al., 1990; Aziz TZ, et al., 1991) or pharmacological inactivation of the STN (Levy R, et al., 2001). These observations imply that STN-HFS should act by silencing STN neurons, which are overactive in Parkinson's disease, and by subsequently reducing their excitatory influence on the output basal ganglia nuclei (Rodriguez-Oroz MC, et al., 2001). However, despite the successful application of the DBS, various electrophysiological studies failed to deliver a uniform explanation of its mechanism, and contradictory effects on the neuronal activity of the basal ganglia have been reported.

Electrical stimulation produces large artifact waveforms whenever neural recordings are performed during stimulation. These artifacts can occlude neuronal spike forms. The template subtraction method, employed by most of the artifact removal techniques, could potentially generate residual artifact due to variability in the stimulation onset time or the variation in artifact waveforms (Harding GW, 1991; Wichmann T, 2000; O'Keeffe DT, et al., 2001; Hashimoto T, et al., 2002; Heffer LF & Fallon JB, 2008; Ryu SB, et al., 2013).

*In vitro* studies in rats suggest that HFS might drive STN neurons into completely or partially following the stimulation train, silence the STN neurons during the stimulation or exceeding the stimulation period by up to several minutes with subsequent reassuming the pacemaking firing (Magariños-Ascone C, et al., 2002; Beurrier C, et al., 2001; Do MT & Bean BP, 2003). Garcia and colleagues observed that stimulation within a range of 80 - 185 Hz suppressed spontaneous firing in STN neurons and induced stimulus-driven firing time-locked to the stimulus pulse (Garcia L, et al., 2003). The stimulus-driven firing was influenced

neither by the blockade of ionotropic or metabotropic glutamate receptors nor by blockade of GABA receptors. There was no difference between the slices from intact and dopamine-depleted rats. A subsequent study (Garcia L, et al., 2005) of STN neurons recorded in whole-cell patch-clamp configuration in rat brain slices showed that within empirically applied therapeutic parameters of STN-HFS in Parkinson's disease, (130 - 185 Hz, pulses of short duration, 60 - 100 μs, 1 - 3 mA amplitude) STN neurons fired regularly and time-locked to the stimuli. This observation supports the hypothesis that, at clinically relevant parameters, HFS overrides the spontaneous activity of STN neurons turning them into stable oscillators entirely driven by the stimulation.

*In vivo* studies in primates reported a decrease in the firing rate or a complete inhibition of STN neurons during stimulation (Moran A, et al., 2011). Recordings in parkinsonian patients showed a decrease in the firing rate accompanied by an increase of the burst-like activity of STN neurons (Galati S, et al., 2006).

Computational analysis studies suggest that the DBS may affect various neuronal elements differently. Not only the somas of the neurons surrounding the electrode may be directly excited or inhibited but also the afferent inputs and fibers passing close to the electrode may be activated by the electric field. The threshold for excitability of axons is lower than that for somata, and myelinated fibers are more easily excitable than unmyelinated ones (Ranck JB Jr, 1975; Moffitt MA, et al., 2004). Moreover, the generated action potentials will propagate in an orthodromic and antidromic direction (McIntyre CC, et al., 2004a; McIntyre CC, et al., 2004b; Miocinovic S, et al., 2006)

The effect that DBS evokes in the relevant efferent nuclei seems more important in the understanding of its mechanism of action than the effect on the cell bodies of the stimulation target.

Numerous results of various *in vivo* and *in vitro* studies laid the foundation for the following hypotheses explaining the phenomena of DBS (Breit S, et al., 2004):

- inactivation of voltage dependent ion channels resulting in a depolarization block in neuronal transmission (Benazzouz A, et al., 1995; 1996; Beurrier C, et al., 2001)

- information jamming by overriding with a stimulation-driven high-frequency pattern (Garcia L, et al., 2003; Hashimoto T, et al., 2003)

- synaptic inhibition by stimulation of inhibitory afferents to the target nuclei (Dostrovsky JO, et al., 2000)

- synaptic depression resulting from stimulation-induced neurotransmitter depletion (Urbano FJ, et al., 2002; Xia R, et al., 2004)

## 1.5 Aim of the study

The complexity of neuronal response to extracellular electrical stimulation and the limitations in experimental techniques hinder our understanding of a precise DBS mechanism. The data collected from previous animal studies are often contradictory, which indicates that the therapeutic effects of DBS may not be explained by simple inhibition or excitation of the STN outputs. This study focuses on characterizing the influence of stimulation of the STN on the basal ganglia nuclei.

We set out to investigate the effects STN stimulation has on the electrophysiological activity of the GPe, the SNr, and the PPN in rats under urethane anesthesia in the context of:

- assessing the modulation of basal ganglia activity by HFS of the STN

- characterizing the neuronal responses to STN stimulation of the basal ganglia nuclei in terms of firing rate and firing pattern
- simultaneous in-vivo recordings in up to three basal ganglia nuclei prior/after STN stimulation

# 2 Materials and Methods

## 2.1 Animals and housing conditions

40 adult Wistar rats (Charles River Laboratories, Sulzfeld, Germany), weighing 245 – 566 g, were used for this study.

The rats were housed under artificial lighting (12 h / 12 h light - dark cycle), temperature (22 °C) and humidity (50 - 60 %) conditions, receiving a standard diet (Kliba Nafag, Provimi Kliba AG, Kaiseraugst, Switzerland) and water available ad libitum. They were kept in isolated, ventilated cage-systems (IVC: 48.0 cm x 37.5 cm x 21.0 cm, Indulab AG, Gams, Switzerland) in groups of 2 - 5 animals per cage.

## 2.2 Ethics

All experiments were carried out in accordance with the German Animal Welfare Act ("Tierschutzgesetz"). The study was approved by the Ethics Committee of the Eberhard Karls University of Tübingen.

## 2.3 Equipment & Software

The setup of the experiment is shown in Figure 3. The rat was mounted in a stereotaxic frame (Stoelting, Wood-Dale, IL, USA, motorized version for StereoDrive, Neurostar, Sindelfingen, Germany) with three motors operating in the x, y and z-axis. All four electrodes were placed in stabilizing metal tubes (custom-made from lumbar puncture needles by Feinmechanik-Labor, Augenklinik Universität Tübingen) between two matrices (Feinmechanik-Labor, Augenklinik Universität Tübingen) and attached to a 4-channel motorized miniature micromanipulator module "i4" ("Independent 4", Neurostar, Sindelfingen, Germany).

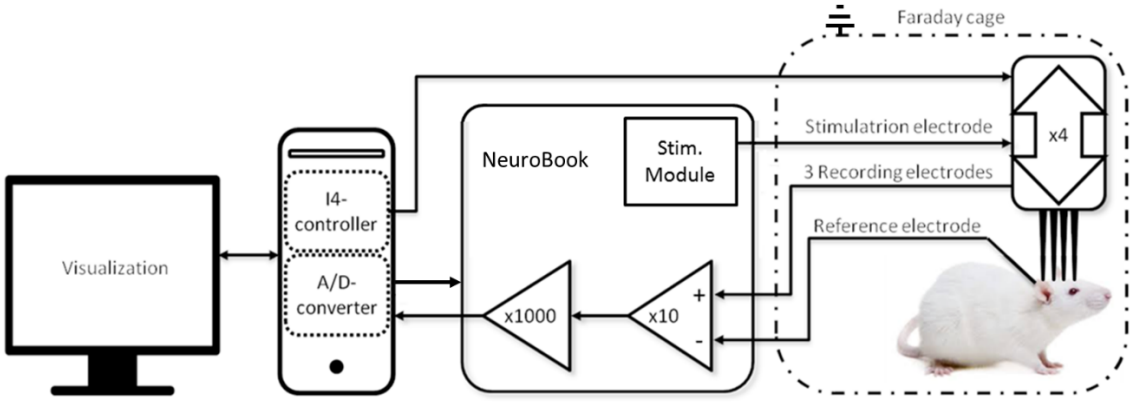


**Figure 3: Schematic setup of the experiment. NeuroBook consists of a preamplifier, amplifier, band-pass filter, stimulus generator, an impedance measurement module, and a recording module. The i4-controller manipulates the 4-channel motorized miniature micromanipulator module.**

The i4 moving module consists of four individual motors, each with an electrode attached to it. This allows the electrodes to be navigated individually into their target brain structures. With 10 x 10 holes each 0.75 mm apart the two guiding matrices allow placing the electrodes within an 6.75 mm x 6.75 mm area of the brain so that the desired coordinates are covered (Figure 4).

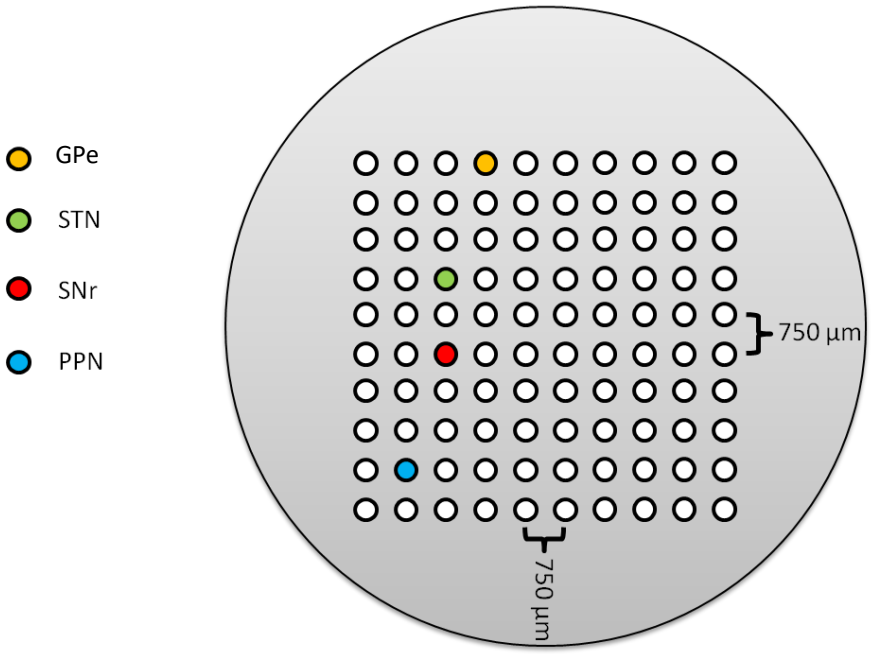


**Figure 4: Electrode placement in the matrix. External globus pallidus (GPe), subthalamic nucleus (STN), substantia nigra pars reticulata (SNr), pedunculopontine nucleus (PPN).**

Tungsten-Microelectrodes (FHC Inc. Bowdoinham, Maine, USA) shown in with epoxy insulation, long thinned profile with a rounded medium taper angle and standard shank (diameter 200 µm) were used.

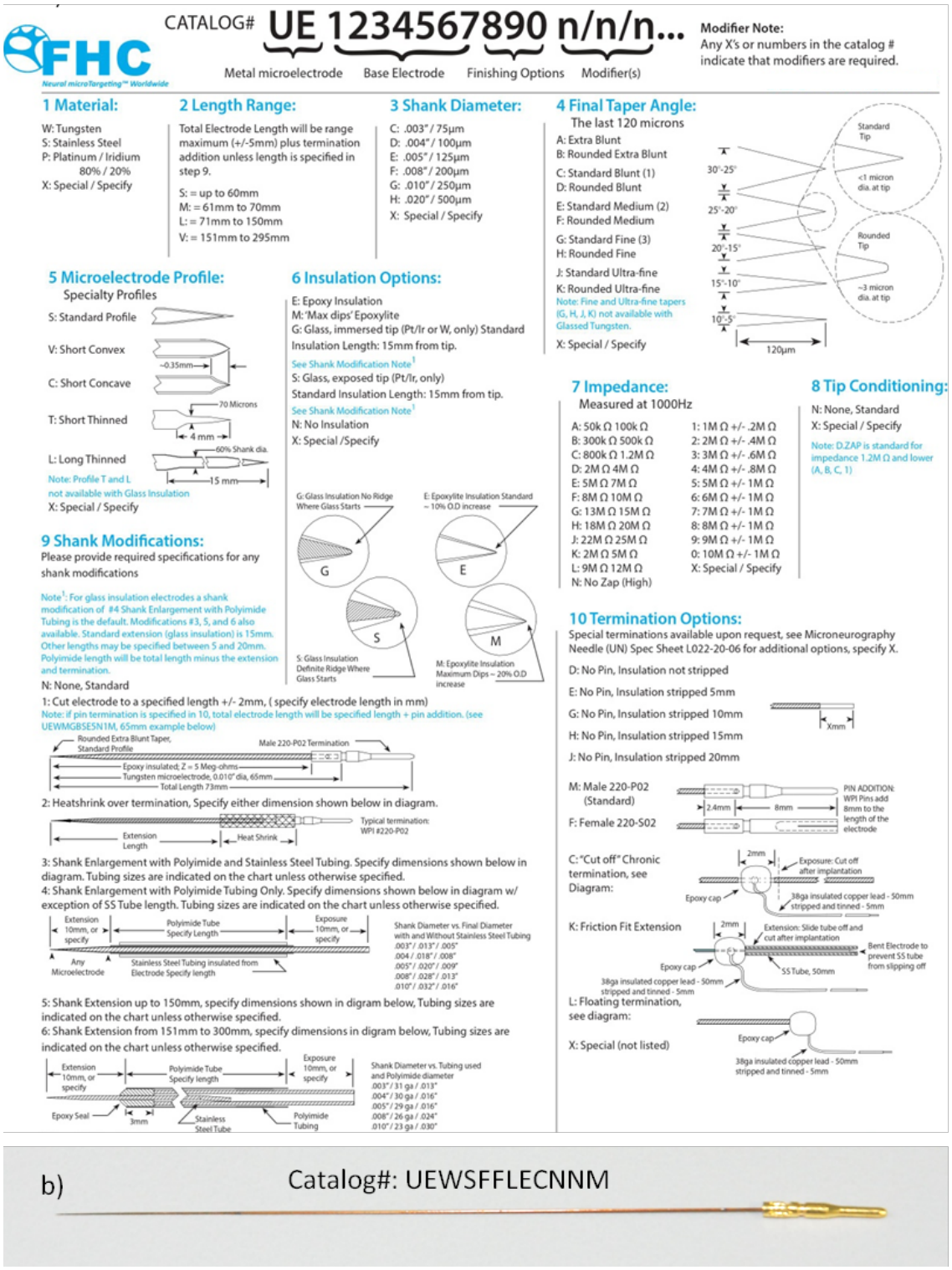


**Figure 5: Electrodes a) Specification of the Tungsten-Microelectrodes, FHC Inc. Bowdoinham Maine, USA b) Picture of the electrode**

The electrodes were 60 mm long, with a standard male termination and their impedance was between 800 kΩ and 1.2 MΩ. The specifications of the electrodes are shown in Figure 5.

The animal, i4 micromanipulator module, guiding matrices and electrodes were all placed in a Faraday cage (Feinmechanik-Labor, Augenklinik Universität Tübingen) minimizing external electromagnetic fields (Figure 6).

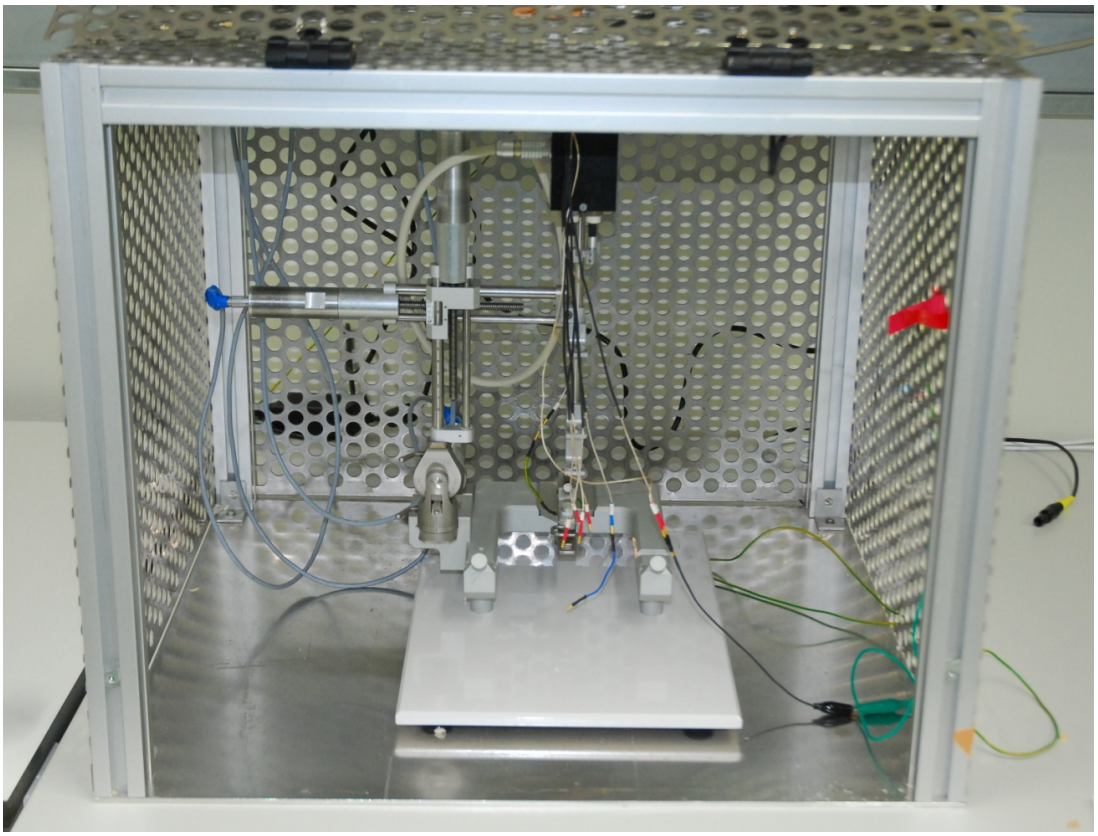

**Figure 6: Faraday cage with stereotactic frame and i4 positioner**

The electrodes were connected to a modified NeuroBook stimulation/recording module which incorporates a preamplifier, an amplifier, a filter, a stimulus generator, an impedance measurement module, and a recording module. The motorized arm of the stereotactic frame can be navigated in all three axes and is controlled by the computer software StereoDrive (Neurostar, Tübingen, Germany). The precise descending movement of every single electrode in the brain was conducted using the software NeuroGuide (Version 1.0.337 Neurostar, Tübingen, Germany). NeuroGuide enables real-time control and visualization of

electrode motion thanks to the integrated rat brain atlas. NeuroGuide also visualizes the signals recorded by NeuroBook in real–time and saves the data to the hard drive. The extracellular field potential picked up by the electrode was preamplified 10-fold and further amplified 1000-fold. Frequencies not falling within the 300 Hz - 5000 Hz range were rejected by a band-pass filter. The signal was subsequently digitized by an A/D converter

## 2.4 Anesthesia and surgery

Animals were weighed and the dose of anesthesia was calculated. 1.2 mg/g of 18 % urethane (Urethane, Sigma-Aldrich Chemie GmbH Munich, Germany) was injected intraperitoneally. The needle was introduced at a 30-degree angle, slightly to the right of midline, one third to halfway between the hind legs and the bottom of the ribcage. The onset of the anesthesia was checked by testing the pedal reflex. No reaction to the pinching of the web between the toes of the extended limb indicated that the anesthesia was sufficiently deep. Before being restrained in the stereotactic frame, the rat was given a dose of analgesia: 5 µg/kg Fentanyl intraperitoneally (Fentanyl®-Janssen, Janssen-Cilag GmbH, Neuss, Germany).

Solution preparation:

18 % Urethane (180 mg/ml): 18 g in 100 ml 0.9 % NaCl

Fentanyl (0.5 µg/ml): 1 ml Fentanyl (50 µg/ml) in 99 ml 0.9 % NaCl

An eye gel was applied to moisten and lubricate the eyes (Oculotect® mono A Augengel, Novartis Pharma GmbH, Nürnberg, Germany, 0.56 mg/g Retinol Palmitate). Furthermore, 10 % Lidocaine spray (Xylocain® Pumpspray Dental, AstraZeneca) was applied into the auditory canal to prevent pain while the animal was fixed to the stereotactic frame.

The extremities and the trunk were covered with a cotton pad coat in order to keep the body temperature stable. The body temperature was continuously

measured with a rectal probe and kept at 36.0 C to 37.5 C. Finally, a 15 mm incision was made in the scalp along the anterior-posterior line and the periosteum was removed mechanically with a scalpel. The margins of the area covering the targeted nuclei were outlined on the skull surface and using a cranial drill a 3.5 mm x 9.5 mm opening was drilled into the bone starting 1 mm rostrally and 1.5 mm laterally to the bregma reference point (Figure 7), exposing the underlying dura mater. The dura mater was carefully removed with a syringe needle operating under a microscope (Carl Zeiss Meditec AG, Jena, Germany). In order to remove excessive tissue, the brain surface was rinsed with 0.9 % NaCl and swabbed with a cotton swab.

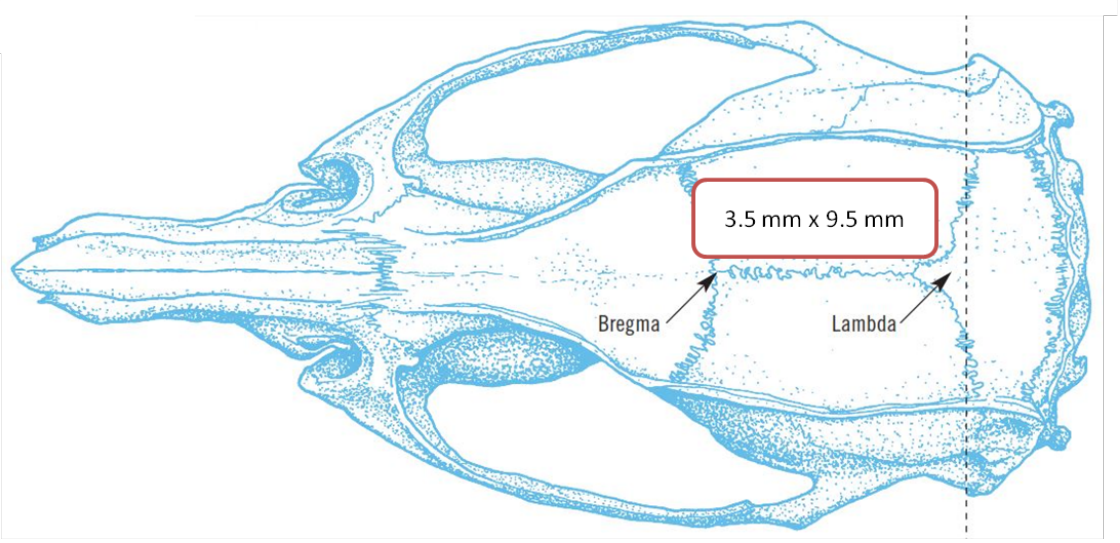


**Figure 7: Skull of an adult Wistar rat with outlined operative field (Illustration from the Rat Brain Atlas of Paxinos and Watson, 2005).**

## 2.5 Electrode positioning

The stereotaxic coordinates targeting the GPe, STN, SNr and PPN were established according to the Rat Brain Atlas (Paxinos and Watson, 2005). All recordings were performed in three trajectories, always in the right hemisphere. The coordinates for trajectories 1 to 3 used for rats weighing between 250 g and 350 g are shown below (Figure 8 through Figure 11). Coordinates for rats weighing over 350 g were adjusted applying linear interpolation in reference to the distance between lambda and bregma in mature Wistar rats (mean weight

436 g) from the Rat Brain Atlas of Paxinos and Watson, if this distance varied from the expected distance of 9 mm.

**Figure 8: STN trajectories**

**a) Table of trajectories 1-3 targeting the STN established using the Rat Brain Atlas (Paxinos and Watson 2005). Dorsally from bregma (x), laterally from bregma (y), starting depth (z) and end position (z')**

**Localization of the STN in coronal brain sections matching:**
**b) trajectory 1 (Bregma -3.48 mm, Paxinos and Watson, 2005)**
**c) trajectory 2 (Bregma -3.60 mm, Paxinos and Watson, 2005)**
**d) trajectory 3 (Bregma -3.36 mm, Paxinos and Watson, 2005)**

a)

| Trajectory | x[mm] | y[mm] | z[mm] | z'[mm] |
|---|---|---|---|---|
| 1 | -3.50 | 2.45 | 8.00 | 8.40 |
| 2 | -3.60 | 2.75 | 7.80 | 8.20 |
| 3 | -3.30 | 2.80 | 7.70 | 8.20 |

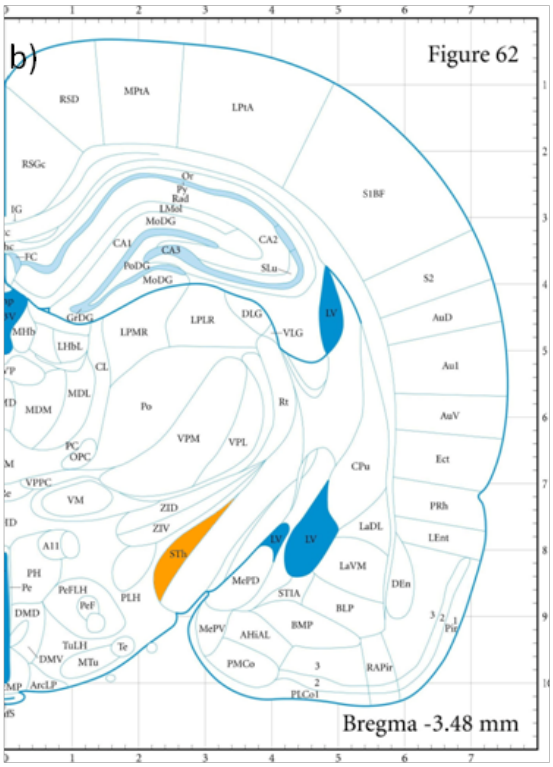


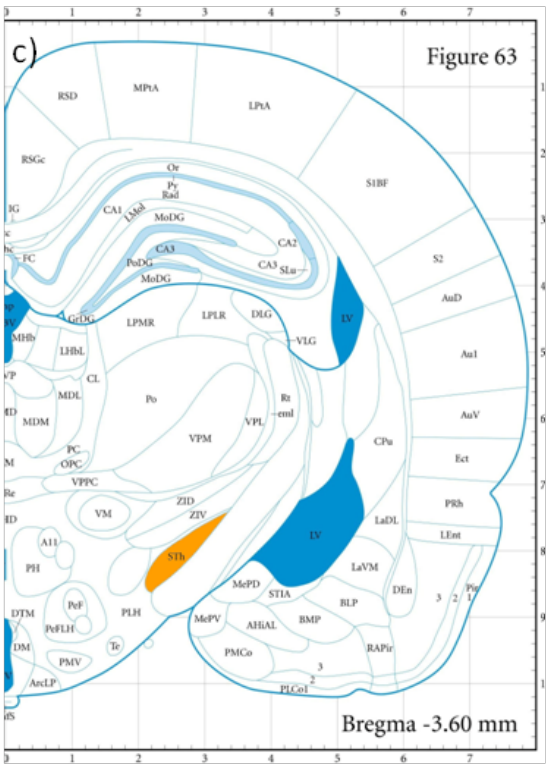


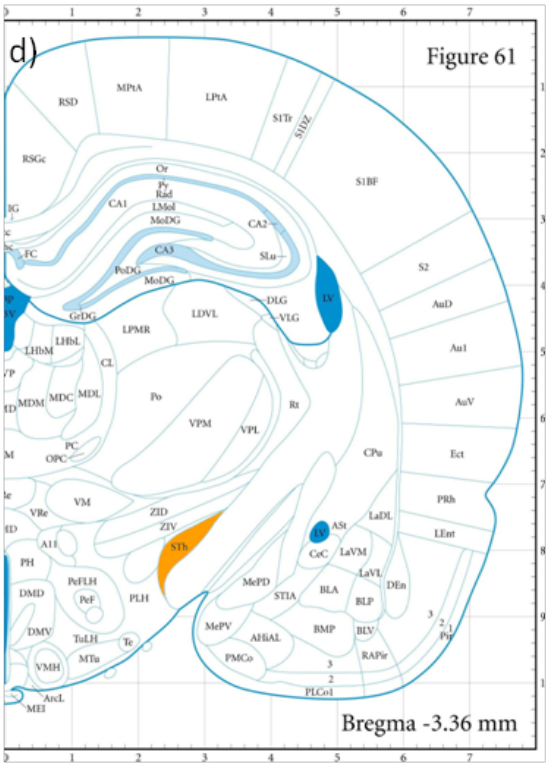

**Figure 9: GPe trajectories**

**a) Table of trajectories 1-3 targeting the GPe established using the Rat Brain Atlas (Paxinos and Watson 2005). Dorsally from bregma (x), laterally from bregma (y), starting depth (z) and end position (z')**

**Localization of the GPe in coronal brain sections matching:**
**b) trajectory 1 (Bregma -1.20 mm, Paxinos and Watson, 2005)**
**c) trajectory 2 (Bregma -1.32 mm, Paxinos and Watson, 2005)**
**d) trajectory 3 (Bregma -1.08 mm, Paxinos and Watson, 2005)**

a)

| Trajectory | x[mm] | y[mm] | z[mm] | z'[mm] |
|---|---|---|---|---|
| 1 | -1.25 | 3.20 | 5.40 | 7.50 |
| 2 | -1.35 | 3.50 | 5.60 | 7.80 |
| 3 | -1.05 | 3.55 | 5.60 | 7.60 |


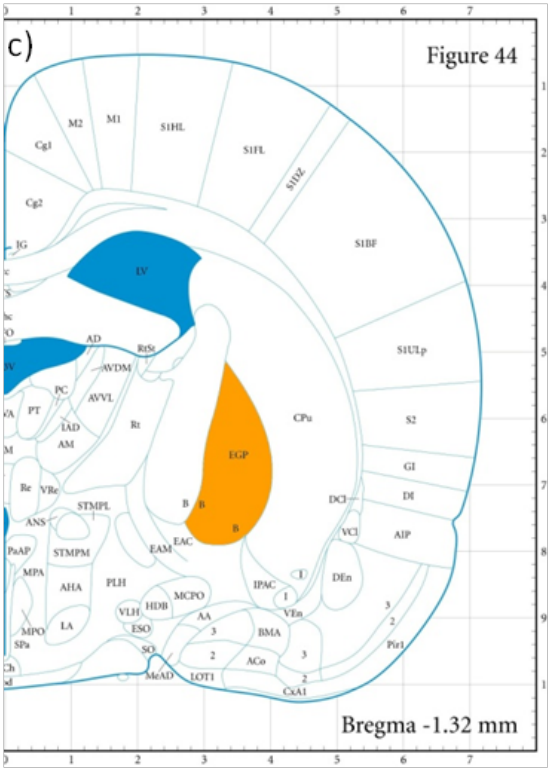


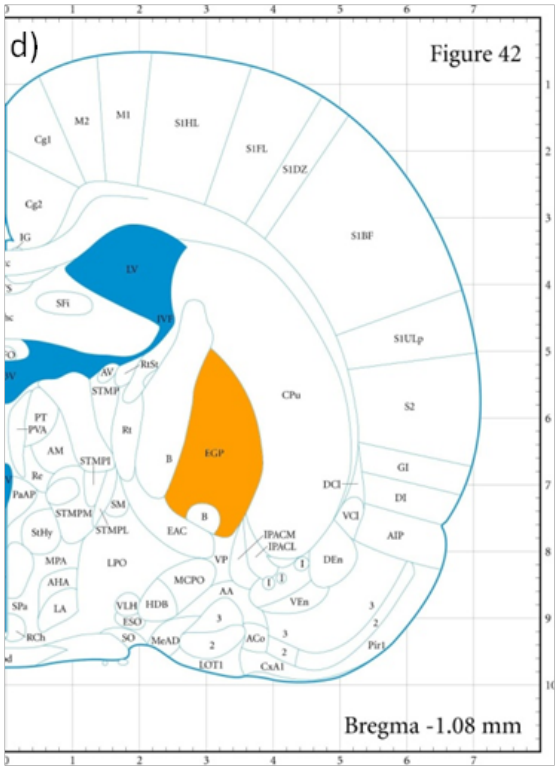

**Figure 10: SNr trajectories**

**a) Table of trajectories 1-3 targeting the SNr established using the Rat Brain Atlas (Paxinos and Watson 2005). Dorsally from bregma (x), laterally from bregma (y), starting depth (z) and end position (z')**

**Localization of the SNr in coronal brain sections matching:**
**b) trajectory 1 (Bregma -5.04 mm, Paxinos and Watson, 2005)**
**c) trajectory 2 (Bregma -5.16 mm, Paxinos and Watson, 2005)**
**d) trajectory 3 (Bregma -4.80 mm, Paxinos and Watson, 2005)**

a)

| Trajectory | x[mm] | y[mm] | z[mm] | z'[mm] |
|---|---|---|---|---|
| 1 | -5.00 | 2.45 | 8.00 | 8.80 |
| 2 | -5.10 | 2.75 | 7.50 | 8.00 |
| 3 | -4.80 | 2.80 | 7.60 | 8.40 |

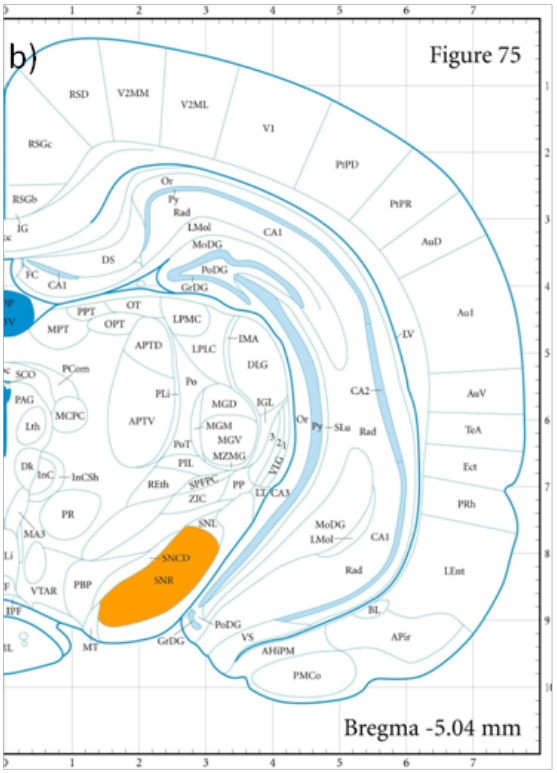


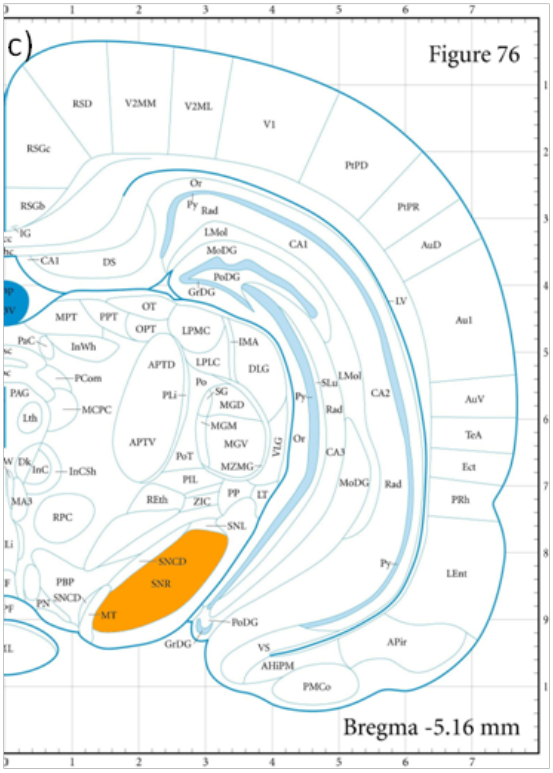


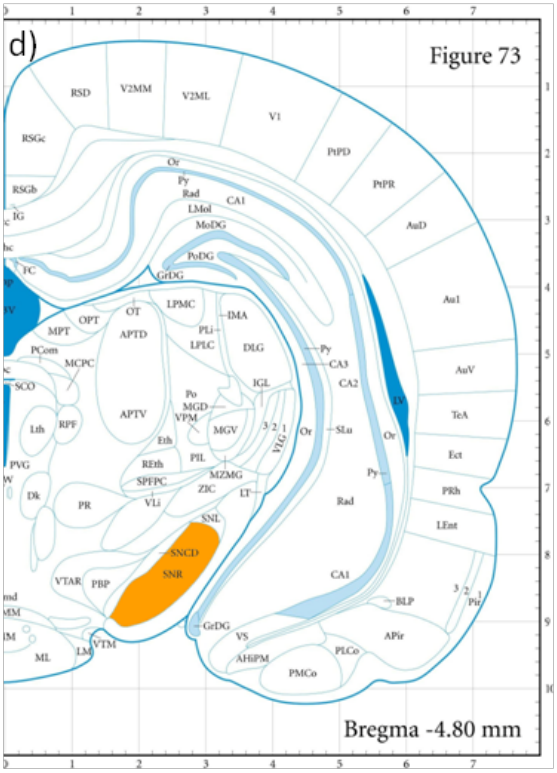

**Figure 11: PPN trajectories**

**a) Table of trajectories 1-3 targeting the PPN established using the Rat Brain Atlas (Paxinos and Watson 2005). Dorsally from bregma (x), laterally from bregma (y), starting depth (z) and end position (z')**

**Localization of the PPN in coronal brain sections matching:**
**b) trajectory 1 (Bregma -7.20 mm, Paxinos and Watson, 2005)**
**c) trajectory 2 (Bregma -7.32 mm, Paxinos and Watson, 2005)**
**d) trajectory 3 (Bregma -7.08 mm, Paxinos and Watson, 2005)**

a)

| Trajectory | x[mm] | y[mm] | z[mm] | z'[mm] |
|---|---|---|---|---|
| 1 | -7.25 | 1.70 | 7.60 | 8.00 |
| 2 | -7.35 | 2.00 | 7.50 | 8.00 |
| 3 | -7.05 | 2.05 | 7.70 | 8.10 |

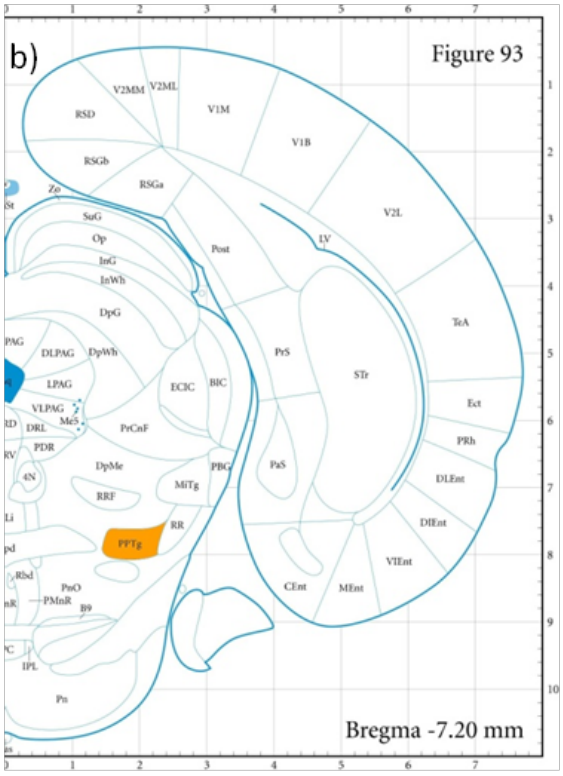


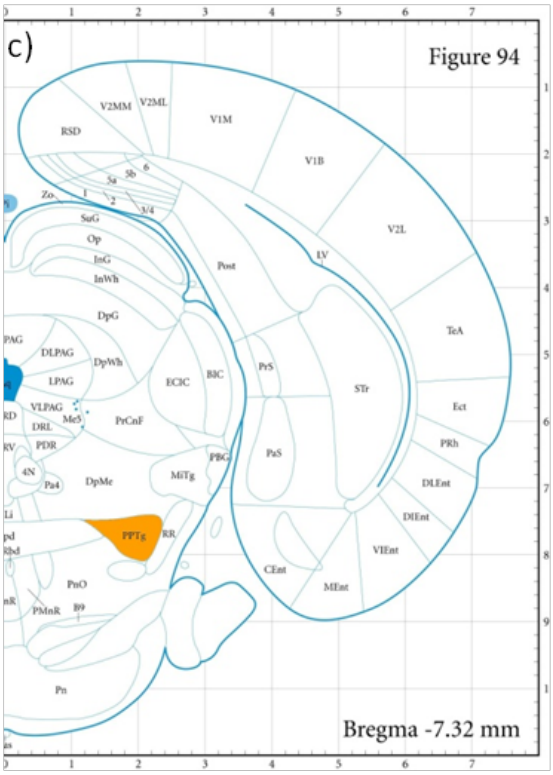


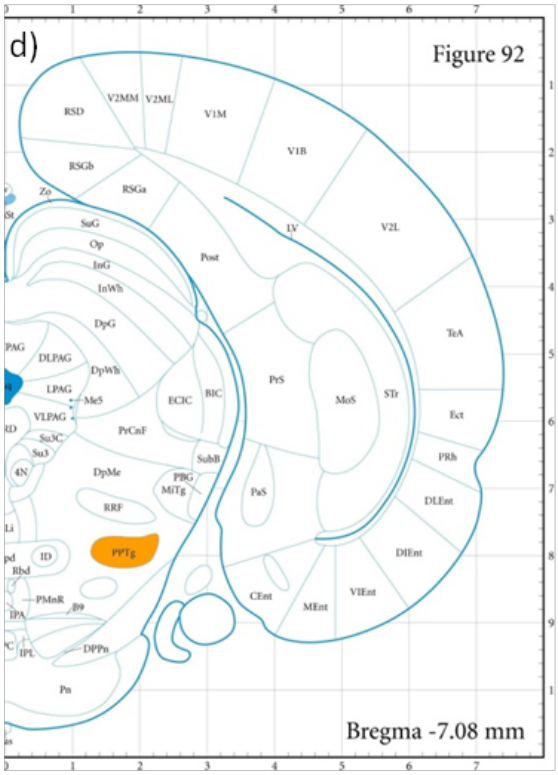

The electrodes were placed in the i4 positioner with the leading electrode (E1-STN) being positioned in the zero position above the bregma. The brain surface was rinsed once again with 0.9 % NaCl and dried with a cotton swab. The Faraday cage was closed to minimize interference with external electromagnetic fields. The coordinates of the first trajectory for the leading electrode (STN) were entered in StereoDrive and all four electrodes in the i4 positioner were moved to their positions above the target nuclei close to the brain surface.

The electrodes were then separately descended in 100 µm steps via NeuroGuide until a signal change was observed indicating that the brain surface was reached.

## 2.6 Stimulation, electrophysiological recordings and data acquisition

In all experiments, all four electrodes were introduced into the right hemisphere. The electrodes were positioned approximately 300 µm above the basal ganglia and subsequently descended in 50 µm steps until the correct depth was reached. With the electrodes positioned correctly and detecting stable signals from a single neuron in each nucleus, the electrophysiological recordings were started.

Spontaneously firing neurons were recorded for approximately 40 seconds to create a baseline. The STN was then stimulated for 20 s with the following HFS parameters: bipolar, monophasic stimulation, 100 µA, pulse width 100 µs at 130 Hz. The post-stimulation action potentials were recorded for 120 seconds. Neurons that were lost right after stimulation were excluded from analysis. Between recordings, the electrodes were descended in 20 µm steps to scan for neurons while exploring the nucleus. Recordings were performed once an active neuron was encountered, and a clear signal with a signal-to-noise ratio greater than 3:1 was detected.

At the end of each recording session, a lesion in the brain tissue was made by passing a constant current of 10 µA through each recording electrode for 5 s.

This allowed pinpointing the exact position of the electrodes on the histology slides to verify if the electrodes were placed correctly within the target nuclei.

Figure 12 shows the NeuroGuide interface visualizing the real-time signals from the target nuclei. Figure 13 illustrates a NeuroGuide recording session in stimulation mode. The E2 (SNr), E3 (PPN) and E4 (GPe) graphs visualize the real-time action potentials picked up by the electrodes while the STN is ready for stimulation ("Stimulation-current" monitoring channel). The prominent spikes represent the firing of a neuron.

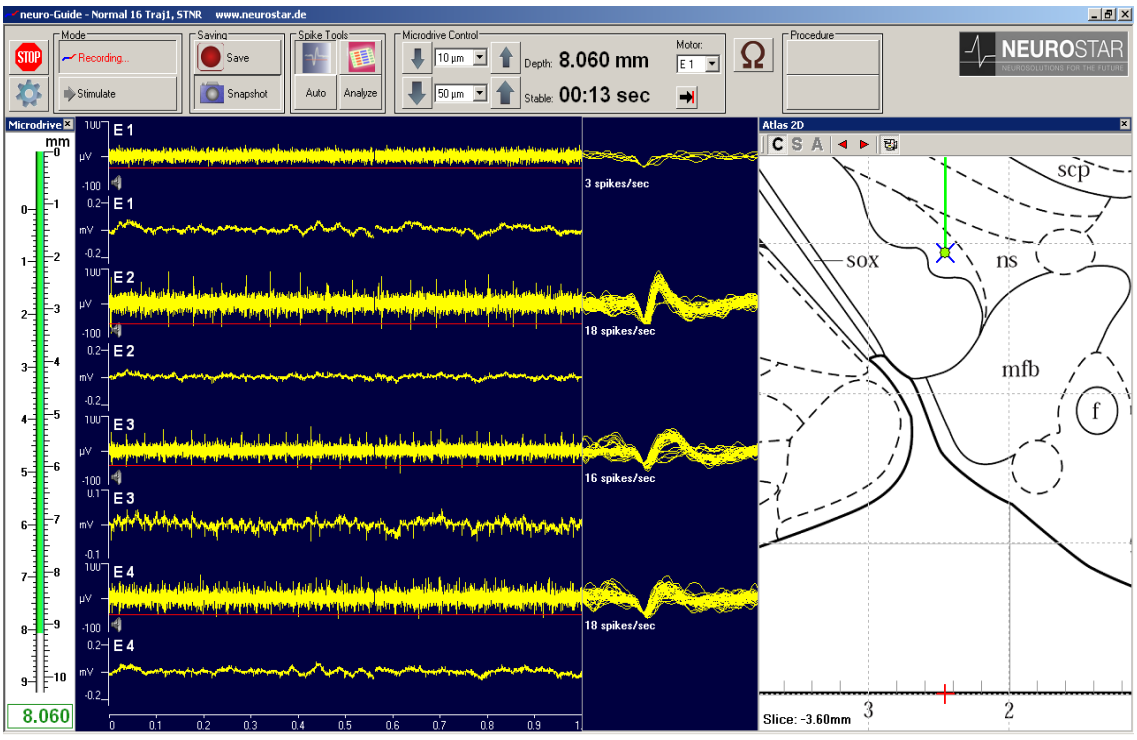


**Figure 12: NeuroGuide interface showing the real-time signals from the target nuclei. Motor E1 controls the electrode E1, which is positioned in the STN (displayed in the atlas on the right side). Electrode E2 is positioned in the SNr, electrode E3 in the PPN and electrode E4 in the GPe.**

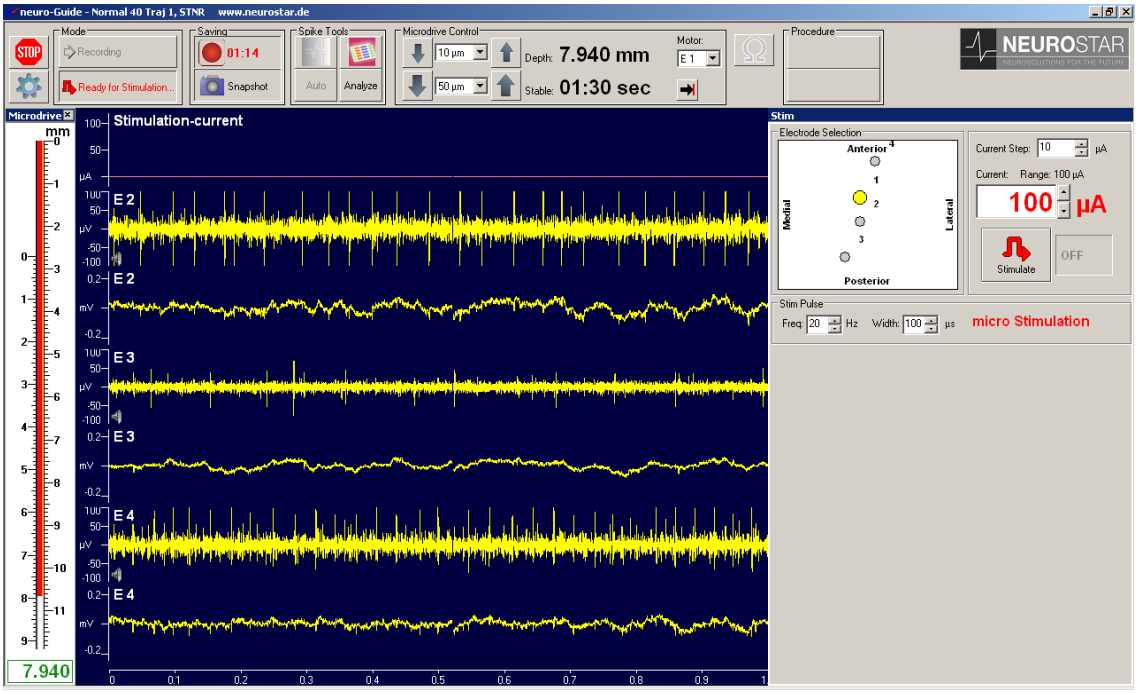


**Figure 13: Recording session in Neuro-Guide - stimulation mode. Electrode E1 (controlled by motor E1) is positioned in the STN, electrode E2 is positioned in the SNr (motor E2), electrode E3 in the PPN (motor E3) and electrode E4 in the GPe (motor E4).**

## 2.7 Histology

### 2.7.1 Chemicals and solution preparation

| | |
|---|---|
| 4 % paraformaldehyde solution | Carl Roth GmbH & Co. KG, Karlsruhe, Germany |
| sucrose | Carl Roth GmbH & Co. KG, Karlsruhe, Germany |
| polyvinylpyrrolidone (40 kg/mol) | Sigma-Aldrich Chemie GmbH Munich, Germany |
| ethylene glycol | Sigma Aldrich Chemie GmbH Munich, Germany |
| PBS | chemical salts from Sigma Aldrich Chemie GmbH Munich, Germany |

| | |
|---|---|
| Cresyl Violet | Sigma Aldrich Chemie GmbH Munich, Germany |
| ethanol | Sigma Aldrich Chemie GmbH Munich, Germany |
| xylene | Sigma Aldrich Chemie GmbH Munich, Germany |
| PERTEX® | Leica Microsystems GmbH, Wetzlar Germany |

Solutions:

| | |
|---|---|
| 10x PBS: | Dissolve 80 g NaCl, 2.4 g $KH_2PO_4$, 2 g KCl and 14.4 g of $Na_2HPO_4$, in 800 ml distilled $H_2O$, set pH to 7.4. Fill to 1 L and sterilize by autoclaving. |
| 30 % sucrose: | 30 g sucrose in 100 ml 0.9 % NaCl-solution |
| Cresyl Violet solution: | 100 mg Cresyl Violet heated up to 60 °C with 100 ml distilled $H_2O$, followed by adding 2 drops of acetic acid, filtered, cooled, stored in a dark bottle |
| antifreeze solution: | 300 g sucrose, 10 g polyvinylpyrrolidone and 300 ml ethylene glycol – dissolved in 700 ml 1x PBS |

### 2.7.2 Perfusion and fixation

Once the experiment was completed, the rat was given a lethal dose of urethane (approx. 720 - 900 mg). The animal was then fixed on a Styrofoam plate, and the abdomen was opened with an incision at the base of the thoracic cage, below the diaphragm. The thoracic cavity was then entered via a diaphragmatic incision, and the descending aorta was clamped with a vascular clamp above the diaphragm. Subsequently, the heart was accessed via a median sternotomy and a small blunt cannula was placed into the ascending aorta through the left ventricular and fixed with a clamp. The right atrium was then opened to allow the blood and perfusion solutions to drain out. The rat was perfused transcardially with 150 ml 0.9 % NaCl to wash out the vascular bed, followed by 150 ml, 4 % paraformaldehyde solution (PFA) to fixate the tissue. After decapitation, the brain was carefully removed from the skull using dissecting forceps. It was then kept in a 4 % PFA solution at 4 °C for 72 hours and subsequently placed into a 30 % sucrose solution. After 48 hours, the brains reached the bottom of the flask, indicating that water was sufficiently removed due to osmosis. In the next step, the brains were placed on dry ice for the preparation of frozen sections.

### 2.7.3 Preparation of frozen sections

The brains were frozen at - 40 °C, cut into 40 µm coronal sections using a microtome (sliding microtome Leica SM2000 R), and stored shortly floating in an antifreeze solution before being mounted onto gelatin-coated slides („SuperFrost® plus“, R. Langenbrinck GmbH, Emmendingen, Deutschland). After mounting, the slides were dried and stained with Cresyl Violet.

### 2.7.4 Cresyl violet staining

Cresyl Violet staining was used to highlight important neuronal structures. Thanks to its cationic nature, Cresyl Violet can bind to the negatively charged phosphate backbone of both DNA and RNA, staining them dark blue (Puchtler H, et al., 1985). As a result, the granular endoplasmic reticulum, also known as the Nissl body, as well as the nuclei of neurons become visible. This method enables recognizing different neuronal structures in the brain architecture and was therefore used to verify the location of the electrodes in the target basal ganglia.

The Cresyl Violet solution was warmed up to 60 °C and the slides were stained in an incubator for approximately 8 min at 60 °C. The slides were then rinsed in distilled water to remove excess stain. Subsequently, they were immersed for 2 min in 70 %, 95 %, and 99 % ethanol followed by immersion in xylene for 3 min. Finally, they were mounted in a Pertex mounting medium and left to dry overnight.

### 2.7.5 Histological control

To validate the position of the electrodes in the nuclei, a marking in the brain tissue was made by passing a constant electric current through the electrodes at the last recording site. Once the stained brain slices were mounted, the localization of the lesion was compared with the nuclei localization in the Rat Brain Atlas (Paxinos and Watson, 2005) under a microscope at 50 x and 100 x magnification. The slides were subsequently scanned using a microscope (Axioplan 2ie Imaging, Zeiss).

## 2.8 Data analysis

To evaluate the response of the target nuclei to STN stimulation, the recordings of intervals 10 seconds prior and 10 seconds post-stimulation were examined. The mean firing rate over the last 10 seconds preceding the stimulation was

termed the “baseline rate”. The mean firing rate in the 10 seconds directly after cessation of stimulation was termed “post-stimulation.” In this way, the stimulation effects could be assessed in the absence of stimulation artifacts that are picked up by recording electrodes in during STN stimulation. A similar *in vivo* study in PD rats performing a treadmill locomotion test showed that motor improvement due to STN stimulation lasted beyond the stimulation period (Shi et al.2006), which supports the above described approach of focusing on the post-stimulation activity which is free of artifacts.

### 2.8.1 Spike Sorting

The recorded data were analyzed using the analysis software SpeedSort (Version 2.1.1b5, Neurostar, Sindelfingen, Germany). SpeedSort is compatible with the experiment software Neuro-Guide and evaluates raw signals from multi-channel recordings. The signals are sorted automatically, based on the multi-factorial information about the spike shape, spike statistics, spike timestamp statistics, as well as the electrode position (x, y, z). Moreover, only signals with a signal-to-noise ratio greater than 3:1 were considered.

### 2.8.2 Firing rate and firing pattern characterization

The firing rate was calculated from the number of spikes (propagated action potentials) detected in a defined time interval and is expressed as spikes/s. The analysis software SpeedSort uses the Kaneoke and Vitek method (Kaneoke Y & Vitek JL, 1996), based on the density of the spike distribution, to determine one of three distinct firing patterns. An accidental firing pattern i.e. "random" is assumed, if the density distribution is in accordance with the Poisson distribution. If the density distribution deviates from the Poisson distribution, the degree of skewness is determined by examining the asymmetry of the distribution function. If the density distribution is significantly different from the Poisson distribution, the skewness of the density distribution is significantly positive, and there is a

minimum of 4 spikes per burst, a salvo-like firing pattern, i.e. "bursting", is assumed. A regular firing pattern i.e. "tonic" is characterized by a symmetric density distribution. An exemplary recording analysis of a tonic firing pattern is shown below (Figure 14).

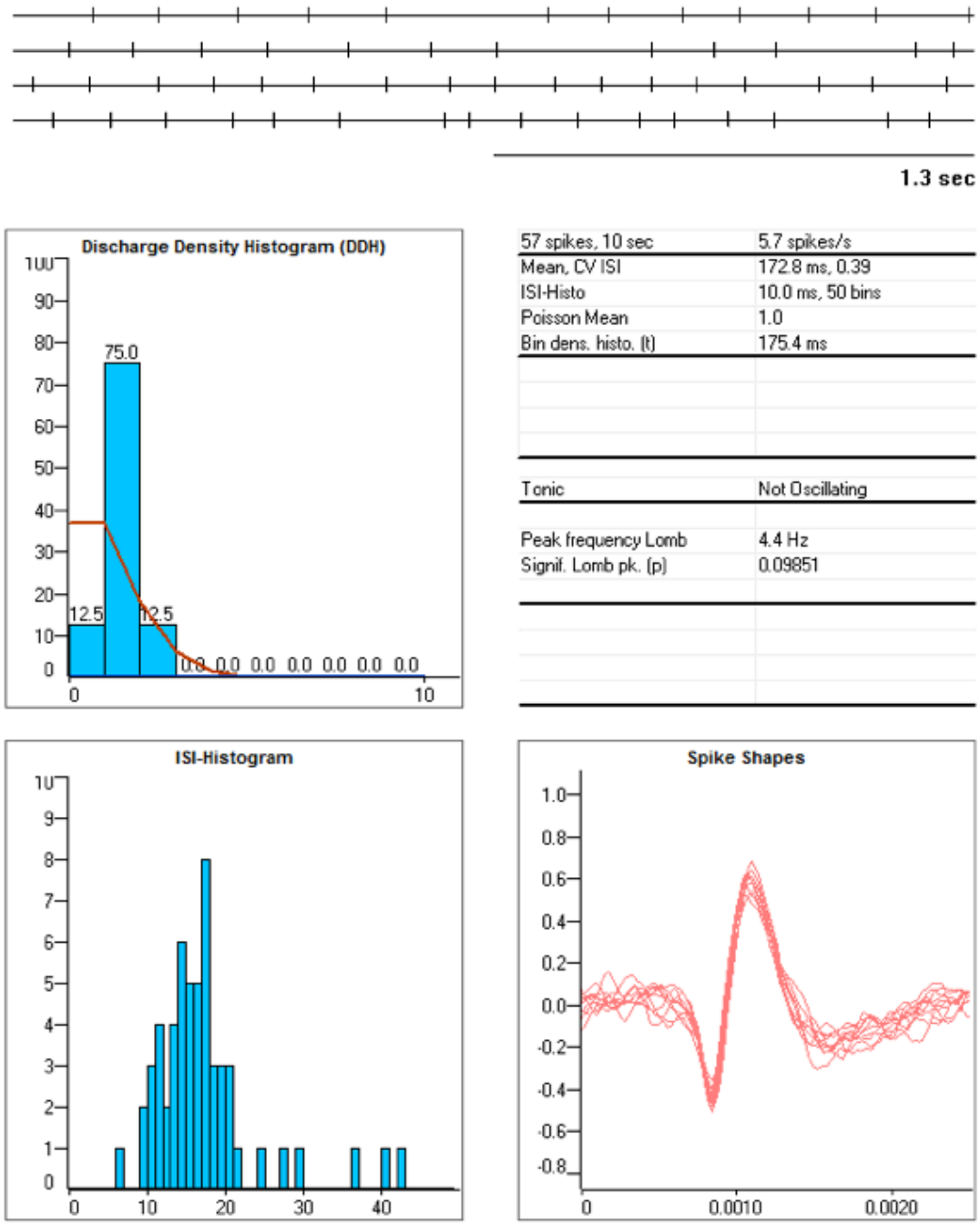


**Figure 14: Firing pattern "tonic" according to the Kaneoke and Vitek method. The timeline is shown on top. The Discharge Density Histogram (DDH) and the Interspike Interval-Histogram (ISI-Histogram) are shown on the left. The Spike Shapes and the calculated values including the mean CV-ISI are shown on the right.**

The coefficient of variation of the interspike intervals (CV-ISI) is a measure of spike train irregularity defined as the standard deviation of the inter-spike interval (ISI) distribution divided by the mean inter-spike interval. A periodic signal has a CV-ISI of 0 and a Poisson process has a CV-ISI of 1. The CV increases with the irregularity of firing pattern.

### 2.8.3 Statistical evaluation

The calculation of the arithmetic mean, standard deviation, standard error of the mean, comparison of the mean firing rates and mean CV-ISIs pre und post stimulation for each nucleus (Wilcoxon signed-rank test), as well as intergroup comparison of mean firing rates (Mann-Whitney U test), was conducted using statistical data analysis software JMP 14.2.0. Results were considered significant at $p < 0.05$.

# 3 Results

A total of 40 rats were used in our experiments. The number of neurons that were available for analysis in each nucleus varied, depending on the signal or anesthesia quality in the individual animals.

All mean values are expressed as the mean and the standard error of the mean (mean ± SEM).

## 3.1 Stimulation induced change in GPe activity

A dataset obtained from 17 rats including recordings of action potentials in 44 distinct neurons was available for analysis of GPe activity under STN stimulation at 130 Hz. Based on the post-stimulation change in the firing rate two types of response were observed: 41 neurons (93 %) decreased and 3 neurons (7 %) increased their firing rate.

The mean firing rate (mean ± SEM) in all GPe neurons prior to stimulation was 20.8 (± 1.2) spikes/s and decreased significantly to 8.3 (± 1.1) spikes/s in the period after stimulation ($p < 0.0001$).

| GPe | Firing rate [spikes/s] | | | CV-ISI | | |
|---|---|---|---|---|---|---|
| | Mean | SD | SEM | Mean | SD | SEM |
| Baseline | 20.8 | 7.8 | 1.2 | 0.51 | 0.17 | 0.02 |
| Post-Stim | 8.3*** | 7.6 | 1.1 | 1.16*** | 0.75 | 0.11 |

**Table 1: Effects of STN stimulation at 130 Hz on the ipsilateral neuronal activity in the GPe. The mean, standard deviation (SD) and standard error of the mean (SEM) are calculated for the firing rate and the coefficient of variation of the interspike intervals (CV-ISI) in all considered GPe neurons. The differences between the post-stimulation (Post-Stim) and baseline means are statistically significant: ***p < 0.0001, n = 44.**

CV-ISI increased in 39 GPe neurons and decreased in 2 neurons, i.e. 95 % of neurons fired more irregularly after stimulation and 5 % of neurons fired more regularly. For 3 neurons, exhibiting a prolonged post-stimulation block, post-stimulation CV-ISI could not be calculated.

The mean coefficient of variation of the interspike intervals (CV-ISI) in of all GPe neurons increased significantly from 0.51 (± 0.02) at baseline to 1.16 (± 0.11) after stimulation ($p < 0.0001$).

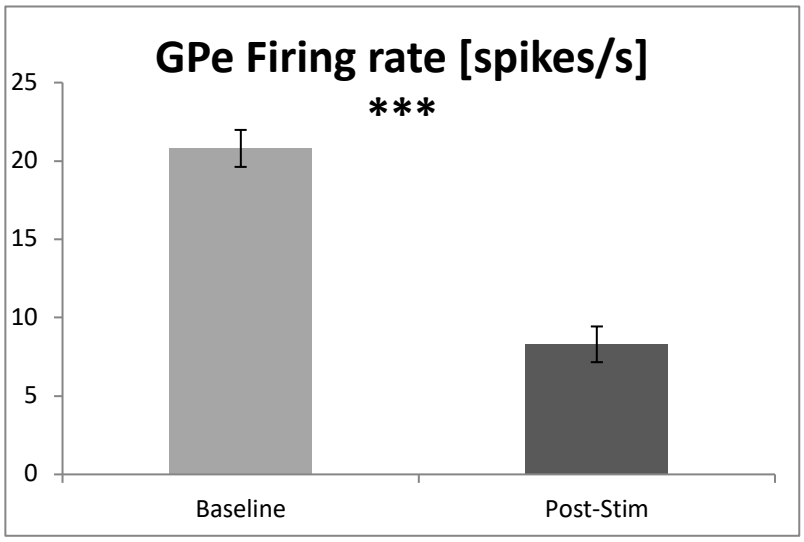


**Figure 15: Comparison of the firing rates in GPe neurons before (Baseline) and after (Post-Stim) ipsilateral STN stimulation with 130 Hz. Error bars indicate SEM. The difference between the post-stimulation and baseline mean is statistically significant: ***p < 0.0001, n = 44.**

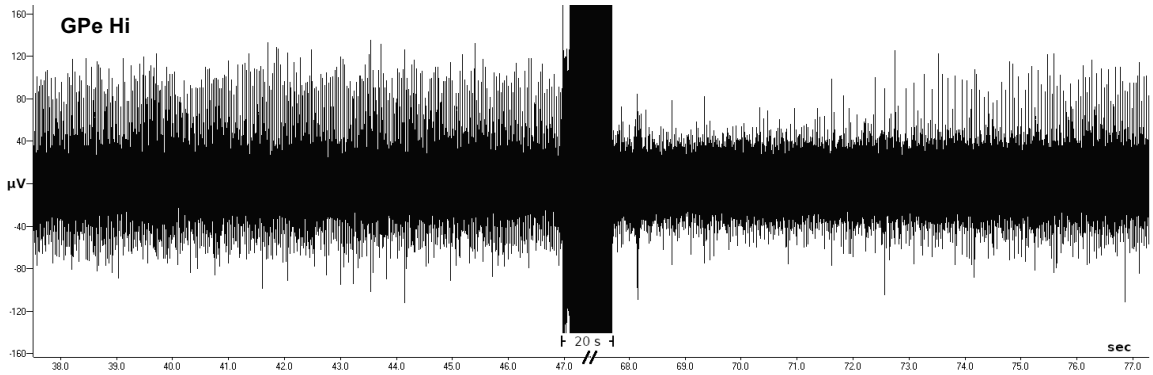


**Figure 16: Exemplary recording of extracellular action potentials of a GPe neuron showing the spontaneous firing before stimulation and a decrease in the firing rate after stimulation. The stimulation period is truncated for illustration purposes.**

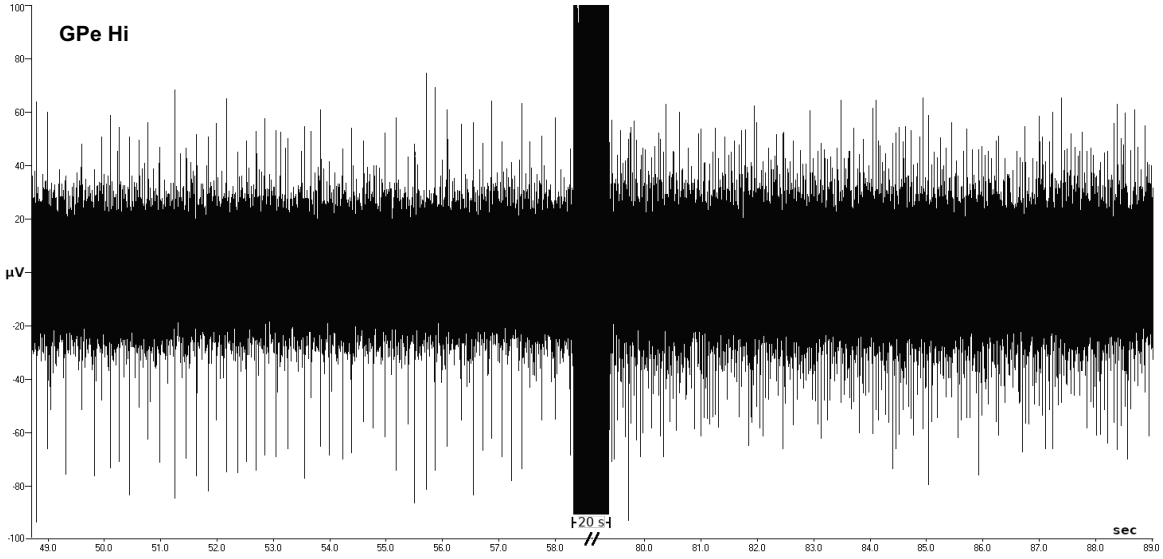


**Figure 17: Exemplary recording of extracellular action potentials of a GPe neuron showing the spontaneous firing before stimulation and an increase in the firing rate after stimulation. The stimulation period is truncated for illustration purposes.**

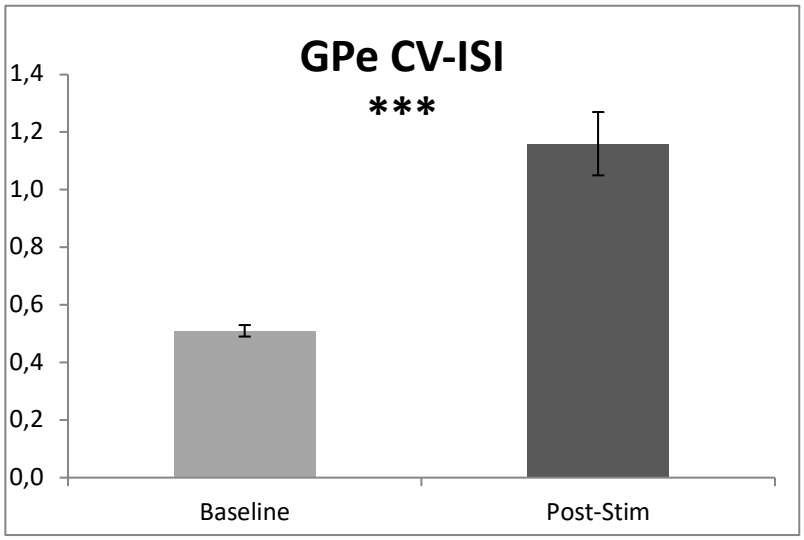


**Figure 18: Comparison of the mean CV-ISI of GPe neurons before (Baseline) and after (Post-Stim) ipsilateral STN stimulation at 130 Hz. Error bars indicate SEM. The difference between the post-stimulation and baseline mean is statistically significant: ***p < 0.0001, n = 44.**

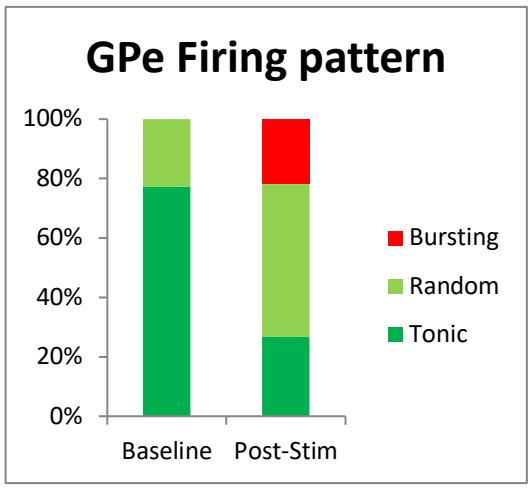


**Figure 19: GPe firing pattern, histogram. Firing pattern distribution of GPe neurons before (Baseline) and after (Post-Stim) STN HFS at 130 Hz.**

| GPe Firing pattern | Baseline | | Post-Stim | |
|---|---|---|---|---|
| | n | % | n | % |
| Tonic | 34 | 77 | 11 | 27 |
| Random | 10 | 23 | 21 | 51 |
| Bursting | 0 | 0 | 9 | 22 |
| Total | 44 | 100 | 41 | 100 |

**Table 2: GPe firing pattern distribution. Distribution of firing pattern in GPe neurons before (Baseline) and after (Post-Stim) STN stimulation at 130 Hz. Neurons exhibiting post-stimulation block could not be assigned by SpeedSort and were therefore not considered.**

The firing pattern distribution of GPe neurons is shown in Figure 19. Before stimulation 77 % of neurons fired tonically, whereas a “random” firing pattern was exhibited by 23 % of GPe neurons. After STN stimulation a “bursting” firing was observed in 22 % of neurons, whereas the number of neurons that fired randomly doubled to 51 %. The occurrence of “tonic” firing decreased to 27 %. Three neurons exhibiting post-stimulation block could not be assigned by SpeedSort and were therefore not considered.

## 3.2 Stimulation induced change in SNr activity

A dataset obtained from 20 rats, including recordings of action potentials in 57 distinct neurons was available for analysis of the SNr response to STN stimulation at 130 Hz. The baseline firing rate of all SNr neurons was 17.6 (± 7.4) spikes/s. Because two divergent responses of SNr neurons were identified based on the post-stimulation change in the firing rate, the statistical analysis was conducted separately for each group. Excitation was observed in 48 neurons (84 %), while the activity of 9 neurons (16 %) was suppressed.

| SNr | | Neurons | Firing rate [spikes/s] | | | CV-ISI | | |
|---|---|---|---|---|---|---|---|---|
| | | n (%) | Mean | SD | SEM | Mean | SD | SEM |
| **Excitation** | Baseline | 9 (16) | 8.2 | 6.7 | 2.2 | 0.63 | 0.36 | 0.12 |
| | Post-Stim | | 19.1** | 6.3 | 2.1 | 0.50* | 0.30 | 0.10 |
| **Inhibition** | Baseline | 48 (84) | 19.4 | 6.1 | 0.9 | 0.50 | 0.20 | 0.02 |
| | Post-Stim | | 8.0*** | 7.1 | 1.0 | 1.05*** | 0.56 | 0.08 |
| | Total | 57 (100) | | | | | | |

**Table 3: Effects of STN stimulation at 130 Hz on the ipsilateral neuronal activity in the SNr. The mean, standard deviation (SD) and standard error of the mean (SEM) are calculated for the firing rate and the coefficient of variation of the interspike intervals (CV-ISI) separately in the group of SNr neurons responding with an increase of the firing rate (Excitation) and decrease of the firing rate (Inhibition). The differences between the post-stimulation (Post-Stim) and baseline means are statistically significant: ***p < 0.0001; **p < 0.01; *p < 0.05.**

The mean firing rate (mean ± SEM) recorded in SNr neurons that were inhibited by the stimulation with 130 Hz was 19.4 (± 0.9) spikes/s prior to stimulation and decreased significantly to 8 (± 1) spikes/s after stimulation ($p < 0.0001$).

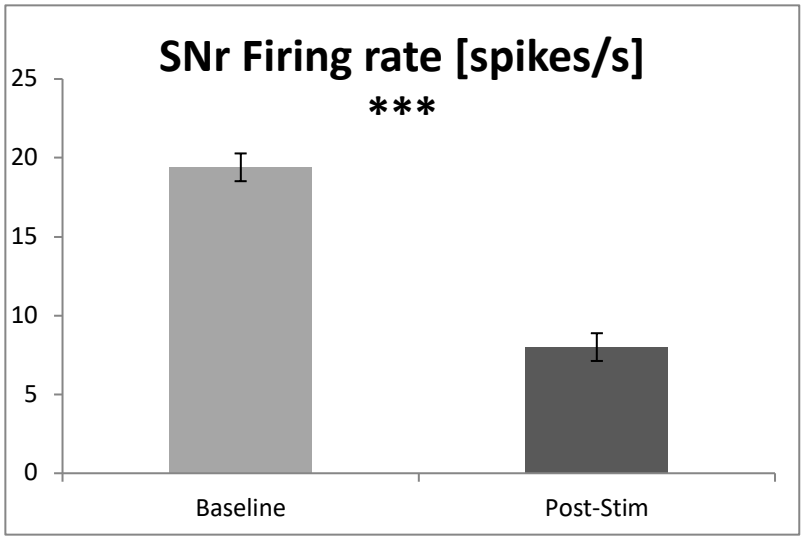


**Figure 20: SNr neurons responding with inhibition, comparison of the mean firing rates before (Baseline) and after (Post-Stim) STN stimulation at 130 Hz. Error bars indicate SEM. The difference between the post-stimulation and baseline mean is statistically significant: ***p < 0.0001, n = 48**

The decrease in firing rate of SNr neurons was associated with a decrease in firing pattern regularity, since the mean CV-ISI increased significantly from 0.50 (± 0.02) at baseline to 1.05 (± 0.08) after stimulation ($p < 0.0001$).

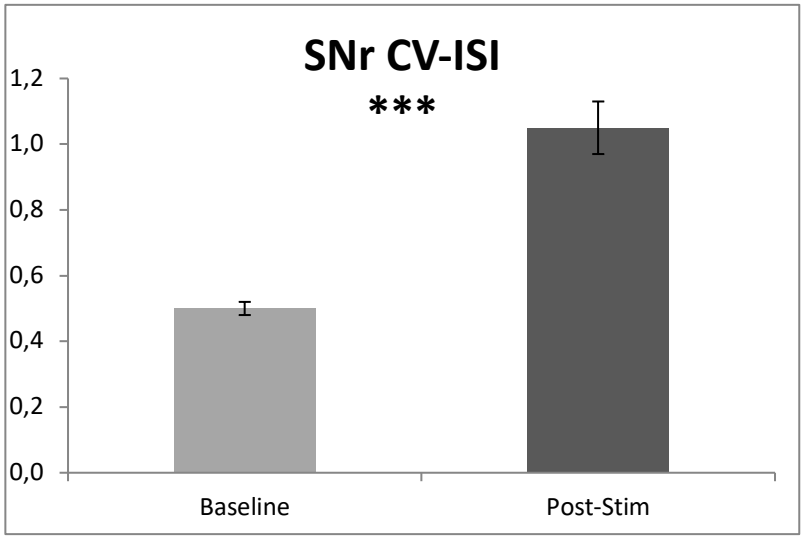


**Figure 21: SNr neurons responding with inhibition, comparison of the mean CV-ISI before (Baseline) and after (Post-Stim) STN stimulation at 130 Hz. Error bars indicate SEM. The difference between the post-stimulation and baseline mean is statistically significant: ***p < 0.0001, n = 48**

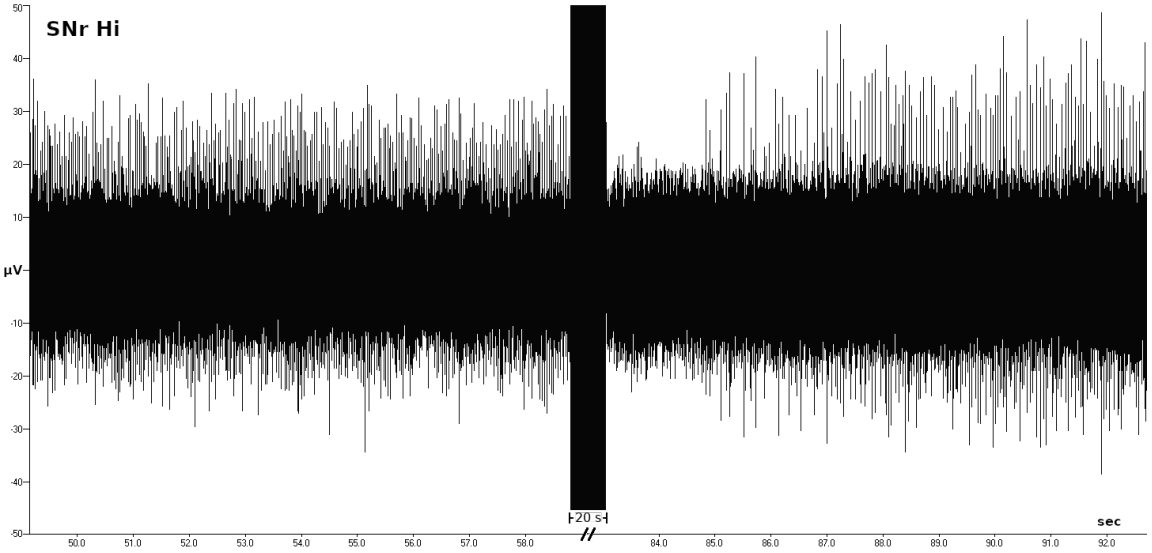


**Figure 22: Exemplary recording of extracellular action potentials of a SNr neuron showing the spontaneous firing before stimulation and a decrease in the firing rate after stimulation. The stimulation period is truncated for illustration purposes.**

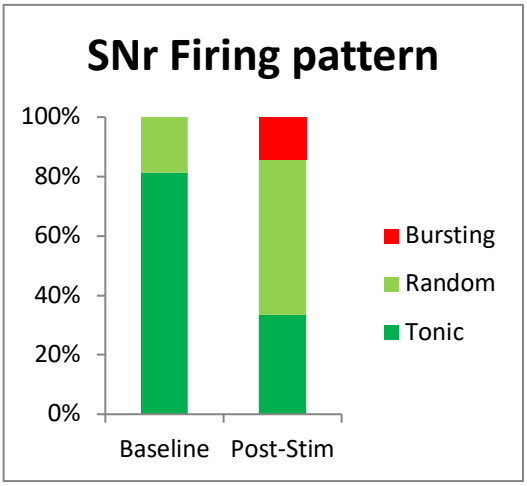


**Figure 23: SNr inhibition, firing pattern histogram. Firing pattern distribution before (Baseline) and after (Post-Stim) stimulation in the group of SNr neurons inhibited by STN HFS at 130 Hz.**

| SNr Firing pattern | Baseline | | Post-Stim | |
|---|---|---|---|---|
| | N | % | N | % |
| Tonic | 39 | 81 | 14 | 33 |
| Random | 9 | 19 | 22 | 53 |
| Bursting | 0 | 0 | 6 | 14 |
| Total | 48 | 100 | 42 | 100 |

**Table 4: Firing pattern distribution, SNr inhibition. Firing pattern distribution before (Baseline) and after (Post-Stim) stimulation in the group of SNr neurons inhibited by STN HFS at 130 Hz. Neurons exhibiting post-stimulation block could not be assigned by SpeedSort and were therefore not considered.**

The firing pattern in the group of SNr neurons inhibited by the STN stimulation is shown in Figure 23. Before stimulation, 81 % of neurons fired tonically and 19 % of neurons fired randomly. After STN stimulation 14 % of neurons exhibited a “bursting” firing pattern, whereas the number of neurons that fired randomly increased to 53 %. The occurrence of “tonic” firing decreased to 33 %. 6 neurons exhibiting post-stimulation block could not be assigned by SpeedSort and were therefore not considered.

In neurons responding with facilitation, the mean firing rate increased significantly from 8.2 (± 2.2) spikes/s at baseline to 19.1 (± 2.1) spikes/s after stimulation ($p < 0.01$).

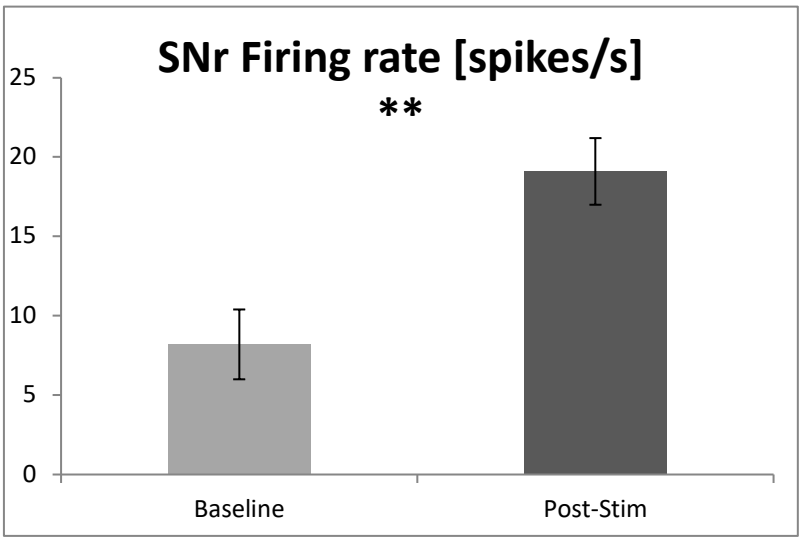


**Figure 24: SNr neurons responding with excitation, comparison of the mean firing rates before (Baseline) and after (Post-Stim) ipsilateral STN stimulation at 130 Hz. Error bars indicate SEM. The difference between the post-stimulation and baseline means is statistically significant: **p < 0.01, n = 9**

The increase in firing rate in SNr neurons was associated with an increase in firing pattern regularity, since the mean CV-ISI decreased significantly from 0.63 (± 0.12) at baseline to 0.50 (± 0.10) after stimulation ($p < 0.05$).

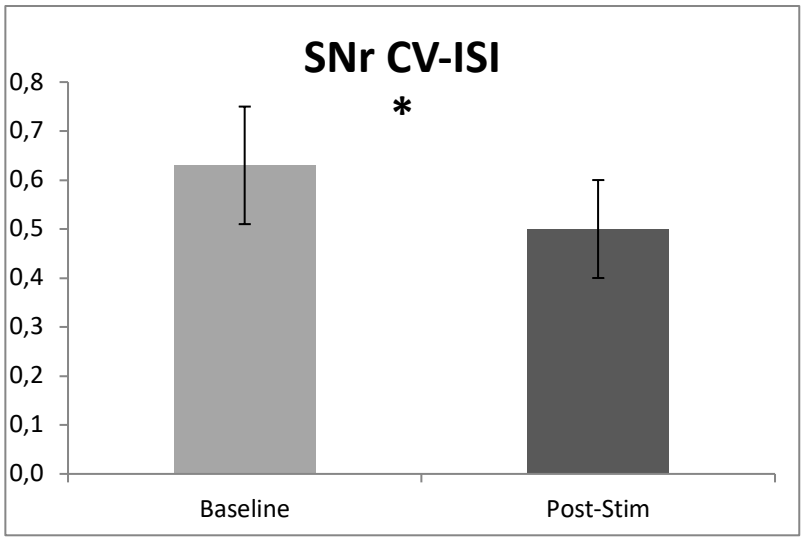


**Figure 25: SNr neurons responding with excitation, comparison of the mean CV-ISI before (Baseline) and after (Post-Stim) ipsilateral STN stimulation at 130 Hz. Error bars indicate SEM. The difference between the post-stimulation and baseline mean is statistically significant: *p < 0.05, n = 9**

The firing pattern distribution of SNr neurons responding with excitation is shown in Figure 27. Before stimulation, 67 % of neurons fired tonically and 33 % of neurons fired randomly. STN stimulation did not change the firing pattern distribution. No “bursting” firing was found in this group. Three neurons that were silent before stimulation could not be assigned by SpeedSort and were therefore not considered.

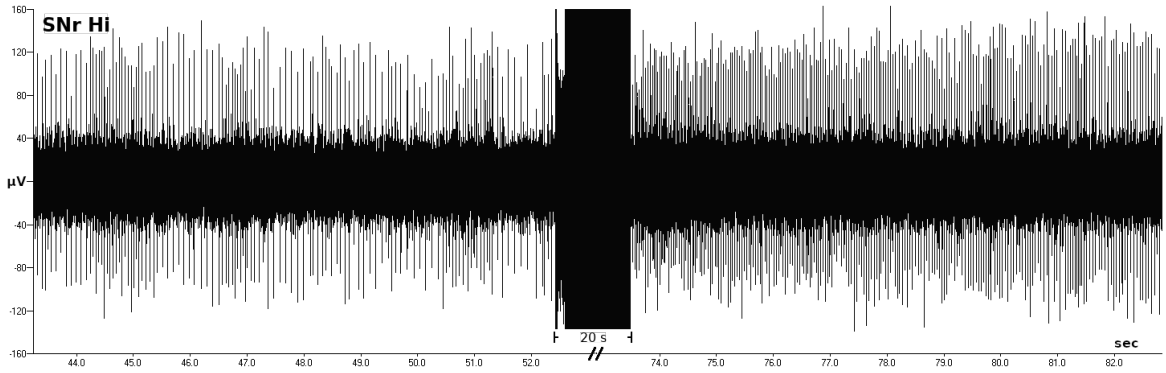


**Figure 26: Exemplary recording of extracellular action potentials of a SNr neuron showing the spontaneous firing before stimulation and an increase in the firing rate after stimulation. The stimulation period is truncated for illustration purposes.**

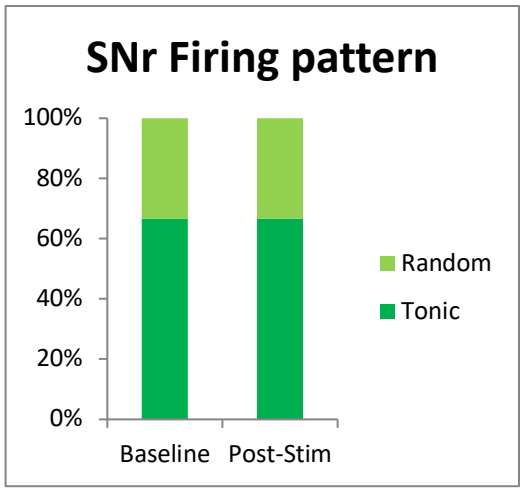


**Figure 27: SNr excitation, firing pattern histogram. Firing pattern distribution before (Baseline) and after (Post-Stim) stimulation in the group of SNr neurons responding with excitation to STN HFS at 130 Hz.**

| SNr Firing pattern | Baseline | | Post Stim | |
|---|---|---|---|---|
| | N | % | N | % |
| Tonic | 4 | 67 | 6 | 67 |
| Random | 2 | 33 | 3 | 33 |
| Bursting | 0 | 0 | 0 | 0 |
| Total | 6 | 100 | 9 | 100 |

**Table 5: Firing pattern distribution, SNr excitation. Firing pattern distribution before (Baseline) and after (Post-Stim) stimulation in the group of SNr neurons responding with excitation to STN HFS at 130 Hz. Neurons that were silent before stimulation could not be assigned by SpeedSort and were therefore not considered.**

## 3.3 Stimulation induced change in PPN activity

A dataset obtained from 24 rats, including recordings of action potentials in 69 distinct neurons, was available for analysis. The mean firing rate (mean ± SEM) in all PPN neurons prior to stimulation was 13.96 (± 0.98) spikes/s. Based on the change in firing rate after STN stimulation at 130 Hz, two groups of neurons could be distinguished. Since the number of PPN neurons responding with facilitation (31 = 45 %) and inhibition (38 = 55 %) was almost equal, the statistical analysis was conducted for each group separately.

| PPN | | Neurons | Firing rate [spikes/s] | | | CV-ISI | | |
|---|---|---|---|---|---|---|---|---|
| | | n (%) | Mean | SD | SEM | Mean | SD | SEM |
| **Excitation** | Baseline | 31 (45) | 11.6 | 8.5 | 1.5 | 0.51 | 0.27 | 0.05 |
| | Post-Stim | | 19.8*** | 10.3 | 1.9 | 0.58 n.s | 0.48 | 0.08 |
| **Inhibition** | Baseline | 38 (55) | 15.7 | 7.4 | 1.2 | 0.58 | 0.32 | 0.05 |
| | Post-Stim | | 6.2*** | 4.9 | 0.8 | 0.93** | 0.64 | 0.11 |
| | Total | 69 (100) | | | | | | |

**Table 6: Effects of STN stimulation at 130 Hz on the ipsilateral neuronal activity in the PPN. The mean, standard deviation (SD) and standard error of the mean (SEM) are calculated for the firing rate and the coefficient of variation of the interspike intervals (CV-ISI) separately in the group of PPN neurons responding with excitation and inhibition. The differences between the post-stimulation (Post-Stim) and baseline means are statistically significant except for CV-ISI in excitation group: ***p < 0.0001; **p < 0.01; n.s. = not significant.**

In the group of PPN neurons responding with facilitation the mean firing rate (mean ± SEM) prior to stimulation was 11.6 (± 1.5) spikes/s and increased significantly to 19.8 (± 1.9) spikes/s after stimulation ($p < 0.0001$).

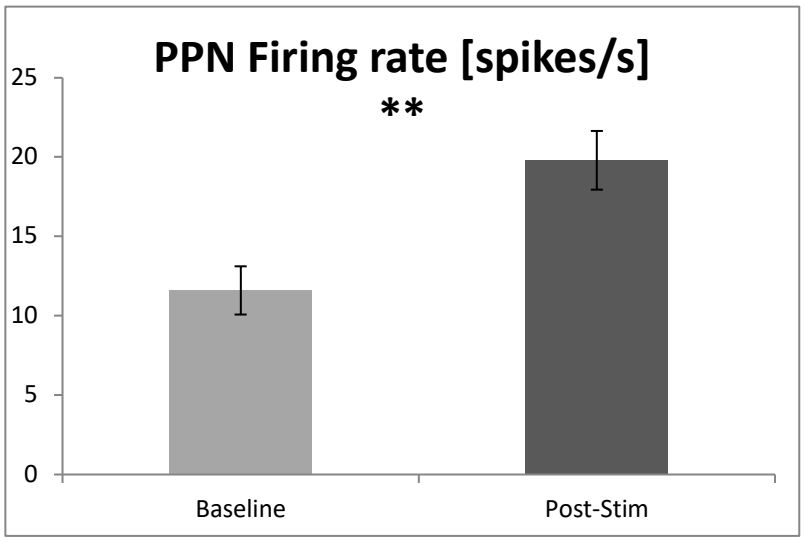


**Figure 28: PPN neurons responding with excitation, comparison of the mean firing rates before (Baseline) and after (Post-Stim) ipsilateral STN stimulation at 130 Hz. Error bars indicate SEM. The difference between the baseline and post-stimulation mean is statistically significant: ***p < 0.0001, n = 31**

The increase of the mean CV-ISI from 0.51 (± 0.05) at baseline to 0.58 (± 0.08) after stimulation was not statistically significant (p > 0.05).

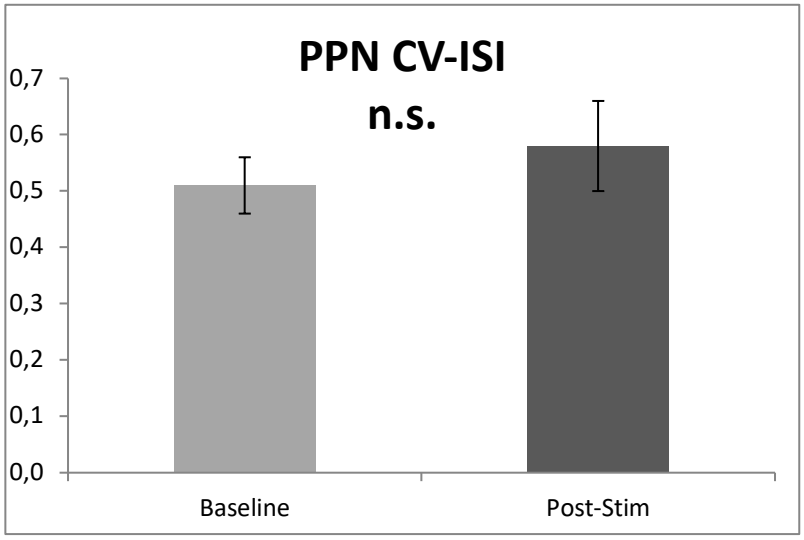


**Figure 29: PPN neurons responding with excitation, comparison of the mean CV-ISI before (Baseline) and after (Post-Stim) ipsilateral STN stimulation at 130 Hz. Error bars indicate SEM. The difference between the post-stimulation and baseline mean is not statistically significant: n.s., n = 31**

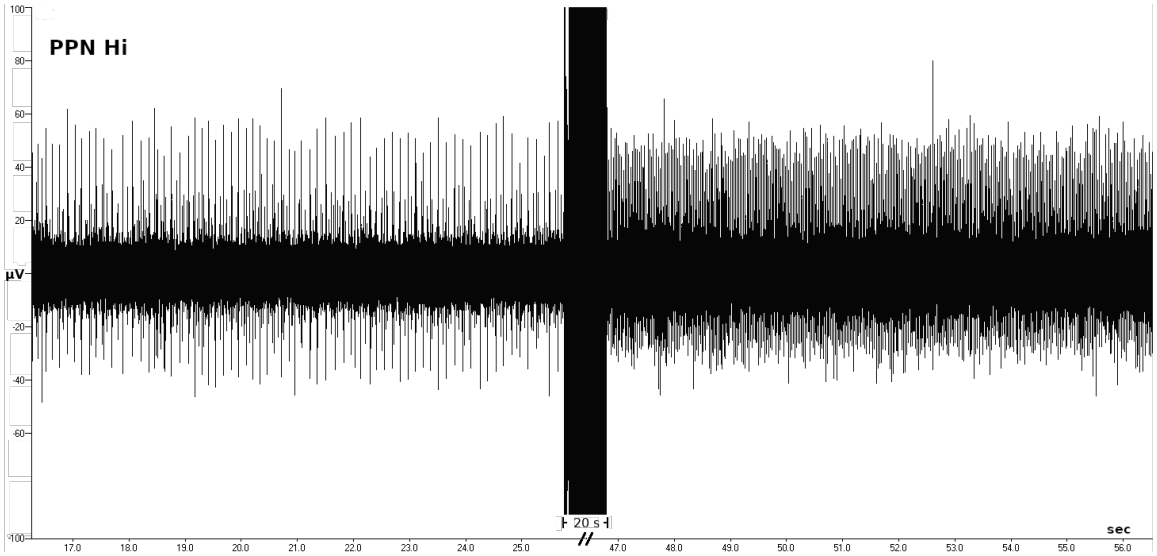


**Figure 30: Exemplary recording of extracellular action potentials of a PPN neuron showing the spontaneous firing before stimulation and an increase in the firing rate after stimulation. The stimulation period is truncated for illustration purposes.**

In 8 out of 31 PPN neurons responding with excitation, a short period (approximately 1 second) of suppressed activity directly after stimulation and prior to a clear increase in the spike-discharge was observed. An example of such a rebound excitation is shown in Figure 31 below.

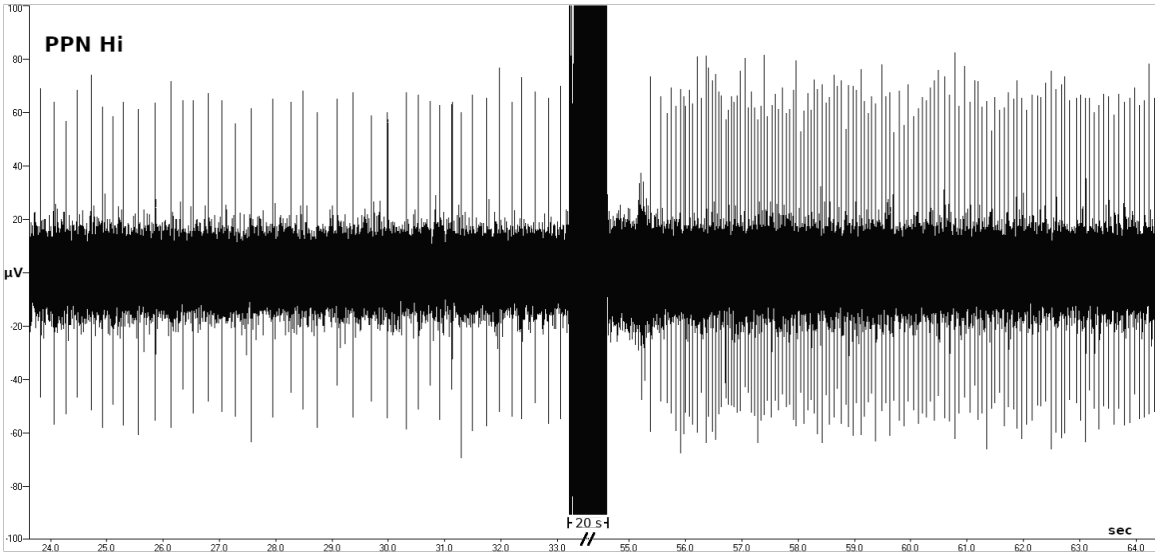


**Figure 31: Exemplary recording of extracellular action potentials of a PPN neuron showing the spontaneous firing before stimulation and a rebound excitation after stimulation. The stimulation period is truncated for illustration purposes.**

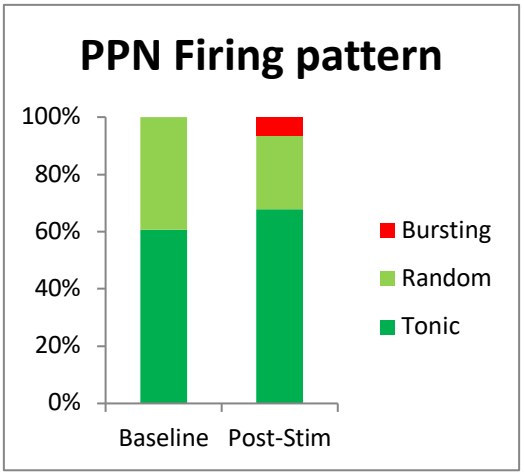


**Figure 32: PPN excitation, firing pattern histogram. Firing pattern distribution before (Baseline) and after (Post-Stim) stimulation in the group of PPN neurons responding with excitation to STN HFS at 130 Hz.**

| PPN Firing pattern | Baseline | | Post-Stim | |
|---|---|---|---|---|
| | N | % | N | % |
| Tonic | 17 | 61 | 21 | 68 |
| Random | 11 | 39 | 8 | 26 |
| Bursting | 0 | 0 | 2 | 6 |
| Total | 28 | 100 | 31 | 100 |

**Table 7: Firing pattern distribution, PPN excitation. Firing pattern distribution before (Baseline) and after (Post-Stim) stimulation in the group of PPN neurons responding with excitation to STN HFS at 130 Hz. Neurons that were silent before stimulation could not be assigned by SpeedSort and were therefore not considered.**

The firing pattern distribution of PPN neurons that were excited by STN stimulation is shown in Figure 32. Before stimulation, 61 % of neurons fired tonically and 39 % fired randomly. After stimulation, “bursting” firing was observed in 6 % of neurons, “random” and “tonic” firing patterns were exhibited by 26 % and 68 % of neurons respectively. 3 neurons that were silent before stimulation could not be assigned by SpeedSort and were therefore not considered.

The mean firing rate recorded in PPN neurons that were inhibited by the STN stimulation was 15.7 (± 1.2) spikes/s at baseline and decreased significantly to 6.2 (± 0.8) spikes/s after stimulation ($p < 0.0001$).

The baseline mean firing rate was significantly higher in the group of neurons that were inhibited by STN stimulation compared to the group responding with excitation (Mann-Whitney U Test, $p < 0.05$).

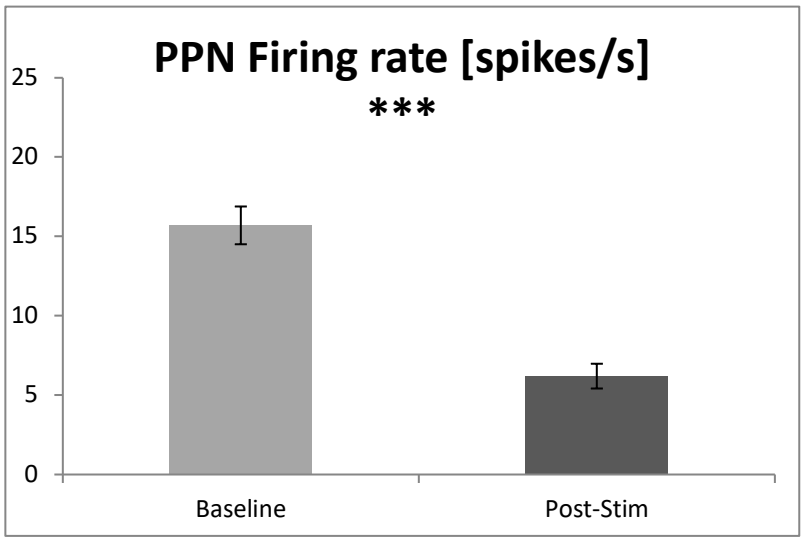


**Figure 33: PPN neurons responding with inhibition, comparison of the mean firing rates before (Baseline) and after (Post-Stim) ipsilateral STN stimulation at 130 Hz. Error bars indicate SEM. The difference between the post-stimulation and baseline mean is statistically significant: ***p < 0.0001, n = 38**

The decrease in firing rate in PPN neurons was associated with a decrease in firing pattern regularity, since the mean CV-ISI increased significantly from 0.58 (± 0.05) at baseline to 0.93 (± 0.11) after stimulation ($p < 0.01$).

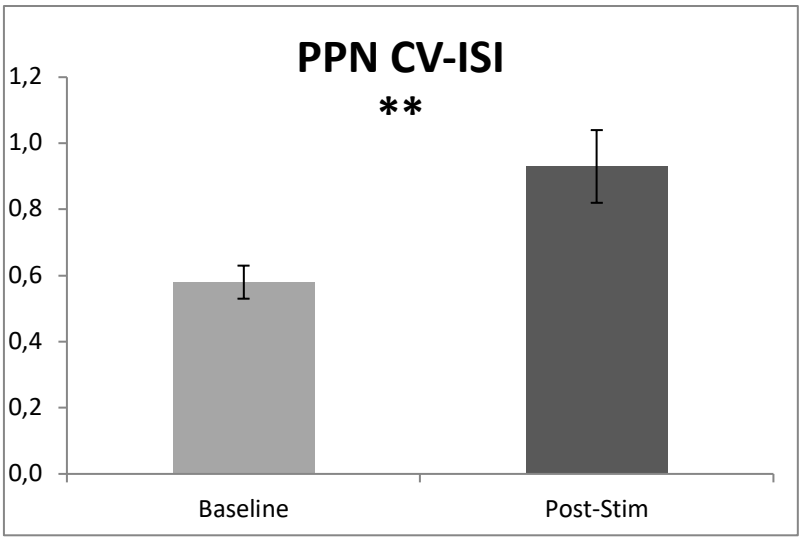


**Figure 34: PPN neurons responding with inhibition, comparison of the mean CV-ISI before (Baseline) and after (Post-Stim) ipsilateral STN stimulation at 130 Hz. Error bars indicate SEM. The difference between the post-stimulation and baseline mean is statistically significant: ***p < 0.0001, n = 38**

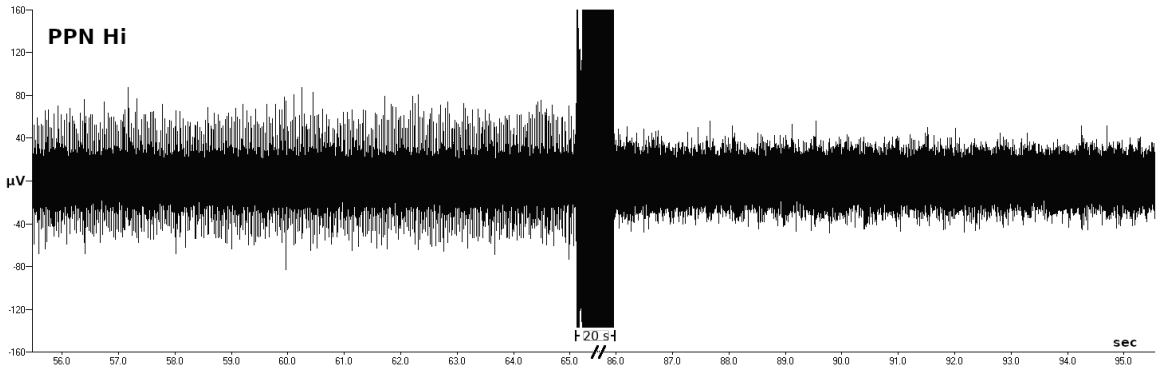


**Figure 35: Exemplary recording of extracellular action potentials of a PPN neuron showing the spontaneous firing before stimulation and a decrease in the firing rate after stimulation. The stimulation period is truncated for illustration purposes.**

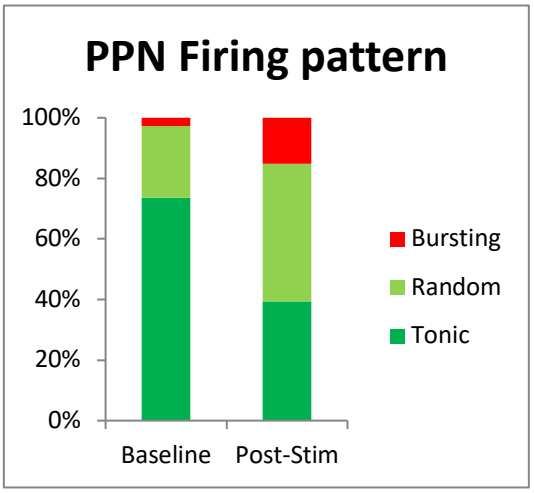


**Figure 36: PPN inhibition, firing pattern histogram. Firing pattern distribution before (Baseline) and after (Post-Stim) stimulation in the group of PPN neurons inhibited by STN HFS at 130 Hz.**

| PPN Firing pattern | Baseline | | Post-Stim | |
|---|---|---|---|---|
| | N | % | N | % |
| Tonic | 28 | 74 | 13 | 39 |
| Random | 9 | 24 | 15 | 46 |
| Bursting | 1 | 2 | 5 | 15 |
| Total | 38 | 100 | 33 | 100 |

**Table 8: Firing pattern distribution, PPN inhibition. Firing pattern distribution before (Baseline) and after (Post-Stim) stimulation in the group of PPN neurons inhibited by STN HFS at 130 Hz. Neurons exhibiting post-stimulation block could not be assigned by SpeedSort and were therefore not considered.**

The firing pattern distribution of PPN neurons responding with inhibition is shown in Figure 36. Before stimulation, 74 % of neurons fired tonically, “random” and “bursting” firing patterns were exhibited by 24 % and 2 % of neurons respectively. After STN stimulation the number of neurons exhibiting “bursting” and “random” firing increased to 15 % and 24 % respectively, while the number of neurons firing tonically decreased to 39 %. 5 neurons exhibiting post-simulation block could not be assigned by SpeedSort and were therefore not considered.

## 3.4 Histological control

Brain tissue markings performed at the end of recordings were used to control electrode positioning. The slides in Figure 37 – 39 below show examples of such markings. Examined structures are directly contrasted and compared with the Cresyl Violet stained slides from the Atlas of Paxinos and Watson. Because usually, the brain tissue penetration channel closes after the removal of the electrodes, the entry points are not always visible.

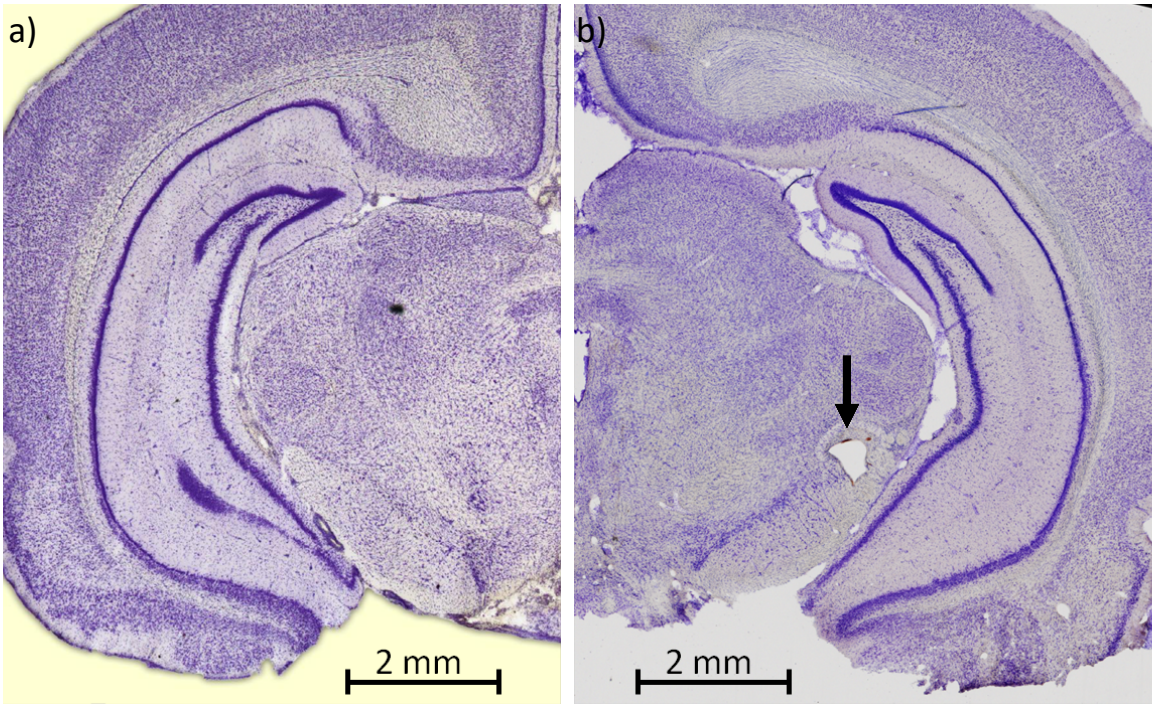


**Figure 37: Exemplary histological control, SNr marking:**

**a) Cresyl Violet stained slide from the Atlas of Paxinos and Watson (Bregma -5.40 mm, Paxinos and Watson, 2005)**

**b) Cresyl Violet staining, marking at the end of 2. trajectory for SNr with coagulated blood at the end of the tissue penetration channel near the marking site (arrow)**

**c) corresponding figure from the atlas (Bregma -5.16 mm, Paxinos and Watson, 2005)**

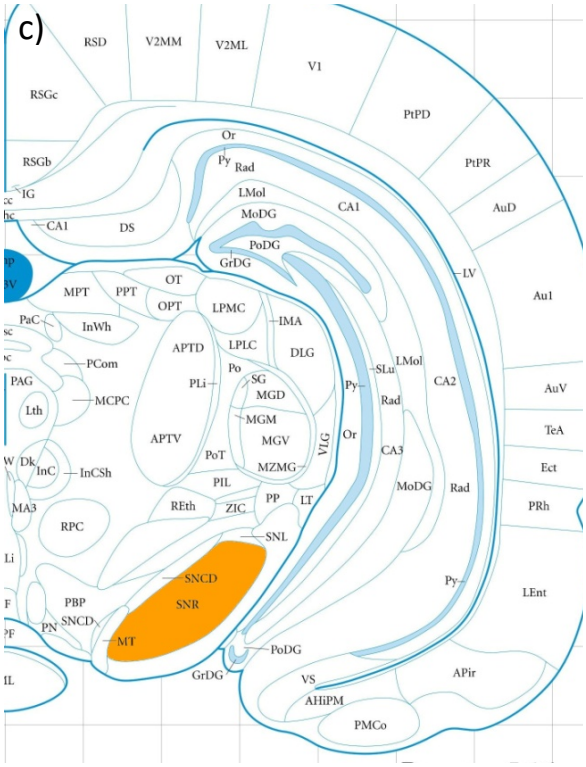

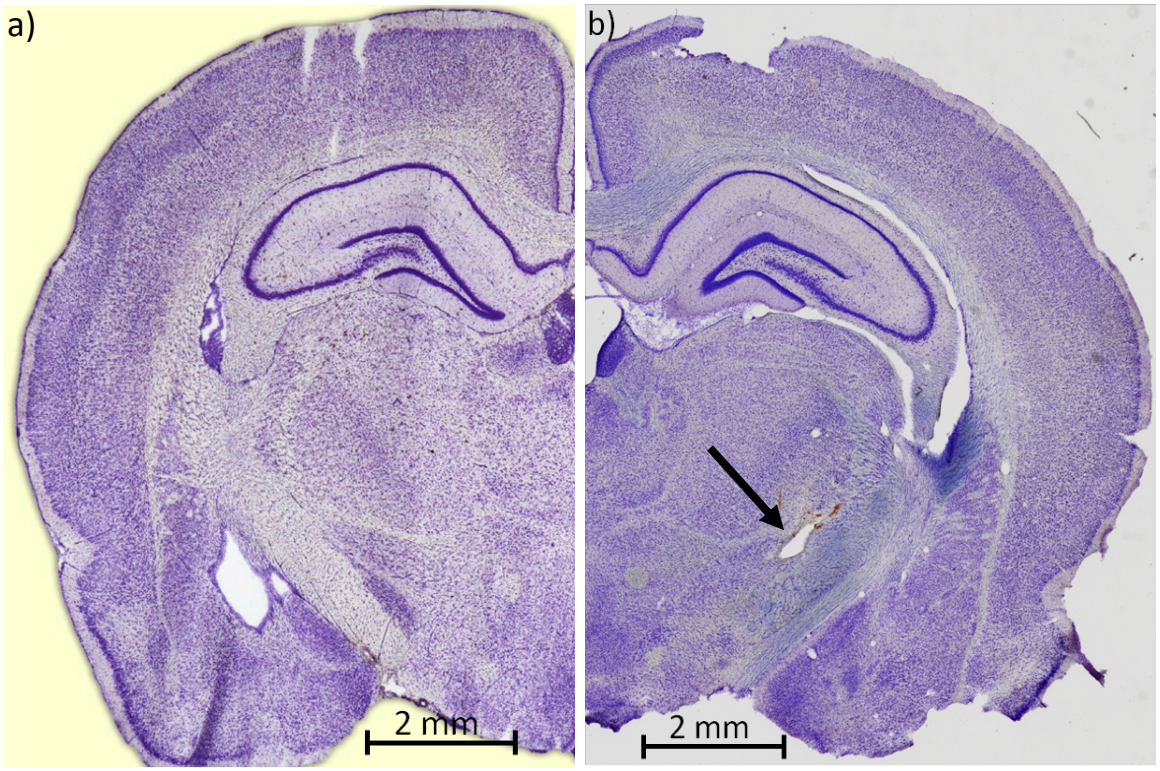


**Figure 38: Exemplary histological control, STN marking:**

**a) Cresyl Violet stained slide from the Atlas of Paxinos and Watson (Bregma -3.48 mm, Paxinos and Watson, 2005)**

**b) Cresyl Violet staining, marking at the end of 2. trajectory for STN with coagulated blood at the end of the tissue penetration channel near the marking site (arrow)**

**c) corresponding figure from the atlas (Bregma -3.60 mm, Paxinos and Watson, 2005)**

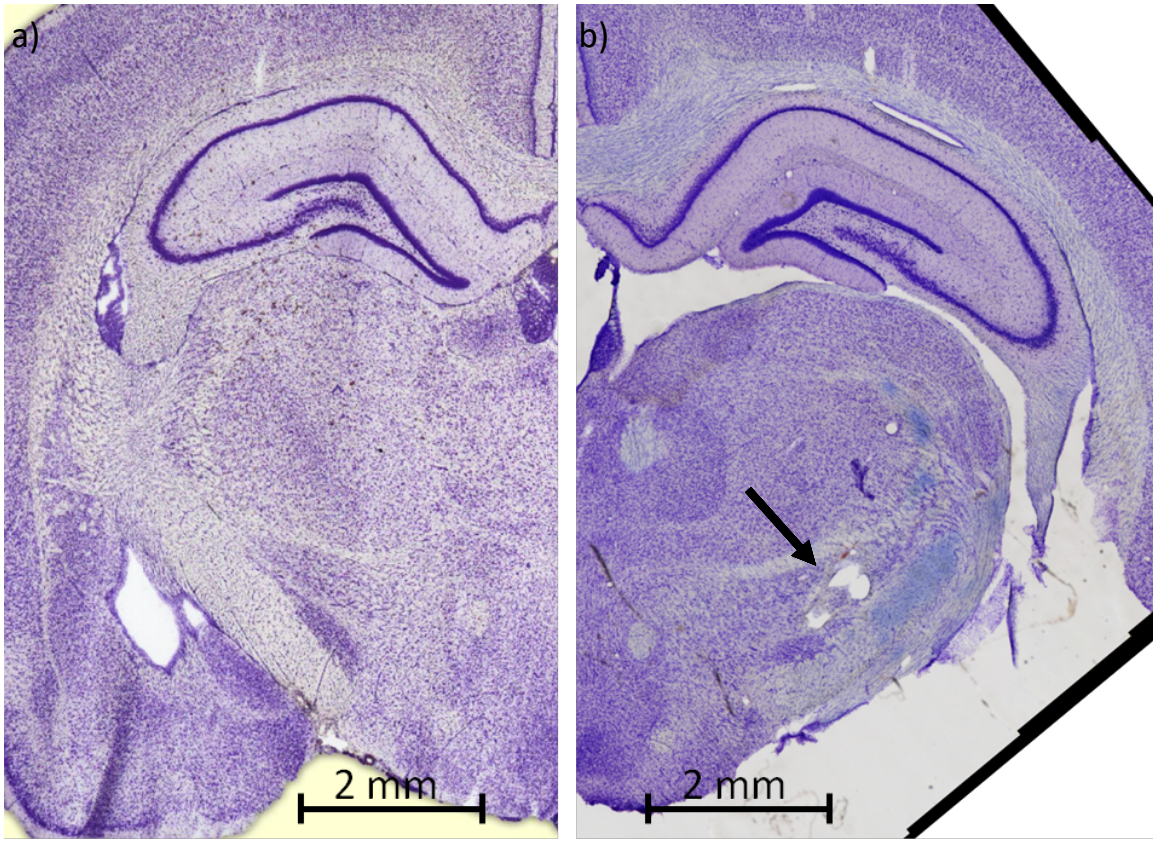


**Figure 39: Exemplary histological control, STN marking:**

**a) Cresyl Violet stained slide from the Atlas of Paxinos and Watson (Bregma -3.48 mm, Paxinos and Watson, 2005)**

**b) Cresyl Violet staining, marking at the end of 1. trajectory for STN with coagulated blood at the end of the tissue penetration channel near the marking site (arrow)**

**c) corresponding figure from the atlas (Bregma -3.48 mm, Paxinos and Watson, 2005)**

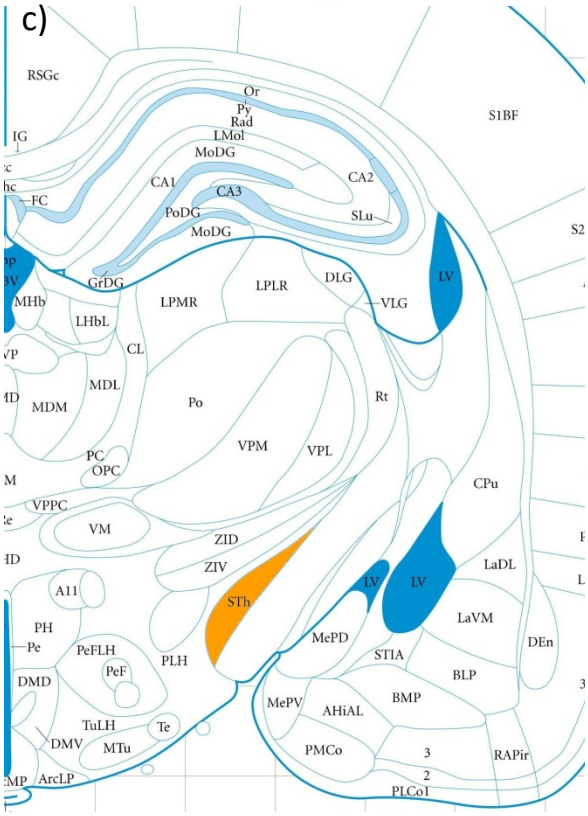

# 4 Discussion

The main results of this study are:

- The ipsilateral STN stimulation at 130 Hz, 100 μA and pulse width of 100 μs for 20 seconds in urethane- anesthetized intact rats inhibits the activity of almost all GPe neurons and the majority of SNr neurons, but also induces an excitation in a minority of the SNr neurons. HFS of the STN leads to an increase and decrease in activity in a similar proportion of PPN neurons.

- HFS of the STN causes a shift towards irregular firing in most of the neurons of all three basal ganglia nuclei and an increase in firing pattern regularity in SNr neurons exhibiting a post-stimulative excitation.

## 4.1 Modulation of GPe activity by STN-HFS

The observed baseline firing rates in GPe neurons correspond well with values obtained in other *in vivo* studies in rats under urethane anesthesia (Burbaud P, et al., 1994) and was slightly higher than reported in awake rats (Shi LH, et al., 2006).

The application of ipsilateral high-frequency STN stimulation elicited a significant decrease in the firing rates in most GPe neurons (93 % cells). Consistent with our results, an *in vivo* study in both normal and PD rats anesthetized with a mix of tiletamine/zolazepam and xylazine showed significant inhibition of GPe neurons during STN stimulation at frequencies higher than 50 Hz (Ryu SB, et al., 2013). It should be noted, though, that these extracellular recordings were only performed in 5 rats, and the neuronal activity of GPe neurons was analyzed during stimulation with the use of an artifact removal technique, subjecting results to artifacts. Our findings are, however, contradictory with the data obtained in the first electrophysiological studies of high-frequency STN stimulation in normal rats describing a post-stimulation increase in the firing rate of all recorded GPe

neurons with a return to baseline activity within 60 - 150 seconds (Benazzouz A, et al., 1995). In the current study, excitation was observed only in 7 % of GPe neurons. The inconsistency with our data might be attributed to a different stimulation duration, a difference in stimulation parameters or anesthesia since the Benazzouz group applied a higher intensity stimulation (300 µA) for a shorter amount of time (5 seconds) in rats anesthetized with chloral hydrate. It is also noteworthy that only 10 GPe cells from 5 rats were included in this study. In line with our observations, a more recent study in awake rodents demonstrated that STN stimulation may not necessarily produce a universal reaction in all GPe neurons (Shi LH, et al., 2006). During 20 s behaviorally effective STN stimulation at 130 Hz in PD rats performing a treadmill locomotion task, the GPe neurons exhibited an almost equal proportion of excitations and inhibitions. The motor improvement lasted beyond the stimulation period, which allowed for data collection not only during the stimulation period but also during the following off stimulation intervals, avoiding stimulation artifacts in the recordings. The ratio of inhibitory to excitatory responses was approximately 2 : 1 during the 3 seconds stimulation period and was reversed in the 2 seconds “off” stimulation period (Shi LH, et al., 2006). The differences in proportions of inhibitions to excitations compared to our data might be due to a different experimental design (awake vs. anesthetized rats) or indicate a dependence of the GPe reaction on the stimulation duration.

The suppression of GPe activity is most likely caused by the inhibition of the excitatory glutamatergic projections from the STN. HFS has been shown to suppress STN neurons in patients with Parkinson’s disease (Filali M, et al., 2004; Welter ML, et al., 2004), in animal PD models (Meissner W, et al., 2005) as well as in intact rodents (Tai CH, et al., 2003). However, subthalamic neurons in brain slices can fire at very high-frequencies (300 - 500 Hz) in response to a intracellular current, which suggests that they are unlikely to develop a substantial depolarization block (Bevan MD & Wilson CJ, 1999). Since GPe and STN are reciprocally connected (Kita H & Kitai ST, 1994), the inhibitory GABAergic GPe inputs into the STN may be directly activated, which would contribute to STN

inhibition, resulting in a consequent reduction in STN excitatory influence onto the GPe. At the same time, GPe axons could be antidromically activated.

The excitation of GPe neurons is in line with the activation of the direct glutamatergic excitatory STN inputs to the GPe. Supporting this hypothesis is the neurochemical data reporting elevated Glu levels in GPe after ipsilateral STN stimulation in intact rats (Windels F, et al., 2000). Moreover, since the threshold for excitability of axons is much lower than that for somata (Ranck JB Jr, 1975) and activation of fibers passing the electrode region seems likely (McIntyre CC, et al., 2004a; McIntyre CC, et al., 2004b; Miocinovic S, et al., 2006), the GPe axons in the STN may be antidromically activated and the evoked action potential may travel to the cell body. The fact that neuroanatomical studies found large varicosities of GPe axons closely apposed to the STN somata and dendrites, lends support to this theory (Sato F, et al., 2000).

We observed a post-stimulation increase in firing irregularity in 95 % of GPe neurons and the mean CV-ISI for all analyzed GPe neurons increased significantly. An increase in the incidence of burst activity in the majority of GPe cells during therapeutically effective STN stimulation has been shown in non - human primates (Hahn PJ, et al., 2008), however the change of the mean CV-ISI was not statistically significant. In contradiction to our data, a significant decrease in burst rate was observed after cessation of effective STN stimulation in awake rats (Shi LH, et al., 2006).

Studies in primate (Miller WC & DeLong MR, 1987) and rodent models of Parkinson's disease (Pan HS & Walters JR, 1988; Soares J, et al., 2004) have reported that the average firing rate of GPe neurons is lower in the parkinsonian state than in normal animals. Extracellular recordings in patients were similar to those in MPTP-treated monkeys (Hutchison WD, et al., 1994; Sterio D, et al., 1994). Although the current study examined the influence of STN stimulation on basal ganglia only in the normal state, considering the above mentioned findings and the fact, that HFS seems to elicit a similar effect on firing rates of GPe neurons in normal and PD animals (Ryu SB, et al., 2013), it might be suggested that the therapeutic effect of STN stimulation can unlikely be explained by a

simple excitation/inhibition model. Since pallidal neurons do not respond to STN stimulation uniformly, more than one mechanism of action seems to be involved in the STN stimulation-induced modulation of pallidal activity, and the net effect for a particular pallidal neuron likely depends on the spatial relationship of its afferents and efferents to the electric field stimulation (Hahn PJ, et al., 2008). Under that hypothesis, the therapeutic effect of STN stimulation is reached through a combination of electrode positioning and stimulation parameters as long as a sufficient proportion of pallidal neurons are shifted away from pathological firing patterns (Hahn PJ, et al., 2008).

## 4.2 Modulation of SNr activity by STN-HFS

The observed mean baseline firing rates of SNr neurons correspond well with values obtained in other *in vivo* studies in rats under urethane anesthesia (Burbaud P, et al., 1994). Most SNr neurons (84 %) responded to ipsilateral high-frequency STN stimulation with a decrease in their firing rate, accompanied by a significant increase of CV-ISI indicating a shift of the firing pattern towards irregularity. Excitation was observed in 16 % of SNr neurons and was accompanied by a significant increase in firing regularity.

Similar results have been reported in several previous studies in anesthetized rats. Benazzouz et al. observed a decrease in activity of 91 % of SNr neurons lasting from 50 to 120 seconds after application of 5 seconds high-frequency STN stimulation (130 Hz). 9 % of neurons exhibited a biphasic response consisting of an increase followed by a significant decrease in the firing rate (Benazzouz A, et al., 1995). Excitation occurred mainly at low frequencies (5 – 50 Hz) and was outweighed by the inhibitory effect at frequencies over 60 Hz, indicating a correlation of the stimulation effect with the stimulation frequency. In a subsequent study, HFS evoked a predominantly inhibitory response of SNr neurons in both normal and PD rats with 6-OHDA lesions of the SNc (Benazzouz A, et al., 2000). Another *in vivo* study in awake rats, reported almost equal numbers of SNr neurons exhibiting excitation and inhibition during and after

STN stimulation at 130 Hz (Shi LH, et al., 2006). Extracellular recordings of SNr activity in patients showed a decrease in the firing rate after 20 seconds STN stimulation with 140 Hz (Maltête D, et al., 2007), as well as an increase the firing rate during a 30 minutes long STN stimulation session (Galati S, et al., 2006).

The inhibition of SNr neurons may likely result from a decreased excitation of the subthalamonigral glutamatergic pathway. Indeed, a simultaneous inhibition of the STN and the SNr during STN stimulation, accompanied by a significant decrease in the expression of messenger RNA for subunit I of the cytochrome c oxidase (*COX1* mRNA) in the STN as well as in the SNr has been observed in both normal and 6-OHDA lesioned rats (Tai CH, et al., 2003). Since the SNr receives GABAergic afferents from the GPe (Smith Y & Bolam JP, 1989), the inhibition of SNr neurons may also be caused by a stimulation-induced increase in the inhibitory GPe input. The inhibitory polysynaptic effect of STN stimulation on the SNr via activation of pallidonigral fibers is supported by neurochemical studies reporting an increase in GABA levels in the SNr after a unilateral STN stimulation (Windels F, et al., 2000; Windels F, et al., 2005). Moreover, an injection of GABA antagonists into the SNr causes a cessation of STN stimulation-induced inhibition (Maurice N, et al., 2003) and a GPe lesion abolishes the increase in SNr GABA levels induced by HFS of the STN (Windels F, et al., 2005). In our experiments inhibition and not excitation was the predominant response of GPe neurons to STN stimulation. However, DBS is expected to evoke action potentials predominantly in axons, from where they may propagate orthodromically and antidromically (Grill M & McIntyre C, 2001). Therefore, it appears possible that only GPe axons may be activated via direct stimulation of GABAergic pallidonigral fibers passing close to the STN resulting in increased GABA levels in the SNr (Maurice N, et al., 2003; Windels F, et al., 2005).

The observed excitation in a portion of SNr neurons may be primarily explained by orthodromic activation of subthalamonigral axons (Hammond C, et al., 1978). Consistent with this hypothesis, an increase in SNr glutamate levels was found after STN stimulation in normal rats (Windels F, et al., 2000). Also, electrical

stimulation could activate some of the STN neurons or just STN axons of the subthalamonigral pathway.

Although the SNr receives both GABAergic and glutamatergic inputs that are believed to act together regulating its activity, SNr cells appear to be relatively insensitive to direct activation by glutamate, but very sensitive to a diminished GABA input, which may release them from tonic inhibition and determine their functional hyperactivity. In the presence of bicuculline, a competitive $GABA_A$ antagonist, SNr cells show consistent excitations. Therefore, modulation of GABA inhibitory input, not the opposing actions of glutamate and GABA, seems to be the primary factor controlling the activity of SNr neurons under physiological conditions (Windels F & Kiyatkin EA, 2004). The predominant GABA role in regulating SNr activity is also in line with ultrastructural studies in the SNr (Gerfen CR & Wilson JW, 1996) revealing that glutamatergic subthalamic projections contact dendrites, whereas GABAergic pallidal terminals have a strategic gating position onto the soma of SNr neurons (Bevan MD & Wilson CJ, 1999; Windels F & Kiyatkin EA, 2006a).

The firing rate model of the pathophysiology in Parkinson's disease assumes an increased activity of the basal ganglia output nuclei. This could be confirmed in PD animal models for the GPe, whereas the data obtained for the SNr is contradictory. A few studies in 6-OHDA-lesioned rats showed increased firing rates of SNr neurons and reported that the firing pattern changed towards more irregular and bursty (Lee JI, et al., 2001; Wang Y, et al., 2010), while no such change (Sanderson P, et al., 1986; Murer MG, et al., 1997) or a reduction in the firing rate was observed in other studies (Rohlfs A, et al., 1997). STN lesion has been shown to regularize the firing pattern and partially revert the spontaneous bursting firing found in the SNr after SNc lesioning (Murer MG, et al., 1997). We observed a significant decrease in CV-ISI in SNr neurons that were excited by STN stimulation, whereas inhibited SNr neurons exhibited a shift towards irregularity in firing with the occurrence of "bursting" firing, which was not observed before stimulation. Contrasted with the findings of Murer et al., our data

indicate that STN stimulation modulates the firing pattern of SNr neurons in a mechanism that is not identical to that of STN lesioning.

## 4.3 Modulation of PPN activity by STN-HFS

PPN neurons exhibited a lower baseline firing rate compared to SNr and GPe neurons, which is in good agreement with other studies (Breit S, et al., 2001; Florio T, et al., 2007). Ipsilateral high-frequency STN stimulation elicited a near equal number of excitatory and inhibitory responses in PPN neurons. The data regarding the influence of STN stimulation on PPN activity is scarce. A similar effect in PPN neurons after cessation of STN stimulation at 130 Hz has previously been observed in rats (Florio T, et al., 2007).

Increased activity of PPN neurons may result from the activation of STN projections to the PPN, as a direct excitatory input from the STN to the PPN has been described in rats (Granata AR & Kitai ST, 1989). Since the PPN is in reciprocal connection with the STN (Hammond C, et al., 1983a; Kita T & Kita H, 2011), antidromic activation of PPN efferents to the STN should also be considered (Florio T, et al., 2007). Given the existence of inhibitory SNr projections to the PPN (Granata AR & Kitai ST, 1991), a reduction of the inhibitory influence from the inhibited SNr could also contribute to the PPN excitation. In line with this hypothesis is the STN stimulation-induced decrease in SNr activity predominantly observed in our study. Since an inhibition of GPi under STN stimulation has been shown in other studies (Benazzouz A, et al., 1995) and inhibitory GABAergic GPi projections to the PPN have been described in the rat (Semba K & Fibiger HC, 1992; Moriizumi T & Hattori T, 1992) and monkey (Shink E, et al., 1997), there is also a possibility of PPN excitation resulting from the attenuated GPi activity.

Inhibition of the PPN may likely be caused by a stimulation-induced inhibition of the excitatory projections from the STN. The inhibitory response of PPN neurons may also be explained by the existence of a polysynaptic inhibitory projection

from the STN to the PPN via the SNr. Since a portion of SNr neurons was activated by STN stimulation, an increase in the inhibitory GABAergic SNr input to the PPN seems conceivable. As the stimulation of the STN has been shown to increase the activity of GPi neurons (Hashimoto T, et al., 2003), an increase of the inhibitory GPi influence on PPN neurons should also be considered. This hypothesis is strengthened by the observation that the inhibitory influence of STN stimulation on PPN neurons disappears in GPi-lesioned rats (Florio T, et al., 2007).

In 8 out of 31 PPN neurons responding with excitation a short period of suppressed activity, directly after stimulation and prior to a clear increase in the spike discharge, was observed. Such rebound excitation after SNr stimulation has been described before in PPN neurons in *in vitro* studies in rat brain slices (Kang Y & Kitai ST, 1990) and, together with our observation, may speak for the STN stimulation-induced indirect PPN modulation via SNr neurons.

The baseline mean firing rate was significantly higher in the group of neurons that were inhibited by STN stimulation compared to the group responding with excitation. Based on the electrophysiological properties, mainly in terms of spontaneous firing rate, three classes of PPN neurons (slow firing, fast firing and a mixed group) have been distinguished in previous *in vitro* studies (Kang Y & Kitai ST, 1990; Takakusaki K, et al., 1996). Together with these observations, our data suggest that the effects STN stimulation has on a particular PPN neuron (or populations of neurons) may correlate with its intrinsic properties.

The absence of a unilateral response to STN stimulation reflects the complex morphology and connectivity of the PPN. Based on the density and arrangement of its cholinergic neurons, the PPN was originally divided into the pars dissipata (rostral) and pars compacta (caudal) (Olszewski J & Baxter D, 1982). The rostral PPN consists mostly of GABAergic neurons and interconnects with the basal ganglia: SNr and GPi. The caudal PPN consists dominantly of cholinergic and glutamatergic neurons, receives inputs from the cortex and projects to the STN, the ventral tegmental area, the thalamus, as well as the superior and inferior colliculi. The difference between those two PPN regions is clearer with regards

to the distribution of the efferents than afferents (Martinez-Gonzalez C, et al., 2011). Considering this localized distribution, STN stimulation could simultaneously produce opposite effects in different PPN regions. The rostral PPN area could be inhibited indirectly by STN induced excitation of SNr neurons (Hammond C, et al., 1983), whereas the caudal PPN area could be antidromically activated via its efferents to the STN (Florio T, et al., 2007; Aravamuthan BR, et al., 2008; Martinez-Gonzalez C, et al., 2009). Alternatively, the rostral PPN area could be activated due to disinhibition via GABAergic projections from the SNr, while the inhibition of the caudal PPN area could result from stimulation-induced inhibition of the excitatory projections from the STN.

We observed an increase in firing irregularity after STN stimulation, which was significant in the group of inhibited PPN neurons. A lesion of the STN in normal rats was found to decrease the mean firing rate and increase the firing irregularity in PPN neurons (Breit S, et al., 2001). The divergent reaction of PPN neurons observed in our experiments, however, indicates that the HFS of the STN extends beyond simply mimicking the effects of an STN lesion.

Although our experiments were only performed in intact rats, regarding the increase in the firing rate and irregularity of firing pattern in PPN neurons found in a 6-OHDA rat model of Parkinson's disease (Breit S, et al., 2001; Jeon MF, et al., 2003), at least in terms of firing regularity, the therapeutic effect of STN stimulation in Parkinson's disease may likely be reached by modulating the activity of PPN neurons in a different mechanism than simply counteracting the changes observed in the parkinsonian state.

## 4.4 Effect of anesthesia on *in vivo* recordings

Electrophysiological tests require long and stable anesthesia. Commonly used anesthetics in rodents are chloral hydrate, urethane, halothane or isoflurane. Continuous administrations of anesthetics (e.g. isoflurane) might cause artifacts in the recordings. Urethane provides stable, long-lasting anesthesia (> 3 hours)

and stable electrophysiological conditions and was therefore chosen for the experiments (Hara K & Harris RA, 2002).

Not only the neurophysical features are different in awake and sleeping animals (Mahon S, et al., 2001; Mahon S, et al., 2006), but the anesthesia itself has an influence on the neuronal activity (Windels F & Kiyatkin EA, 2006b). The specific pharmacological action of anesthetics on neurons and basal ganglia circuits is poorly characterized and the number of studies comparing these parameters in both awake and anesthetized animals is limited. The anesthesia-related alterations in discharge rate may depend upon the type of anesthetic used and might have dissimilar effects in different brain structures. Studies in rodents exploring functional connectivity using resting-state functional magnetic resonance imaging (rsfMRI) in the awake state and under six different anesthesia protocols, showed that urethane and propofol correspond best to the awake state (Paasonen J, et al., 2018). Nevertheless, all anesthetics seem to influence neuronal activity in one way or another. Therefore, the factor of general anesthesia should be considered in the interpretation of results and evaluation of their relevance with regards to similar data obtained using different protocols.

# 5 Summary

Deep brain stimulation (DBS) of the subthalamic nucleus (STN) alleviates all cardinal symptoms in Parkinson's disease patients. However, the underlying mechanism of high-frequency stimulation (HFS) of the STN is poorly understood. Extensive electrophysiological *in vitro* and *in vivo* research has failed to deliver a uniform explanation of the DBS phenomena. The data concerning the influence of STN stimulation on the neuronal activity of the basal ganglia are often contradictory.

The current study was performed in intact, urethane-anesthetized rats. It explores the effects of high-frequency STN stimulation on the electrophysiological activity of the external globus pallidus (GPe), the substantia nigra pars reticulata (SNr), and the pedunculopontine nucleus (PPN). To assess the modulation of neuronal activity by stimulation, extracellular single-cell recordings were performed before and after HFS of the STN, in up to three basal ganglia nuclei simultaneously, which provides a significant advantage over previous studies exploring the modulation of a single basal ganglia nucleus.

The results of the present work show that HFS of the STN modulates the activity of all examined basal ganglia nuclei. STN stimulation inhibits GPe activity, most likely due to stimulation-induced inhibition of the excitatory glutamatergic projections from the STN. The majority of the SNr neurons were inhibited by STN stimulation, suggesting a similar monosynaptic modulatory mechanism. However, a minority of SNr neurons displayed increased activity after STN stimulation. This effect is most likely polysynaptic, involving the inhibitory pallidonigral projection. PPN neurons were found to respond to STN stimulation both by decreased and increased activity in the same proportion. Inhibition of the PPN is probably caused by stimulation-induced inhibition of the excitatory projections from the STN, whereas excitation of the PPN occurs most likely due to disinhibition via GABAergic projections from the SNr.

Taken together, the results of this study demonstrate that HFS of the STN modulates the activity of the whole basal ganglia network, suggesting that the

clinical effect of STN-DBS in the treatment of Parkinson's disease represents a complex phenomenon that extends beyond the restoration of the pathological hyperactive basal ganglia output.

# 6 Zusammenfassung

Die Tiefe Hirnstimulation (DBS) des Nucleus subthalamicus (STN) wird seit den 1990er Jahren zur Therapie sämtlicher Leitsymptome des Parkinson Syndroms erfolgreich eingesetzt. Der Wirkmechanismus der Hochfrequenzstimulation (HFS) des STN ist allerdings weiterhin unzureichend verstanden. Umfangreiche elektrophysiologische *in vitro* und *in vivo* Studien konnten keine einheitliche Erklärung der DBS-Phänomene liefern. Die experimentelle Datenlage zum Einfluss der HFS des STN auf die neuronale Aktivität der Basalganglien ist oft widersprüchlich.

Ziel der vorliegenden Arbeit war die Untersuchung der Auswirkungen der STN-HFS auf die elektrophysiologische Aktivität des externen Globus pallidus (GPe), der Substantia nigra pars reticulata (SNr) und des Nucleus pedunculopontinus (PPN).

Hierfür wurden in intakten, Urethan-narkotisierten Ratten extrazelluläre Einzelzellableitungen der drei genannten Basalganglien-Kerne vor und nach der HFS des STN durchgeführt. Im Gegensatz zu früheren Studien, die nur einzelne Basalganglien untersuchten, stellt die hier zur Anwendung kommende gleichzeitige Ableitung mehrerer Kerngebiete eine Weiterentwicklung zur Beurteilung der Modulation der neuronalen Aktivität dar.

Die Ergebnisse der vorliegenden Arbeit zeigen, dass die STN-HFS die Aktivität sämtlicher untersuchten Basalganglien-Kerne moduliert. Die STN-Stimulation hemmt die Aktivität des GPe, am ehesten durch stimulationsinduzierte Hemmung der exzitatorischen glutamatergen STN-Efferenzen. Die Mehrheit der SNr-Neurone wurde durch die STN-Stimulation gehemmt, was auf einen ähnlichen monosynaptischen Modulationsmechanismus hindeutet. Eine Minderheit der SNr-Neurone zeigte jedoch nach der STN-Stimulation eine erhöhte Aktivität. Dieser Effekt ist vermutlich polysynaptisch unter Beteiligung der inhibitorischen pallidonigralen Projektion. PPN-Neurone reagierten auf die STN-Stimulation teils mit verringerter, teils mit erhöhter Aktivität, in ähnlichem Anteil. Die Hemmung des PPN wird vermutlich durch eine stimulationsinduzierte Inhibition der

exzitatorischen Afferenzen vom STN hervorgerufen, wohingegen die Aktivierung des PPN durch eine Enthemmung über GABAerge Afferenzen von der SNr zu erklären ist.

Zusammengenommen zeigen die Ergebnisse dieser Studie, dass die STN-HFS die Aktivität des gesamten Basalganglien-Netzwerks moduliert. Dieses deutet darauf hin, dass die klinische Wirkung der STN-DBS in der Behandlung des Parkinson Syndroms ein komplexes Phänomen darstellt, das über die Wiederherstellung des pathologisch hyperaktiven Basalganglien-Ausgangs hinausgeht.

# 7 Bibliography


Alexander GM & Crutcher MD, 1990. Functional architecture of basal ganglia circuits: neural substrates of parallel processing. *Trends Neurosci,* Volume 13(7), pp. 266-271.

Aravamuthan BR, Stein JF & Aziz TZ, 2008. The anatomy and localization of the pedunculopontine nucleus determined using probabilistic diffusion tractography. *Br J Neurosurg,* Volume 22, pp. 25-32.

Aziz TZ, Peggs D, Sambrook MA & Crossman AR, 1991. Lesion of the subthalamic nucleus for the alleviation of 1-methyl-4-phenyl-1,2,3,6-tetrahydropyridine (MPTP)-induced parkinsonism in the primate. *Mov Discord,* Volume 6(4), pp. 288-292.

Baldermann JC, et al., 2016. Deep Brain Stimulation for Tourette-Syndrome: A Systematic Review and Meta-Analysis. *Brain Stimul,* Volume 9(2), pp. 296-304.

Bari A, D. et al., 2018. Neuromodulation for substance addiction in human subjects: A review. *Neurosci Biobehav Rev,* Volume 95, pp. 33-43.

Benabid AL, et al., 1991. Long-term suppression of tremor by chronic stimulation of the ventral intermediate thalamic nucleus. *Lancet,* Volume 337(8738), pp. 403-406.

Benabid AL, et al., 1987. Combined (thalamotomy and stimulation) stereotactic surgery of the VIM thalamic nucleus for bilateral Parkinson disease. *Appl Neurophysiol,* Volume 50(1-6), pp. 344-346.

Benazzouz A, et al., 1996. Alleviation of experimental hemiparkinsonism by high-frequency stimulation of the subthalamic nucleus in primates: a comparison with L-Dopa treatment. *Mov Disord,* Volume 11(6), pp. 627-632.

Benazzouz A, et al., 2000. Effect of high-frequency stimulation of the subthalamic nucleus on the neuronal activities of the substantia nigra pars reticulata and ventrolateral nucleus of the thalamus in the rat. *Neuroscience,* Volume 99(2), pp. 289-295.

Benazzouz A, et al., 1993. Reversal of rigidity and improvement in motor performance by subthalamic high-frequency stimulation in MPTP-treated monkeys. *Eur J Neurosci,* Volume 5(4), pp. 382-389.

Benazzouz A, Piallat B, Pollak P & Benabid AL, 1995. Responses of substantia nigra pars reticulata and globus pallidus complex to high frequency stimulation of the subthalamic nucleus in rats: electrophysiological data. *Neurosci Lett.,* Volume 189(2), pp. 77-80.

Bergman H, Wichmann T & DeLong MR, 1990. Reversal of experimental parkinsonism by lesions of the subthalamic nucleus. *Science,* Volume 249(4975), pp. 1436-1438.

Bernheimer H, et al., 1973. Brain dopamine and the syndromes of Parkinson and Huntington. *J Neurol Sci,* Volume 20(4), pp. 415-455.

Beurrier C, Bioulac B, Audin J & Hammond C, 2001. High-frequency stimulation produces a transient blockade of voltage-gated currents in subthalamic neurons. *J Neurophysiol,* Volume 85(4), pp. 1351-1356 .

Bevan MD & Bolam JP, 1995. Cholinergic, GABAergic, and glutamate-enriched inputs from the mesopontine tegmentum to the subthalamic nucleus in the rat. *J Neurosci,* Volume 15(11), pp. 7105-7120.

Bevan MD & Wilson CJ, 1999. Mechanisms underlying spontaneous oscillation and rhythmic firing in rat subthalamic neurons. *J Neurosci,* Volume 19(17), pp. 7617-7628.

Blahak C, et al., 2009. Rapid response of parkinsonian tremor to STN-DBS changes: direct modulation of oscillatory basal ganglia activity. *Mov Disord,* Volume 24(8), pp. 1221-1225.

Blomstedt P & Hariz MI, 2010. Deep brain stimulation for movement disorders before DBS for movement disorders. *Parkinsonism Relat Disord,* Volume 16(7) , pp. 429-433.

Bosch C, et al., 2012. Preservation of the hyperdirect pathway of basal ganglia in a rodent brain slice. *Neuroscience,* Volume 215, pp. 31-41.

Breit S, Bouali-Benazzouz R, Benabid AL & Benazzouz A, 2001. Unilateral lesion of the nigrostriatal pathway induces an increase of neuronal activity of the pedunculopontine nucleus, which is reversed by the lesion of the subthalamic nucleus in the rat. *Eur J Neurosci,* Volume 14(11), pp. 1833-1842.

Breit S, Schulz JB & Benabid AL, 2004. Deep brain stimulation. *Cell Tissue Res,* Volume 318(1), pp. 275-288.

Burbaud P, Gross C & Bioulac B, 1994. Effect of subthalamic high frequency stimulation on substantia nigra pars reticulata and globus pallidus neurons in normal rats. *J Physiol Paris,* Volume 88(6), pp. 359-361.

Canteras NS, Shammah-Lagnado SJ, Silva BA & Ricardo JA, 1988. Somatosensory inputs to the subthalamic nucleus: a combined retrograde and anterograde horseradish peroxidase study in the rat. *Brain Res,* Volume 458(1), pp. 53-64.

Canteras NS, Shammah-Lagnado SJ, Silva BA & Ricardo JA, 1990. Afferent connections of the subthalamic nucleus: a combined retrograde and anterograde horseradish peroxidase study in the rat. *Brain Res,* Volume 513(1), pp. 43-59.

Charara A & Parent A, 1994. Brainstem dopaminergic, cholinergic and serotoninergic afferents to the pallidum in the squirrel monkey. *Brain Res,* Volume 640(1-2), pp. 155-170.

Connolly BS & Lang AE, 2014. Pharmacological treatment of Parkinson disease: a review. *JAMA,* Volume 311(16), pp. 1670-1683.

Cragg SJ, et al., 2004. Synaptic release of dopamine in the subthalamic nucleus. *Eur J Neurosci,* Volume 20(7), pp. 1788-1802.

Crossman AR, 1987. Primate models of dyskinesia: the experimental approach to the study of basal ganglia-related involuntary movement disorders. *Neuroscience,* Volume 21(1), pp. 1-40.

DeLong MR, Crutcher MD & Georgopoulos AP, 1985. Primate globus pallidus and subthalamic nucleus: functional organization. *J Neurophysiol,* Volume 53(2), pp. 530-543.

DeLong M & Wichmann T, 2012. Deep brain stimulation for movement and other neurologic disorders. *Ann N Y Acad Sci,* Volume 1265, pp. 1-8.

Deniau JM, Menetrey A & Thierry AM, 1994. Indirect nucleus accumbens input to the prefrontal cortex via the substantia nigra pars reticulata: a combined anatomical and electrophysiological study in the rat. *Neuroscience,* Volume 61(3), pp. 533-545.

Dexter DT & Jenner P, 2013. Parkinson disease: from pathology to molecular disease mechanisms. *Free Radic Biol Med,* Volume 62, pp. 132-144.

Do MT & Bean BP, 2003. Subthreshold sodium currents and pacemaking of subthalamic neurons: modulation by slow inactivation. *Neuron,* Volume 39(1), pp. 109-120.

Dorsey ER, et al., 2007. Projected number of people with Parkinson disease in the most populous nations, 2005 through 2030. *Neurology,* Volume 68(5), pp. 384-386.

Dostrovsky JO, et al., 2000. Microstimulation-induced inhibition of neuronal firing in human globus pallidus. *J Neurophysiol,* Volume 84(1), pp. 570-574.

Elder CM & Vitek JL, 2001. The motor thalamus: Alteration of neuronal activity in the parkinsonian state. In: Kultas-Ilinsky K & Ilinsky IA, eds. *Basal Ganglia and Thalamus in Health and Movement Disorders.* New York: Kluwer Academic.

Engelender S, 2008. Ubiquitination of α-synuclein and autophagy in Parkinson's disease. *Autophagy,* Volume 4(3), pp. 372-374.

Fasano A, et al., 2015. Axial disability and deep brain stimulation in patients with Parkinson disease. *Nat Rev Neurol,* Volume 11(2), pp. 98-110.

Filali M, et al., 2004. Stimulation-induced inhibition of neuronal firing in human subthalamic nucleus. *Exp Brain Res,* Volume 156(3), pp. 274-281.

Filion M & Tremblay L, 1991. Abnormal spontaneous activity of globus pallidus neurons in monkeys with MPTP-induced parkinsonism. *Brain Res,* Volume 547(1), pp. 142-151.

Florio T, et al., 2007. High-frequency stimulation of the subthalamic nucleus modulates the activity of pedunculopontine neurons through direct activation of excitatory fibres as well as through indirect activation of inhibitory pallidal fibres in the rat. *Eur J Neurosci,* Volume 25(4)., pp. 1174-1186.

Fujishiro H, et al., 2008. Cardiac sympathetic denervation correlates with clinical and pathologic stages of Parkinson's disease. *Mov Disord,* Volume 23(8), pp. 1085-1092.

Futami T, Takakusaki K & Kitai ST, 1995. Glutamatergic and cholinergic inputs from the pedunculopontine tegmental nucleus to dopamine neurons in the substantia nigra pars compacta. *Neurosci Res,* Volume 21(4), pp. 331-342.

Galati S, et al., 2006. Biochemical and electrophysiological changes of substantia nigra pars reticulata driven by subthalamic stimulation in patients with Parkinson's disease. *Eur J Neurosci,* Volume 23(1), pp. 2923-2928.

Garcia L, et al., 2003. Dual effect of high-frequency stimulation on subthalamic neuron activity. *J Neurosci,* Volume 23(25), pp. 8743-8751.

Garcia L, et al., 2005. Impact of high-frequency stimulation parameters on the pattern of discharge of subthalamic neurons. *J Neurophysiol,* Volume 94(6), pp. 3662-3669.

Garcia-Rill E, 1991. The pedunculopontine nucleus. *Progress in Neurobiology,* Volume 36(5), pp. 363-389.

Gerfen CR, et al., 1990. D1 and D2 dopamine receptor-regulated gene expression of striatonigral and striatopallidal neurons. *Science,* Volume 250(4986), pp. 1429-1432.

Gerfen CR & Wilson JW, 1996. The basal ganglia; Handbook of Chemical Neuroanatomy. In: Swanson LW, Björklund A & Hökfelts T, eds. *Integrated Systems of the CNS Part III.* Amsterdam: Elsevier, pp. 371-468.

Gildenberg PL, 2005. Evolution of neuromodulation. *Stereotact Funct Neurosurg,* Volume 83(2-3), pp. 71-79.

Granata AR & Kitai ST, 1989. Intracellular analysis of excitatory subthalamic inputs to the pedunculopontine neurons. *Brain Res,* Volume 488(1-2), pp. 57-72.

Granata AR & Kitai ST, 1991. Inhibitory substantia nigra inputs to the pedunculopontine neurons. *Exp Brain Res,* Volume 86(3), pp. 459-466.

Graybiel AM, Delong MR & Kitai ST, 2003. *The Basal Ganglia VI.* New York: Springer.

Greenland JC & Barker RA, 2018. The Differential Diagnosis of Parkinson’s Disease. In: Stoker TB & Greenland JC, eds. *Parkinson’s Disease: Pathogenesis and Clinical Aspects.* Brisbane (AU): Codon Publications.

Grill M & McIntyre C, 2001. Extracellular excitation of central neurons: Implications for the mechanisms of deep brain stimulation. *Thalamus & Related Systems,* Volume 1(3), pp. 269-277.

Guatteo E, Cucchiaroni ML & Mercuri NB, 2009. Substantia nigra control of basal ganglia nuclei. *Journal of Neural Transmission, Supplement,* Volume 73, pp. 91-101.

Hahn PJ, et al., 2008. Pallidal burst activity during therapeutic deep brain stimulation. *Experimental neurology,* Volume 211(1), pp. 243-251.

Hammond C, Deniau JM, Rizk A & Feger J, 1978. Electrophysiological demonstration of an excitatory subthalamonigral pathway in the rat. *Brain Res,* Volume 151(2), pp. 235-244.

Hammond C, et al., 1983a. Anatomical and electrophysiological studies on the reciprocal projections between the subthalamic nucleus and nucleus tegmenti pedunculopontinus in the rat. *Neuroscience,* Volume 9(1), pp. 41-52.

Hammond C, Shibazaki T & Rouzaire-Dubois B, 1983. Branched output neurons of the rat subthalamic nucleus: electrophysiological study of the synaptic effects on identified cells in the two main target nuclei, the entopeduncular nucleus and the substantia nigra. *Neuroscience,* Volume 9(3), pp. 511-520.

Hancock DB, et al., 2007. Smoking, caffeine, and nonsteroidal anti-inflammatory drugs in families with Parkinson disease. *Arch Neurol,* Volume 64(4), pp. 576-580.

Hara K & Harris RA, 2002. The anesthetic mechanism of urethane: the effects on neurotransmitter-gated ion channels. *Anesth Analg,* Volume 94(2), pp. 313-318.

Harding GW, 1991. A method for eliminating the stimulus artifact from digital recordings of the direct cortical response. *Comput Biomed Res,* Volume 24(2), pp. 183-195.

Hariz MI, Blomstedt P & Zrinzo L, 2010. Deep brain stimulation between 1947 and 1987: the untold story. *Neurosurg Focus,* Volume 29(2), pp. 1-10.

Hashimoto T, et al., 2003. Stimulation of the subthalamic nucleus changes the firing pattern of pallidal neurons. *J Neurosci,* Volume 23(5), pp. 1916-1923.

Hashimoto T, Elder CM & Vitek JL, 2002. A template subtraction method for stimulus artifact removal in high-frequency deep brain stimulation. *J Neurosci Methods,* Volume 113(2), pp. 181-186.

Hassani OK, François C, Yelnik J & Féger J, 1997. Evidence for a dopaminergic innervation of the subthalamic nucleus in the rat. *Brain Res,* Volume 749(1), pp. 88-94.

Hassani OK, Mouroux M & Féger J, 1996. Increased subthalamic neuronal activity after nigral dopaminergic lesion independent of disinhibition via the globus pallidus. *Neuroscience,* Volume 72(1), pp. 105-115.

Hassler R, et al., 1960. Physiological observations in stereotaxic operations in extrapyramidal motor disturbances. *Brain,* Volume 83, pp. 337-350.

Hazrati LN & Parent A, 1992. Projection from the deep cerebellar nuclei to the pedunculopontine nucleus in the squirrel monkey. *Brain Res,* Volume 585(1-2), pp. 267-271.

Heffer LF & Fallon JB, 2008. A novel stimulus artifact removal technique for high-rate electrical stimulation. *J Neurosci Methods,* Volume 170(2), pp. 277-284.

Hikosaka O, Takikawa Y & Kawagoe R, 2000. Role of the basal ganglia in the control of purposive saccadic eye movements. *Physiol Rev,* Volume 80(3), pp. 953-978.

Hirsch EC, et al., 2003. The role of glial reaction and inflammation in Parkinson's disease. *Ann N Y Acad Sci,* Volume 991, pp. 214-228.

Hutchison WD, et al., 1994. Differential neuronal activity in segments of globus pallidus in Parkinson's disease patients. *Neuroreport,* Volume 5(12), pp. 1533-1537.

Jeon MF, et al., 2003. Effect of ipsilateral subthalamic nucleus lesioning in a rat parkinsonian model: study of behavior correlated with neuronal activity in the pedunculopontine nucleus. *J Neurosurg*, Volume 99(4), pp. 762-767.

Jessell TM, Emson PC, Paxinos G & Cuello AC, 1978. Topographic projections of substance P and GABA pathways in the striato- and pallido-nigral system: a biochemical and immunohistochemical study. *Brain Res,* Volume 152(3), pp. 487-498.

Kaneoke Y & Vitek JL, 1996. Burst and oscillation as disparate neuronal properties. *J Neurosci Methods,* Volume 68(2), pp. 211-223.

Kang Y & Kitai ST, 1990. Electrophysiological properties of pedunculopontine neurons and their postsynaptic responses following stimulation of substantia nigra reticulata. *Brain Res,* Volume 535(1), pp. 79-95.

Kawaguchi Y, Wilson CJ, Augood SJ & Emson PC, 1995. Striatal interneurones: chemical, physiological and morphological characterization. *Trends Neurosci,* Volume 18(12), pp. 527-535.

Kita H & Kitai ST, 1987. Efferent projections of the subthalamic nucleus in the rat: light and electron microscopic analysis with the PHA-L method. *J Comp Neurol,* Volume 260(3), pp. 435-452.

Kita H & Kitai ST, 1994. The morphology of globus pallidus projection neurons in the rat: an intracellular staining study. *Brain Res,* Volume 636(2), pp. 308-319.

Kita T & Kita H, 2011. Cholinergic and non-cholinergic mesopontine tegmental neurons projecting to the subthalamic nucleus in the rat. *Eur. J. Neurosci,* Volume 33(3), pp. 433-443.

Lavoie B & Parent A, 1994a. Pedunculopontine nucleus in the squirrel monkey: Distribution of cholinergic and monoaminergic neurons in the mesopontine tegmentum with evidence for the presence of glutamate in cholinergic neurons. *J Comp Neurol,* Volume 344(2), pp. 190-209.

Lavoie B & Parent A, 1994b. Pedunculopontine nucleus in the squirrel monkey: projections to the basal ganglia as revealed by anterograde tract-tracing methods. *J Comp Neurol.,* Volume 344(2), pp. 210-231.

Lee JI, et al., 2001. Increased burst firing in substantia nigra pars reticulata neurons and enhanced response to selective D2 agonist in hemiparkinsonian rats after repeated administration of apomorphine. *J Korean Med Sci,* Volume 16(5), pp. 636-642.

Levy R, et al., 2001. Lidocaine and muscimol microinjections in subthalamic nucleus reverse Parkinsonian symptoms. *Brain,* Volume 124(10), pp. 2105-2018.

Limousin P, et al., 1998. Electrical stimulation of the subthalamic nucleus in advanced Parkinson's disease. *N Engl J Med,* Volume 339(16), pp. 1105-1111.

Limousin P, et al., 1995. Effect of parkinsonian signs and symptoms of bilateral subthalamic nucleus stimulation. *Lancet,* Volume 345(8942), pp. 91-95.

Magariños-Ascone C, Pazo JH, Macadar O & Buño W, 2002. High-frequency stimulation of the subthalamic nucleus silences subthalamic neurons: a possible cellular mechanism in Parkinson's disease. *Neuroscience,* Volume 115(4), pp. 1109-1117.

Mahon S, Deniau JM & Charpier S, 2001. Relationship between EEG potentials and intracellular activity of striatal and cortico-striatal neurons: an in vivo study under different anesthetics. *Cereb Cortex,* Volume 11(4), pp. 360-73.

Mahon S, et al., 2006. Distinct patterns of striatal medium spiny neuron activity during the natural sleep-wake cycle. *J Neurosci,* Volume 26(48), pp. 12587-12595.

Mallet N, et al., 2012. Dichotomous organization of the external globus pallidus. *Neuron,* Volume 74(6), pp. 1075-1086.

Maltête D, et al., 2007. Subthalamic stimulation and neuronal activity in the substantia nigra in Parkinson's disease. *J Neurophysiol,* Volume 97(6), pp. 4017-4022.

Martinez-Gonzalez C, Bolam JP & Mena-Segovia J, 2011. Topographical Organization of the Pedunculopontine Nucleus. *Front Neuroanat,* Volume 5, pp. 1-10.

Martinez-Gonzalez C, Micklem BR, Bolam JP & Mena-Segovia J, 2009. *Neurons containing calcium-binding proteins are topographically organized in the pedunculopontine nucleus.* Chicago, IL, Society for Neuroscience.

Mason P, 2017. Medical Neurobiology. In: 2nd ed. New York: Oxford University Press, pp. 433-434.

Maurice N, Thierry AM, Glowinski J & Deniau JM, 2003. Spontaneous and evoked activity of substantia nigra pars reticulata neurons during high-frequency stimulation of the subthalamic nucleus. *J Neurosci,* Volume 23(30), pp. 9929-9936.

McIntyre CC, et al., 2004a. Electric field and stimulating influence generated by deep brain stimulation of the subthalamic nucleus. *Clin Neurophysiol,* Volume 115(3), pp. 589-595.

McIntyre CC, Savasta M, Kerkerian-Le Goff L & Vitek JL, 2004b. Uncovering the mechanism(s) of action of deep brain stimulation: activation, inhibition, or both. *Clin Neurophysiol,* Volume 115(6), pp. 1239-1248.

Meissner W, et al., 2005. Subthalamic high frequency stimulation resets subthalamic firing and reduces abnormal oscillations. *Brain,* Volume 128(10), pp. 2372-2382.

Mesulam MM, Geula C, Bothwell MA & Hersh LB, 1989. Human reticular formation: cholinergic neurons of the pedunculopontine and laterodorsal tegmental nuclei and some cytochemical comparisons to forebrain cholinergic neurons. *J Comp Neurol,* Volume 283(4), pp. 611-633.

Miller WC & DeLong MR, 1987. Altered tonic activity of neurons in the globus pallidus and subthalamic nucleus in the primate MPTP model of parkinsonism. In: Carpenter MB & Jayaraman A, eds. *The Basal Ganglia II.* New York: Plenum Press, pp. 415-427.

Mintz I, Hammond C, Guibert B & Leviel V, 1986. Stimulation of the subthalamic nucleus enhances the release of dopamine in the rat substantia nigra. *Brain Res,* Volume 376(2), pp. 406-408.

Miocinovic S, et al., 2006. Computational analysis of subthalamic nucleus and lenticular fasciculus activation during therapeutic deep brain stimulation. *J Neurophysiol,* Volume 96(3), pp. 1569-1580.

Moffitt MA, McIntyre CC & Grill WM, 2004. Prediction of myelinated nerve fiber stimulation thresholds: limitations of linear models. *IEEE Trans Biomed Eng,* Volume 51(2), pp. 229-236.

Moran A, et al., 2011. Dynamic stereotypic responses of Basal Ganglia neurons to subthalamic nucleus high-frequency stimulation in the parkinsonian primate. *Front Syst Neurosci,* Volume 5(21), pp. 1-11.

Morgan JP, 1982. The first reported case of electrical stimulation of the human brain. *J Hist Med Allied Sci,* Volume 37(1), pp. 51-64.

Moriizumi T & Hattori T, 1992. Separate neuronal populations of the rat globus pallidus projecting to the subthalamic nucleus, auditory cortex and pedunculopontine tegmental area. *Neuroscience,* Volume 46(3), pp. 701-710.

Murer MG, Riquelme LA, Tseng KY & Pazo JH, 1997. Substantia nigra pars reticulata single unit activity in normal and 6-0HDA-lesioned rats: effects of intrastriatal apomorphine and subthalamic lesions. *Synapse,* Volume 27(4), pp. 278-293.

Muthusamy KA, et al., 2007. Connectivity of the human pedunculopontine nucleus region and diffusion tensor imaging in surgical targeting. *J Neurosurg,* Volume 107(4), pp. 814-820.

Nakano K, et al., 1990. Topographical projections from the thalamus, subthalamic nucleus and pedunculopontine tegmental nucleus to the striatum in the Japanese monkey, Macaca fuscata. *Brain Res,* Volume 537(1-2), pp. 54-68.

Nambu A, et al., 2000. Excitatory cortical inputs to pallidal neurons via the subthalamic nucleus in the monkey. *J Neurophysiol,* Volume 84(1), pp. 289-300.

Nambu A, Tokuno H & Takada M, 2002. Functional significance of the cortico-subthalamo-pallidal 'hyperdirect' pathway. *Neurosci Res,* Volume 43(2), pp. 111-117.

Nauta HJ & Cole M, 1978. Efferent projections of the subthalamic nucleus: an autoradiographic study in monkey and cat. *J Comp Neurol,* Volume 180(1), pp. 1-16.

Noyce AJ, et al., 2012. Meta-analysis of early nonmotor features and risk factors for Parkinson disease. *Ann Neurol,* Volume 72(6), pp. 893-901.

Obeso JA, et al., 2008. Functional organization of the basal ganglia: therapeutic implications for Parkinson's disease. *Mov Disord,* Volume 23, pp. 548-559.

O'Keeffe DT, Lyons GM, Donnelly AE & Byrne CA, 2001. Stimulus artifact removal using a software-based two-stage peak detection algorithm. *J Neurosci Methods,* Volume 109(2), pp. 137-145.

Olszewski J & Baxter D, 1982. *Cytoarchitecture of the human brain stem.* Basel: Karger.

Orimo S, et al., 2005. Cardiac sympathetic denervation precedes neuronal loss in the sympathetic ganglia in Lewy body disease. *Acta Neuropathol,* Volume 109(6), pp. 583-588.

Paasonen J, et al., 2018. Functional connectivity under six anesthesia protocols and the awake condition in rat brain. *Neuroimage,* Volume 172, pp. 9-20.

Pan HS & Walters JR, 1988. Unilateral lesion of the nigrostriatal pathway decreases the firing rate and alters the firing pattern of globus pallidus neurons in the rat. *Synapse,* Volume 2(6), pp. 650-656.

Parent A & Hazrati LN, 1995a. Functional anatomy of the basal ganglia. I. The cortico-basal ganglia-thalamo-cortical loop. *Brain Res Brain Res Rev,* Volume 20(1), pp. 91-127.

Parent A & Hazrati LN, 1995b. Functional anatomy of the basal ganglia. II. The place of subthalamic nucleus and external pallidum in basal ganglia circuitry. *Brain Res Brain Res Rev,* Volume 20(1), pp. 128-154.

Paxinos G & Watson C, 2005. *The Rat Brain in Stereotaxic Coordinates - The New Coronal Set 5th Edition.* 5th Edition ed. Amsterdam ; Boston: Academic Press Elsevier.

Pelloux Y & Baunez C, 2013. Deep brain stimulation for addiction: why the subthalamic nucleus should be favored. *Curr Opin Neurobiol,* Volume 23(4), pp. 713-720.

Percheron G, Yelnik J & Francois C, 1984. A Golgi analysis of the primate globus pallidus. III. Spatial organization of the striato-pallidal complex. *J Comp Neurol,* Volume 227(2), pp. 214-227.

Perkins MN & Stone TW, 1980. Subthalamic projections to the globus pallidus: an electrophysiological study in the rat. *Exp Neurol,* Volume 68(3), pp. 500-511.

Pollak P, et al., 1993. Effects of the stimulation of the subthalamic nucleus in Parkinson disease. *Revue Neurol,* Volume 149(3), pp. 175-176.

Pringsheim T, Jette N, Frolkis A & Steeves TD, 2014. The prevalence of Parkinson's disease: a systematic review and meta-analysis. *Mov Disord,* Volume 29(13), pp. 1583-1590.

Puchtler H, Meloan SN & Spencer M, 1985. Current chemical concepts of acids and bases and their application to anionic (“acid”) and cationic (“basic”) dyes. *Histochemistry,* Volume 82(4), pp. 301-306.

Rabey JM & Hefti F, 1990. Neuromelanin synthesis in rat and human substantia nigra. *J Neural Transm Park Dis Dement Sect,* Volume 2(1), pp. 1-14.

Ranck JB Jr, 1975. Which elements are excited in electrical stimulation of mammalian central nervous system: a review. *Brain Res,* Volume 98(3), pp. 417-440.

Rodriguez-Oroz MC, et al., 2001. The subthalamic nucleus in Parkinson's disease: somatotopic organization and physiological characteristics. *Brain,* Volume 124(9), pp. 1777-1790.

Rohlfs A, et al., 1997. Hemispheric asymmetries in spontaneous firing characteristics of substantia nigra pars reticulata neurons following a unilateral 6-hydroxydopamine lesion of the rat nigrostriatal pathway. *Brain Res,* Volume 761(2), pp. 352-356.

Rye DB, Lee HJ, Saper CB & Wainer BH, 1988. Medullary and spinal efferents of the pedunculopontine tegmental nucleus and adjacent mesopontine tegmentum in the rat. *J Comp Neurol,* Volume 269(3), pp. 315-341.

Rye DB, Saper CB, Lee HJ & Wainer BH, 1987. Pedunculopontine tegmental nucleus of the rat: Cytoarchitecture, cytochemistry, and some extrapyramidal connections of the mesopontine tegmentum. *J Comp Neurol,* Volume 259(4), pp. 483-528.

Ryu SB, et al., 2013. Neuronal Responses in the Globus Pallidus during Subthalamic Nucleus Electrical Stimulation in Normal and Parkinson's Disease Model Rats. *Korean J Physiol Pharmacol,* Volume 17(4), pp. 299-306.

Sadikot AF & Rymar VV, 2009. The primate centromedian-parafascicular complex: anatomical organization with a note on neuromodulation. *Brain Res Bull,* Volume 78(2-3), pp. 122-130.

Sanderson P, Mavoungou R & Albe-Fessard D, 1986. Changes in substantia nigra pars reticulata activity following lesions of the substantia nigra pars compacta. *Neurosci Lett,* Volume 67(1), pp. 25-30.

Saper CB & Loewy AD, 1982. Projections of the pedunculopontine tegmental nucleus in the rat: evidence for additional extrapyramidal circuitry. *Brain Res,* Volume 252(2), pp. 367-372.

Sato F, Lavallée P, Lévesque M & Parent A, 2000. Single-axon tracing study of neurons of the external segment of the globus pallidus in primate. *J Comp Neurol,* Volume 417(1), pp. 17-31.

Scarnati E, Proia A, Di Loreto S & Pacitti C, 1987. The reciprocal electrophysiological influence between the nucleus tegmenti pedunculopontinus and the substantia nigra in normal and decorticated rats. *Brain Res,* Volume 423(1-2), pp. 116-124.

Semba K & Fibiger HC, 1992. Afferent connections of the laterodorsal and the pedunculopontine tegmental nuclei in the rat: a retro- and antero-grade transport and immunohistochemical study. *J Comp Neurol,* Volume 323(3), pp. 387-410.

Sem-Jacobsen CW, 1966. Depth-electrographic observations related to Parkinson’s disease. Recording and electrical stimulation in the area around the third ventricle. *J Neurosurg,* Volume 24(1), pp. 388-402.

Shi LH, Luo F, Woodward DJ & Chang JY, 2006. Basal ganglia neural responses during behaviorally effective deep brain stimulation of the subthalamic nucleus in rats performing a treadmill locomotion tes. *Synapse,* Volume 59(7), pp. 445-457.

Shink E, Bevan MD, Bolam JP & Smith Y, 1996. The subthalamic nucleus and the external pallidum: two tightly interconnected structures that control the output of the basal ganglia in the monkey. *Neuroscience,* Volume 73(2), pp. 335-357.

Shink E, Sidibe M & Smith Y, 1997. Efferent connections of the internal globus pallidus in the squirrel monkey: II. Topography and synaptic organization of pallidal efferents to the pedunculopontine nucleus. *J Comp Neurol,* Volume 382(3), pp. 348-363.

Smith Y & Bolam JP, 1989. Neurons of the substantia nigra reticulata receive a dense GABA-containing input from the globus pallidus in the rat. *Brain Res,* Volume 493(1), pp. 160-167.

Smith Y & Parent A, 1988. Neurons of the subthalamic nucleus in primates display glutamate but not GABA immunoreactivity. *Brain Res,* Volume 453(1-2), pp. 353-356.

Soares J, et al., 2004. Role of external pallidal segment in primate parkinsonism: comparison of the effects of 1-methyl-4-phenyl-1,2,3,6-tetrahydropyridine-induced parkinsonism and lesions of the external pallidal segment. *J Neurosci,* Volume 24(29), pp. 6417-6426.

Steigerwald F, et al., 2008. Neuronal activity of the human subthalamic nucleus in the parkinsonian and nonparkinsonian state. *J Neurophysiol,* Volume 100(5), pp. 2515-2524.

Steriade M, Pare D, Parent A & Smith Y, 1988. Projections of cholinergic and non-cholinergic neurons of the brainstem core to relay and associational thalamic nuclei in the cat and macaque monkey. *Neuroscience,* Volume 25(1), pp. 47-67.

Sterio D, et al., 1994. Neurophysiological properties of pallidal neurons in Parkinson's disease. *Ann Neurol,* Volume 35(5), pp. 586-591.

Tai CH, et al., 2003. Electrophysiological and metabolic evidence that high-frequency stimulation of the subthalamic nucleus bridles neuronal activity in the subthalamic nucleus and the substantia nigra reticulata. *FASEB J,* Volume 17(13), pp. 1820-1830.

Takakusaki K, Shiroyama T, Yamamoto T & Kitai ST, 1996. Cholinergic and noncholinergic tegmental pedunculopontine projection neurons in rats revealed by intracellular labeling. *J Comp Neurol,* Volume 371(3), pp. 345-361.

Temperli P, et al., 2003. How do parkinsonian signs return after discontinuation of subthalamic DBS. *Neurology,* Volume 60(1), pp. 78-81.

Tepper JM & Lee CR, 2007. GABAergic control of substantia nigra dopaminergic neurons. *Progress in Brain Res,* Volume 160, pp. 189-208.

Thanvi BR & Lo TCN, 2004. Long term motor complications of levodopa: clinical features, mechanisms, and management strategies. *Postgraduate medical journal,* Volume 80(946), pp. 452-458.

Tsang EW, et al., 2010. Involvement of the human pedunculopontine nucleus region in voluntary movements. *Neurology,* Volume 75(11), pp. 950-959.

Urbano FJ, Leznik E & Llinas RR, 2002. Cortical activation patterns evoked by afferent axons stimuli at different frequencies: an in vitro voltage-sensitive dye imaging study. *Thalamus Rel Syst,* Volume 1(4), pp. 371-378.

Vila M, et al., 1997. Consequences of nigrostriatal denervation on the functioning of the basal ganglia in human and nonhuman primates: an in situ hybridization study of cytochrome oxidase subunit I mRNA. *J Neurosci,* Volume 17(2), pp. 765-73.

Vila M, et al., 2000. Evolution of changes in neuronal activity in the subthalamic nucleus of rats with unilateral lesion of the substantia nigra assessed by metabolic and electrophysiologica. *Eur J Neurosci,* Volume 12(1), pp. 337-344.

Viswanathan A, Jimenez-Shahed J, Baizabal Carvallo JF & Jankovic J, 2012. Deep brain stimulation for Tourette syndrome: target selection. *Stereotact Funct Neurosurg,* Volume 90(4), pp. 213-224.

Wang D, et al., 2018. Advanced research on deep brain stimulation in treating mental disorders. Experimental and therapeutic medicine. *Exp Ther Med,* Volume 15(1), pp. 3-12.

Wang HL & Morales M, 2009. Pedunculopontine and laterodorsal tegmental nuclei contain distinct populations of cholinergic, glutamatergic and GABAergic neurons in the rat. *Eur J Neurosci,* Volume 29(2), pp. 340-358.

Wang Y, et al., 2010. Noradrenergic lesion of the locus coeruleus increases apomorphine-induced circling behavior and the firing activity of substantia nigra pars reticulata neurons in a rat model of Parkinson's disease. *Brain Res,* Volume 1310, pp. 189-199.

Welter ML, et al., 2004. Effects of high-frequency stimulation on subthalamic neuronal activity in parkinsonian patients. *Arch Neurol,* Volume 61(1), pp. 89-96.

Wichmann T, 2000. A digital averaging method for removal of stimulus artifacts in neurophysiologic experiments. *J Neurosci,* Volume 98(1), pp. 57-62.

Windels F, et al., 2000. Effects of high frequency stimulation of subthalamicnucleus on extracellular glutamate and GABA insubstantia nigra and globus pallidus in the normal rat. *Eur J Neurosci,* Volume 12(11), pp. 4141-4146.

Windels F, Carcenac C, Poupard A & Savasta M, 2005. Pallidal origin of GABA release within the substantia nigra pars reticulata during high-frequency stimulation of the subthalamic nucleus. *J Neurosci,* Volume 25(20), pp. 5079-5086.

Windels F & Kiyatkin EA, 2004. GABA, Not Glutamate, Controls the Activity of Substantia Nigra Reticulata Neurons in Awake, Unrestrained Rats. *J Neurosci,* Volume 24(30), pp. 6751-6754.

Windels F & Kiyatkin EA, 2006a. GABAergic mechanisms in regulating the activity state of substantia nigra pars reticulata neurons. *Neuroscience,* Volume 140(4), pp. 1289-1299.

Windels F & Kiyatkin EA, 2006b. General anesthesia as a factor affecting impulse activity and neuronal responses to putative neurotransmitters. *Brain Res,* Volume 1086(1), pp. 104-116.

Witt, M. et al., 2009. Biopsies of olfactory epithelium in patients with Parkinson's disease. *Mov Disord,* Volume 24(6), pp. 906-914.

Woolf NJ & Butcher LL, 1986. Cholinergic systems in the rat brain: III. Projections from the pontomesencephalic tegmentum to the thalamus, tectum, basal ganglia, and basal forebrain. *Brain Res Bull,* Volume 16(5), pp. 603-637.

Xia R, et al., 2004. *Modulation of protein expression in vitro by electrical stimulation as a function of frequency.* Rome, Eighth International Congress on Parkinson's Disease and Movement Disorders.

Zhang K, et al., 2010. Long-term results of thalamic deep brain stimulation for essential tremor. *J Neurosurg,* Volume 112, pp. 1271-1276.

# 8 Erklärung zum Eigenanteil

Hiermit erkläre ich, Barbara Slewa, die vorliegende Dissertation selbständig verfasst zu haben. Die Arbeit wurde in der Abteilung Neurologie mit Schwerpunkt Neurodegenerative Erkrankungen und im Hertie-Institut für klinische Hirnforschung unter der Betreuung von Herrn PD Dr. Sorin Breit durchgeführt.

Die Konzeption der Studie erfolgte durch meinen Doktorvater Herrn PD Dr. Sorin Breit. Nach Anleitung meines Betreuers und Dr. Ruven Schäuffele, wurden sämtliche Tierversuche, die Präparation der Gehirne, sowie die histologische Aufarbeitung von mir eigenhändig durchgeführt. Das Feinmechanik-Labor der Augenklinik Tübingen stellte den faradayschen Käfig, die Führungsstäbe, sowie die zwei Elektrodenhalterungen (Matrizen) her.

Die Auswertung der Daten erfolgte nach Rücksprache mit PD Dr. med Sorin Breit eigenständig. Zur Klärung von Fragen bei der statischen Auswertung, erfolgte eine Beratung durch Prof. Dr. Martin Eichner im Institut für Klinische Epidemiologie und angewandte Biometrie.

Die Literaturrecherche, Analyse sowie die Interpretation der erhobenen Daten wurde von mir eigenständig durchgeführt mit Hilfestellung von PD Dr. med Sorin Breit. Das Manuskript der vorliegenden Dissertation wurde von mir persönlich verfasst, und von PD Dr. med Sorin Breit gegengelesen. Es wurden keine weiteren als die von mir angegebenen Quellen verwendet.

Berlin, den 06.01.2020

Barbara Slewa

# 9 Danksagung

Ich bedanke mich vor allem ganz herzlich bei meinem Doktorvater Herrn PD Dr. Sorin Breit für die Überlassung des interessanten Themas, sowie für die engagierte Unterstützung, die er mir in jeder Phase der Experimente und Erstellung dieser Doktorarbeit leistete.

Den Mitarbeitern der AG Jucker danke ich für das Bereitstellen der Geräte und Räumlichkeiten zur Durchführung der Histologie und dem Feinmechanik-Labor der Augenklinik Tübingen für die Herstellung des faradayschen Käfigs, der Führungsstäbe, sowie der Matrizen.

Bei Prof. Dr. Martin Eichner aus dem Institut für Klinische Epidemiologie und angewandte Biometrie bedanke ich mich für die statistische Beratung.

Einen besonderen Dank möchte ich meinen Eltern, auf deren Unterstützung ich mich immer verlassen konnte, und meinem Mann, für die motivierenden Worte und das Korrekturlesen, aussprechen.